ELECTROANALYTICAL AND CHROMATOGRAPHIC INVESTIGATIONS OF THE ANTINEOPLASTIC AGENT CISPLATIN AND RELATED SPECIES

by

Paula Anne Shearan B.Sc.

A thesis submitted for the Degree

of

Doctor of Philosophy

Dublin City University September 1989

Declaration

I hereby declare that the contents of this thesis, except where otherwise stated, are based entirely on my own work, which was carried out in the School of Chemical Sciences, Dublin City University.

Paula Shearan.

Paula Shearan

Malcolm R. Smyth

Malcolm R. Smyth

(Supervisor)

To my parents, Anne and Kevin

Acknowledgements

I wish to acknowledge the following people and thank them sincerely for their help:

School of Chemical Sciences for their financial support, and the Pharmacology Department, UCD, for their support and guidance;

The staff at DCU, School of Chemical Sciences, especially the technical staff, Teresa, Ita, Mick, Peig, Fintan and Veronica;

Dr Mary Meaney for her support, advice and "editing";
Dr Jose-Maria Fernandez Alvarez for his help and "lively" discussions;
Aodhmar for her time and patience;

My fellow post-graduate students especially Eleanor, Andrew, Eileen, Bernie and Mary;

Philip O'Dea and Sinead Dunne for their help;

My family for their support through all my years in college;

and finally Dr. Malcolm Smyth, my supervisor, for his help, guidance, advice and "red biro".

CONTENTS

ABSTRACT

Electroanalytical and Chromatographic Investigations of the Antineoplastic Agent Cisplatin and Related Species

Paula Shearan

The analysis of cisplatin has been investigated using a variety of electrochemical and chromatographic techniques.

Methods were developed for the simultaneous determination of cisplatin and its major hydrolysis products by HPLC with ultra-violet (UV) and electrochemical (EC) detection. The first method involved the use of reversed-phase separation using sulphonic acids as ion-pair reagents. Using a mercury based detector, limits of detection were 5 ug/ml. The second procedure involved the use of an alumina stationary phase.

The interaction of cisplatin with both human serum albumin (HSA) and the amino acid cystine was then investigated using adsorptive stripping voltammetry (AdSV). A mechanism was proposed for the electroreduction of these biologically important molecules. A fractional coefficient for the binding of cisplatin to HSA at pH 7.4 was calculated to be 0.32. The reactivity of hydrolysis products of cisplatin was shown to be greater than that of the parent drug.

Finally, a method was developed for the direct determination of inorganic platinum in urine using differential pulse polarography (DPP) and AdSV, following complexation with ethylenediammine. The method developed was compared with a graphite furnace atomic absorption spectrometric (GFAAS) technique.

CHAPTER ONE

CHEMICAL, PHYSICAL AND BIOLOGICAL PROPERTIES OF CISPLATIN

1.1. INTRODUCTION

Metal co-ordination chemistry, particularly that of the platinum group metals, has proved a successful area in the search for new anticancer drugs. Cis-dichlorodiammineplatinum (II), commonly known as cisplatin, is one such metal complex which is active as an antineoplastic agent. It is now an established drug; however, it was not until the early and mid 1960's that it was recognised to have such properties, and its history is perhaps a prime example of serendipity in science and medicine.

Cisplatin was first reported in 1845 by Peyrone, and was originally known as Peyrone's chloride [1]. Werner [2] in 1893 first distinguished the two isomers, and assigned each isomer a different name, and perhaps, more importantly, ascribed the geometries which we are now familar with today (Figure 1.1.). The cis- form is the therapeutically active compound and will be primarily considered in this section. Although the compound has been known for well over a century, its antineoplastic properties were not realised until the 1960's.

In 1965, Rosenberg [1] found that the application of an electric field to a suspension of Escherichia coli prevented cell division of the bacteria. His fortuitous use of platinum (Pt) electrodes, primarily for their inertness,led to interesting and unexpected results. A long and careful series of control experiments showed that the electric currents had not prevented cell division, but had caused the Pt

electrodes to dissolve to some extent. The ammonium chloride in the growth medium led to the formation of $(NH_4)_2PtCl_6$ [3]. This compound was able to react photochemically to form any of several compounds of the general formula $[Pt(NH_3)_nCl_{6-n}]^{(2-n)}$, where n = 1, 2 or 3 [3]. Rosenberg and co-workers showed that $Pt(NH_3)_2Cl_4$, formed after ultraviolet (UV) light irradiation, was the active compound [4,5]. By testing the synthetic isomers of $Pt(NH_3)_2Cl_4$ and the related platinum(II) salt, $Pt(NH_3)_2Cl_2$, it was established that only the cis-isomers were active [4,5].

It was reasoned that since cell division but not growth was stopped, perhaps these compounds would prove effective against cancerous cells, the most rapidly dividing cells in an organism. The first results were reported in 1969 by Rosenberg et al. using cisplatin [6], where it was found that the dosage level that killed half a sample (LD_{50}) of Swiss white mice was determined to be 14 mg/kg. Levels below the LD_{50} were then tested for tumour growth inhibitory action against transplanted Sarcoma 180 (one of about 100 standard test tumours). Tumour growth was almost completely inhibited at 8 mg/kg, less than the LD_{10} [6].

Because of the early success of this antitumour agent, analogues of cisplatin were soon considered, and scores of compounds with either subsitution of chloride by other halides, nitrate, nitrite and other singly charged anions, or substitution of ammonia were investigated [7-11]. Following a

decade of research on analogs of his original compound, Rosenberg in 1979 [1] cited the following observations on the antineoplastic activity of such platinum complexes:

(i) the complex should be electrically neutral;

(ii) not all ligands should leave or exchange;

(iii) the 2 mono- or 1 bi-dentate leaving group(s) should be in the cis- position;

(iv) the tightly bound ligand(s) should be a substitutionally inert amine; and

(v) the leaving ability of the labile ligand(s) should be of intermediate lability.

First clinical trials began in 1972, and success in the three phases of clinical evaluation (i.e. phase I,II,III) led to the approval of cisplatin as a human anticancer agent. Government approval came in the United States through the Food and Drug Administration (FDA) in December 1978, and in the United Kingdom through the Department of Health and Social Security in March 1979 [12]. In 1983, cisplatin became the U.S.'s biggest selling antitumour drug [13].

1.2. CHEMICAL AND PHYSIOCHEMICAL PROPERTIES OF CISPLATIN

The structure of cisplatin is shown in Figure 1.1. It is a square planar complex formed by a central atom of platinum surrounded by chlorine atoms and ammonia groups in the cis- configuration. It is stable in powder form for over two years in a cool, dark place, and at least a year at room temperature. The solid is only slightly soluble in water. The chemical properties necessary for identifying the compound are listed in Table 1.1.

1.2.1. Hydrolysis reactions of cisplatin

After administration of the drug, usually through injection or infusion in the blood stream, a variety of chemical reactions may occur. Due to the fact that the chloride ion concentration in blood is rather high (103 mM), the cisplatin molecule retains its chloride ions and remains electrochemically neutral. Therefore hydrolysis reactions are relatively unimportant here [14]. Consequently, the high Cl^- concentration in blood significantly hampers the binding of cisplatin to blood proteins. However, significant losses of cisplatin do occur, since 50 -70% of the adminstered drug is excreted within 24 hours [15]. The remaining cisplatin eventually diffuses through the walls of various cells, and now, because of the much lower Cl^- concentration inside the

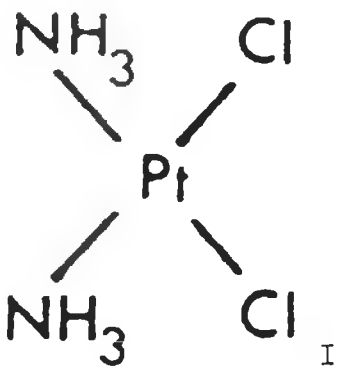

I

Figure 1.1. Structure of cisplatin

Table 1.1. Physical characteristics of cisplatin

Description	orange yellow solid
Melting point	207^{0}C
Relative molecular mass	300.1
Solubility	a) water: 1 mg/ml
	b) dimethylformamide (pure): 24 mg/ml
UV absorption	(0.8 mg/ml, 0.1 M HCl)
	max 301.1 nm ;
	min 246 nm

cell (4 mM), hydrolysis reactions can take place. Based on the work of Martin [16], it is now generally accepted that the hydrolysis scheme, as shown in Figure 1.2., operates inside the cell. The existence of these hydrolysis species of cisplatin has been established by chloride ion titrimetry [17,18]. Of the hydrolysis species, cis-$[Pt(NH_3)_2(H_2O)Cl]^+$ is the predominant species that undergoes reactions with all kinds of molecules present inside the cell (DNA, RNA and proteins).

1.2.2. The chemistry of cisplatin in aqueous media - nucleophlic displacement of the chloride ligand

On studying the hydrolysis processes of the drug, addition of chloride to aqueous solutions of cisplatin would be expected to stabilise cisplatin by shifting the aquation equilibrium to the left. Since the equilibrium constant for the displacement of the second chloride ligand by water is small ($K_2 = 1.11 \times 10^{-4}$ M) [18] compared to that for the displacement of the first chloride ligand ($K_1 = 3.63 \times 10^{-3}$ M) [18], then evaluation of the aquation behaviour can be simplified by consideration of the first hydrolysis step only. The rate of the loss of cisplatin at any time can be given by:

$$\frac{-d[I]}{dt} = k_1[I] - k_{-1}[II][Cl^-] \qquad (1.1)$$

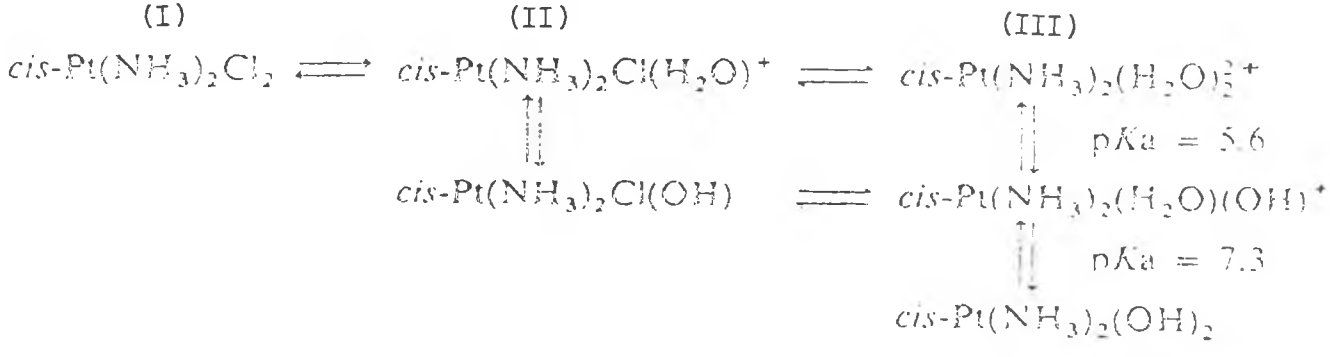

Figure 1.2. Hydrolysis of cisplatin

where I = $[Pt(NH_3)_2Cl_2]$ and

II = $[Pt(NH_3)_2(H_2O)Cl]^+$

At equilibrium, the rate of the forward and reverse reactions are equal, then $-d[I]/dt = 0$. The equilibrium constant for the first hydrolysis step may therefore be defined as:

$$K_1 = \frac{k_1}{k_{-1}} \cdot \frac{[II][Cl^-]}{[I]} \qquad (1.2)$$

From (1.2) it is clear that as $[Cl^-]$ is increased, the ratio of [II]/[I] must decrease (as K_1) is a constant). Hence, the addition of chloride to such aqueous systems should force the equilibrium position to the left, therefore increasing the fraction present as intact cisplatin.

Kinetic studies on the loss of cisplatin in aqueous solutions were first reported by Martin and co-workers [17,18]. Greene et al. [19] were the first to study systematically the stabilising effect of the chloride ion on the hydrolysis reaction, utilising UV spectroscopy and chloride ion titrimetry. The data presented was in good agreement with Martin et al. [17,18]. Hincal et al. [20] carried out a more extensive study to determine the rate constant for the forward reaction involving the first hydrolysis step. Each of the studies [19,20] found substantial stabilisation of cisplatin in aqueous systems upon the addition of chloride.

1.3. TRANSPORT

Cisplatin can either diffuse passively through the cell membrane to enter the cell, or it may require a carrier molecule to transport it. A study was carried out by Gale et al. [21] to distinguish between these two cases and was based on Michaelis-Menten kinetics for the formation of a carrier-substrate intermediate complex, and the Lineweaver-Burk equation for the analysis of such rates. The results mitigate against a carrier transport mechanism, and it is presumed at present that the platinum drug passively diffuses through the plasma membrane of the cell.

1.4. MODE OF ACTION

Since the aquated forms of cisplatin have been shown to be very reactive, much speculation on the mode of action of cisplatin has centred on the aquated forms of the drug.

As outlined above once inside the cell, and following hydrolysis, the products are capable of binding to a variety of molecules therein. Although the exact mechanism of action is still uncertain, the drug and hydrolysis products appear to exert their cytotoxic effects by directly binding with DNA. Pascoe and Roberts [22] showed that DNA is predominantly bound with cisplatin. Their binding data is shown in Table 1.2.

Table 1.2. Binding data for cisplatin with biological molecules.

Macromolecule	DNA	mRNA	rRNA	tRNA	Proteins
Pt/mole	22	0.125	0.033	6.7×10^{-4}	6.7×10^{-4}

Earlier studies by Horacek and Drobnik [23] using spectrophotometric techniques revealed that the affinity of cisplatin for DNA is much lower when the chloride levels are increased, suggesting that it is the aquated forms that are responsible for activity. Also, Rosenberg [24] and Lippard [25,26] suggested that in the intracellular fluids where the chloride concentration is low, cisplatin is converted to its hydrolysis species, and it is these that bind with DNA to create antineoplastic activity.

The molecular mechanism for the cisplatin-DNA binding is still uncertain. It is known that cisplatin and its hydrolysis species do not intercalate between the base pairs of DNA [27,28]. There is also good reason to believe that reactions with the phosphate and sugar moieties of the double helix strands either do not occur, or, if they do to any extent, are not significant for the anticancer activity. Other possible reactions do occur, and these include intrastrand crosslinks [28], DNA-protein crosslinks [29], interstrand crosslinks [30], and finally, reactions with individual bases.

1.5. METABOLISM OF THE DRUG

Hoechelle and Van Camp [31] first reported the biotransformation of the drug in mice (both with or without tumours), for both cis- and trans-dichlorodiammineplatinum(II). The excretion of these drugs follows a bi-phasic pattern, usually described by a 2-compartment model, given mathematically by:

$$\text{rate of elimination} = Ae^{-\alpha t} + Be^{-\beta t} \qquad (1.3)$$

where $t_{1/2,\alpha} = 0.693/\alpha$ and $t_{1/2,\beta} = 0.693/\beta$

The initial rapid phase α has a half-life falling in the range of 1/2 and 3/4 of an hour. The second much slower phase, follows the first, and because of much lower concentrations, data for the half-life is imprecise. Values of $t_{1/2,\beta}$ have been variously reported as 37.5 hours, 5 days, 17.5 days and 44.9 days, depending on the animal [31]. Ultimately, nearly 90% of cisplatin is excreted into urine (mostly during the first few hours to days), but detectable amounts may persist in the urine for weeks [32].

1.6. CLINICAL USES OF THE DRUG

Cytotoxicity of the drug depends on the extent of reaction with DNA, the capacity of the particular cell to excise damage from the template DNA, and the ability of the cell to synthesise DNA even after damage. Any differences are reflected in the sensitivity of various cell types to cisplatin. The drug, however, does not work equally well in all parts of the body [33].

The best results have been obtained with testicular and ovarian cancers, and indeed, the initial approval of the drug in 1978 was for the treatment of these two forms of cancer [34]. Testicular cancers represent about 1% of all male malignant tumours. Before the availability of cisplatin, 90% of patients with advanced nonseminomatous testicular cancer died. However, with an overall response rate of 60%, cisplatin, is now recognised as one of the most active drugs in testicular cancers, and it therefore has been incorporated into combinations with other chemotherapeutic agents with remarkably good results. The basis for active testicular cancer combinations is that of the vinblastine and bleomycin combination reported by Samuels and co-workers [35,36], where response rates with vinblastin and bleomycin have been reported as 76%. Einhorn and Donahue [37] noted particularly good results when cisplatin was again used in combination therapy with the two drugs already mentioned: of 20 patients treated, 15 achieved a complete remission and 5 achieved partial remission. Cisplatin probably found notoriety during

its use in the treatment against testicular cancer of the horse jockey, Bob Champion, who after remission, went on to ride the Grand National winner, Aldiniti.

Ovarian cancer is the most fatal gynaecological malignancy, and estimates are that 1 in 100 American women will die from it [38]. Early treatments using cisplatin showed significantly better results compared to previously used drugs [39,40]. In the years between 1975-1979, 235 women were treated with cisplatin, with 28% showing complete or partial remission [41]; and with various combination chemotherapies, all including cisplatin, 52% of 251 women responded to the treatment in the years 1977-1979. Other significant outcomes with cisplatin treatment have been with cervical and prostatic cancers, which have progressed from unresponsive to resistant [42]. In fact, the drug in combination therapy became headline news at the end of May 1989, for its reported success in the treatment of advanced cervical cancer. Very good results have also been obtained in the treatment of bladder, head and neck, lung and colon cancers [43].

1.7. TOXICITIES AND SIDE-EFFECTS

As with virtually all chemotherapeutic agents used against cancer, cisplatin has, by virtue of its cytotoxic nature, undesirable side-effects. Nausea and vomiting accompany cisplatin use in most patients, commencing 1 to 2 hours after dosage administration and lasting up to 4 to 6 hours later. This

situation is often ameliorated by slow infusion of the drug over a 24 hour period. These and other adverse effects are dose-dependent and often dose-limiting. Kidney damage was encountered in preliminary testing on humans, and this slowed the initial approval process. The kidney damage function, causing a decrease in the filtering capacity of the kidneys, can now be largely controlled via hydration of the patient by infusion of normal saline for several hours before drug administration, followed by the use of forced diuresis using mannitol. This hydration and diuresis before, during and after cisplatin administration has reduced the incidence and severity of nephrotoxicity by reducing the urinary platinum concentration and decreasing the renal residence time of the drug.

There are non-life threatening side-effects due to cisplatin therapy. Hearing loss, in the range of 4 - 8 kHz, occurs in about 30% of all patients [44]. The loss is irreversible, and can progress into the spoken range of 1 to 4 kHz if the drug regime is not altered. Hence, careful monitoring of the patient for any hearing loss, and discontinuation of cisplatin treatment if it is found, is an effective deterent.

Hypersensitive reactions are also experienced during therapy, ranging from skin rash, facial flushing, wheezing and hypotension [32].

There is not a selective up-take of cisplatin by any particular tissue type, and platinum has been found almost everywhere in the body following administration. A typical therapeutic dose of cisplatin gives a concentration of Pt of

about 1 ppm or 5 uM in tumour tissues.

1.8. CONCLUSIONS

A closer understanding of the interactions of cisplatin with biologically relevant molecules and the isolation of these products have been hindered by the lack of specific analytical methodology. Whilst studies of platinum distribution and clearance from various systems are many, the main problem with them is that they suffer from the inability to distinguish cisplatin and those platinum-containing compounds resulting from ligand substitution in cisplatin by other species. The introductions to Chapters 4 and 5 highlight the major analytical techniques commonly used for the detection of this antineoplastic agent and its hydrolysis products.

1.9. REFERENCES

1. Rosenberg B., Cancer Treatment Rep., 1979,63,1433.
2. Werner M., Z. Anorg. Chem., 1898,3,267.
3. Rosenberg B., VanCamp L., Krigas T., Nature , 1965,205,698.
4. Rosenberg B., VanCamp L., Grimley E., and Thomson A.J., J. Biol.Chem., 1967,242,1347.
5. Rosenberg B., Renshaw E., VanCamp L., Hartwick J., and Drobnick J., J. Bacteriol., 1967,93,716.
6. Rosenberg B., Vancamp L., Trosko J.E., and Mansour V.H., Nature , 1969,222,385.
7. Connors T.A., Jones M., Ross W.C.J., Braddock P.D., Khokhor A.R., and Tobel M.L., Chem. Biol. Interact., 1972,5,415.
8. Cleare M.J., and Hoeschelle J.D., Platinum Met. Rev., 1973,17,2.
9. Cleare M.J., and Hoeschelle J.D., Bioinorg. Chem., 1973,2,1987.
10. Munchausen L.L., and Rahn R.O., Cancer Chemother. Rep., 1975,59,643.
11. Cleare M.J., Hydes P.C., Malerbi B.W., and Watkins D M., Biochimie , 1978,60,835.
12. Cleare M.J., Platinum Met. Rev., 1979,23,53.
13. Riley C.M., and Sternson L.A., Pharmacy International., 1984,15.
14. Reedijk J., and Lohman P.H.M., Pharm. Week. Scientific Edn., 1985,7,173.
15. Rosenberg B., Plat. Met. Rev., 1971,15,42.

16. Martin R.B., In: Lippard S.J. ed: Platinum, gold and other metal chemotherapeutic agents: Chemistry and Biochemistry, Washington, American Chemical Society, 1983, 231, 44.
17. Reishus J.W., and Martin D.S., J. Amer. Chem. Soc., 1961, 83, 2457
18. Lee K.W., and Martin D.S., Inorg. Chim. Acta., 1976, 17, 105.
19. Greene R.F., Chatterji D.C., Hiranaka P.K., and Gallelli J.F., Am. J. Hosp. Pharm., 1978, 36, 38.
20. Hincal A.A., Long D.F., and Repta A.J., J. Parent. Drug Assoc., 1979, 33, 107.
21. Gale G.R., Morris C.R., Atkins L.M., and Smith A.B., Cancer Res., 1973, 33, 813.
22. Pascoe J.M., and Roberts J.J., Biochem. Pharmacol., 1974, 23, 1445
23. Horacek P.T., and Drobnik J., Biochem. Biophy. Acta., 1971, 254, 241.
24. Rosenberg B., Interdiscip. Sci. Rev., 1978, 3, 134.
25. Lippard S.J., Acc. Chem. Res., 1978, 11, 211.
26. Gangong W.F., Review of Medical Physiology, 8th Edn, Lange Medical Publications, Los Altos, CA, 1977, 455.
27. Howe-Grant M., Wu K.C., Bauer W.R., and Lippard S.J., Biochemistry, 1976, 15, 4339.
28. Roberts J.J., and Pascoe J.M., Nature, 1972, 235, 282.
29. Zwelling L.A., and Kohn K.W., Cancer Treat. Rep., 1979, 63, 1439.
30. Mansy S., Rosenberg B., and Thomson A.J., J.A.C.S., 1973, 93, 1633.

31. Hoeschelle J.D., and VanCamp L., In: Advances in Antimicrobial and Antineoplastic Chemotherapy, Vol II. Baltimore (University Part Press, 1972,241.
32. Loehrer P.J., and Einhorn L.H., Ann. Int. Med., 1984,100,704.
33. Roberts J. J., In: Pinedo H.M. ed: Cancer Chemotherapy Amsterdam: Exerptia Medica; 1982,95.
34. Garmon L., Sci. News, 1982,121,312.
35. Samuels M.L., Holoye P.Y., and Johnson D.E., Cancer, 1975 36,318.
36. Samuels M.L., Johnson D.E., and Holoye P.Y., Cancer Chemother. Rep., 1975,59,563.
37. Einhorn L.H., and Donohue J.P., J. Urol., 1977,117,65.
38. Wiltshaw E., Platinum Met. Rev., 1979,23,96.
39. Wiltshaw E., and Kroner T., Cancer Treat. Rep., 1976,60,55.
40. Wiltshaw E., Subramarian S., Alexopoulos C., and Barker G., Cancer Treat. Rep., 1979,63,1545.
41. Rosencweig M., Von Hoff D.D., Abele R., and Muggia F.H., Cancer Chemotherapy Annual 1, H.M. Pinedo (Ed), Elsevier, New York, 1979, p107.
42. Durant J.R., in Cisplatin: Current Status and New Developments: Prestayko A.W; Crooke S.J and Carter S.T (Eds), Elsevier, New York, 1982, p331.
43. Van Hoff D.D., and Rosencweig M., Advances in Pharmacology and Chemotherapy, 1980,16,273.
44. Rosencweig M., Van Hoff D.D., Slavik M., and Mugia F.M., Ann Intern. Med., 1977,86,803.

CHAPTER TWO

THEORY

2.1. ELECTROANALYTICAL TECHNIQUES

2.1.1. Fundamental concepts of electroanalytical techniques

2.1.1.1. Modes of mass transport of electroactive species to an electrode surface

During electrolysis, three modes of transfer are important [1]:

(i) migration;

(ii) convection; and

(iii) diffusion.

An excess of supporting electrolyte eliminates the migrational modes of transfer of the electroactive species in solution. Because the ions of the supporting electrolyte are in excess compared to the electroactive species, it is these ions that carry practically the total charge within the solution. Therefore, migration currents of the electroactive species are negligible. For example, the migration current, expressed in terms of transference number, t, of a univalent cation in the absence of a supporting electrolyte may be written as follows:

$$t = c_+ \lambda_+ / c_+ \lambda_+ + c_- \lambda_- \qquad (2.1)$$

where c_+ and c_- are the concentrations of the electroactive

cation and anion respectively, and λ_+ and λ_- are their respective ionic mobilities. If one considers a 100-fold addition of a univalent supporting electrolyte, the transference number of the electroactive cation is decreased to

$$t = \frac{c_+ \lambda_+}{c_+ \lambda_+ + c_- \lambda_- + 100c'_+ \lambda_+ + 100c'_- \lambda_-} \qquad (2.2)$$

where c'_+ and c'_- are the concentrations of the cationic and anionic species in the electrolyte and, λ_+ and λ_- their respective ionic mobilities. Therefore, the addition of a supporting electrolyte, whose ions can neither be oxidised of reduced, causes the transference number of the electroactive species to decrease.

Mass transfer by convection occurs under the influence of stirring or temperature gradients in solution. Although this mode of mass transfer of electroactive species to the electrode surface is utilised in stripping voltammetry, it is not desirable in polarographic studies. Hence, the elimination of convective mass transfer is achieved by maintaining the solution in a quiescent state.

The diffusion mode of mass transfer is a spontaneous process. All species (charged or uncharged) undergo diffusion. In polarographic studies, electroactive species may only be transported to the electrode surface by diffusion, which is achieved by the elimination of migrational and convective modes of mass transfer.

2.1.1.2. Main features of the electrode process

The rate of the redox reaction taking place at the electrode depends on the rate at which the species move from the bulk of the solution to the electrode (mass transfer) and the rate at which electrons tranfer from the electrode to solution species and vice-versa (charge transfer).

A simple electrochemical reaction can be depicted as follows:

$$O + ne \rightleftharpoons R$$

where O and R are the oxidised and reduced forms of the electroactive species. Conversion of O to R involves the following steps:

(i) diffusion of O from the bulk solution to the electrode surface;

(ii) transfer of electrons at the electrode surface to form R;and

(iii) diffusion of R from the electrode surface into the bulk solution.

Homogenous chemical reactions which may precede or follow the heterogeneous charge transfer step can also contribute to the overall electrode reaction.

2.1.1.3. Faradaic and capacitance currents

The total current (i_t) in an electrochemical reaction arises from two main processes at the electrode surface, namely the faradaic current (i_f) and the capacitance current (i_c):

$$i_t = i_f + i_c \qquad (2.3)$$

The faradaic current arises from electron transfer across the electrode-solution interface resulting from the oxidation or reduction of an electroactive species. The size of this faradaic current is dependent on mass transfer processes, and whether the electrolysis is restricted by diffusion, electron transfer, chemical kinetics or adsorption [1]. It also depends on the surface area of the electrode and the applied potential.

The capacitance, or charging, current results because of the change in structure of the electrode-solution interface with changing the potential on the surface area of the electrode. At the electrode-solution interface, a separation of charge takes place that makes the electrode behave like a capacitor. At a given potential, a charge exists on the electrode and an equal and opposite charge in the solution. This "array" of charged species and oriented dipoles existing at the interface is called the "electrical double layer". When the potential of the working electrode is changed, a current must flow to charge or discharge the capacitor. Because no

electron transfer is involved in this process, this type of current is termed "non-faradaic".

For a dropping mercury electrode (DME) of area A, growing with time t, the charge q required to bring the double layer to any potential E is given by:

$$q = C_{de}A(E_m-E) \qquad (2.4)$$

where C_{de} is the capacity of the double layer per unit area and E_m is the electrocapillary maximum i.e. the potential where q = 0.

The potential remains virtually constant over the lifespan of a single mercury drop, so the capacitance current is virtually a function of change in the electrode area. As the mercury drop grows, current must flow to bring the electrical double layer up to the potential designated by the electrode potential. Hence the capacitance current can be expressed mathematically as follows:

$$i_c = 0.0057C_{de}(E_m-E)m^{2/3}t^{-1/3} \qquad (2.5)$$

From equation (2.5) it can be seen that when $E = E_m$, the capacitance current is zero; it is negative when E is more positive than E_m, and positive when E is more negative than E_m. As already highlighted, a combination of i_f and

i_c results in the total current observed. However, in polarographic and voltammetric studies, only faradaic currents are of interest. As will be outlined in later sections, many techniques are now able to discriminate against the capacitance current, hence improving the limits of detection of voltammetric methods of analysis.

2.1.2. Polarography and voltammetry

2.1.2.1. Introduction

The electroanalytical techniques outlined in this section owe their origin to the introduction of direct current (DC) polarography by Jaroslav Heyrovsky in the early 1920's. This polarographic technique was used as the first instrumental method for trace metal analysis, and the subsequent award of the Nobel Prize in 1959 to Heyrovsky marked the importance attached by the scientific community to the introduction of this technique. For about 30 years, the technique grew in popularity. In the late 1950's, however, there was a decline in its application due mainly to the growing competition from chromatographic and spectroscopic methods. The limited sensitivity of DC polarography and the added difficulty involved in the interpretation of polarographic waves also contributed to this decline. However, the 10 years between 1955 and 1965 saw variations introduced in the basic polarographic technique. The discovery of pulse polarography by Barker in the early 1960's [17], which resulted in increases in sensitivity and lower limits of detection, renewed interest in this electroanalytical technique. The early 1970's heralded the use of voltammetry in the important area of environmental analysis, while the coupling of liquid chromatography with electrochemical (LCEC) detection offered the analyst a selective and sensitive tool for the determination of a wide

variety of compounds in complex biological media (e.g. plasma, serum, urine, tissues).

In the following sections , the theory behind direct current (DC) and pulse polarography, as well as adsorptive stripping voltammetry (AdSV) are included.

2.1.2.2. Direct current polarography

Polarography is the voltammetric technique where the working electrode is a dropping mercury electrode (DME). The resulting current is measured as a function of the applied potential. The potential applied between the DME and a counter electrode is varied linearly with time. A plot resulting in a current-potential curve or "polarogram" shows the variation of current with the continously applied potential. A typical DC polarogram for the reduction of cadmium ion (Cd^{2+}) is shown in Figure 2.1.

In region A, as the applied potential is scanned negatively from an initial potential of 0.0 V vs SCE, the current changes minimally, resulting from the sum of the capacitance or charging current and faradaic current, due to the reduction of trace impurities in solution. This current is known as the residual current. In region B, the reduction potential of the Cd^{2+} ions is noted as a major increase in current. The cadmium ions are reduced as follows:

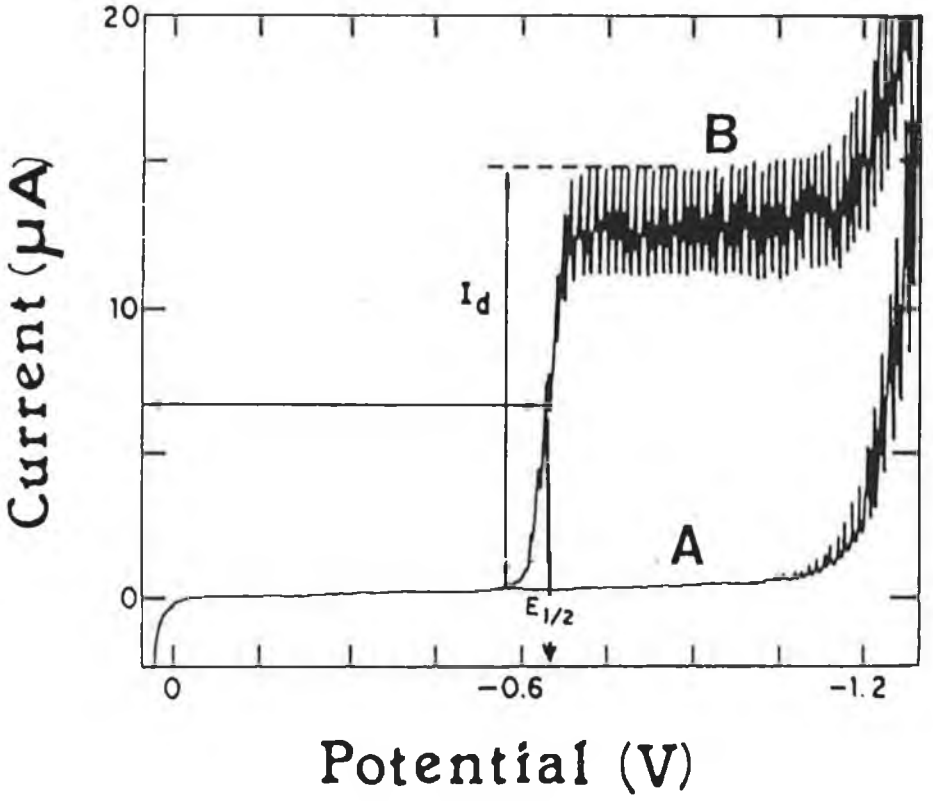

Figure 2.1. Polarograms for (A) 1 M hydrochloric acid and (B) 4 x 10^{-4} M Cd^{2+} in 1 M hydrochloric acid. $E_{1/2}$ is the half-wave potential, while i_d represents the diffusion current.

$$Cd^{2+} + 2e^- \underset{}{\overset{Hg}{\rightleftharpoons}} Cd(Hg)$$

As the rate of reduction increases with increase in the applied potential, the current reaches a plateau or limiting value when the potential becomes sufficiently negative so that the concentration of cadmium ions at the electrode surface is effectively zero. This current is limited by the rate of diffusion of the species to be reduced, and as such, the limiting current is referred to as the diffusion current (i_d). The potential where the current is one-half of its limiting value is called the half-wave potential, $E_{1/2}$. This is a most important feature of the polarogram, as the $E_{1/2}$ value is characteristic of the substance undergoing redox reactions, and hence may be used for qualitative characterisation purposes. Values of $E_{1/2}$ are almost independent of concentration of the electroactive species, but are a function of parameters such as electrolyte, pH, solvent system and the nature of the electroactive species [2].

The diffusion current i_d is directly proportional to the bulk concentration (C^o) of the electroactive species from the Ilkovic equation:

$$i_d = 607nD^{1/2}m^{2/3}t^{1/6}C^o \qquad (2.6)$$

where m and t are the rate of mercury flow (mg s^{-1}) and drop time (s) respectively. To determine the diffusion current it is necessary to subtract the residual current from the total current.

2.1.2.3. Limiting currents in polarography

Most limiting currents in DC polarography are diffusion controlled; however, they may be controlled by kinetic, adsorption or catalytic processes.

2.1.2.3.1. Diffusion-controlled limiting currents

The equation that defines the diffusion current has been based on three laws, i.e. Faraday's law and Fick's first and second laws of diffusion.

Faraday's law may be expressed as follows:

$$i = nFdN/dt \qquad (2.7)$$

where i is the electrolysis current, n is the number of electrons transferred in the electrode process, F is the Faraday constant and dN/dt is the number of the moles of electroactive substance reaching the electrode in unit time. Fick's first law of diffusion may be written as:

$$dN/dt = DA\ dC^{O}/dt \qquad (2.8)$$

where dN is the amount (expressed as the number of moles) of substance that diffuse across any plane perpendicular to, and at distance x from an

electrode of surface area A, dC^0/dx is the concentration gradient and D is the diffusion coefficient. If the mass transfer of electroactive species to the electrode is controlled only by diffusion, then the diffusion current is determined by the concentration gradient at the electrode surface; thus:

$$i = nFAD(dC^0)/dx)_{x=0} \qquad (2.9)$$

Ficks second law states:

$$dC^0/dt = D(d^2C^0/d^2x^2) \qquad (2.10)$$

When equation (2.10) is substituted into equation (2.9), assuming that the concentration of electroactive species at the electrode surface is zero, the equation for current flowing towards a planar stationary electrode is given by the Cottrell equation:

$$i_t = \frac{nFAD^{1/2}C^o}{(\pi t)^{1/2}} \qquad (2.11)$$

where i_t is the current flowing at any time t. However, corrections to the above must be made when the electrode is considered to be a growing drop [3,4]. In this case:

$$i_t = 708nD^{1/2}C^o{}_m{}^{2/3}t^{1/6} \qquad (2.12)$$

If the mean diffusion current is considered instead of the instantaneous current, then the numerical coefficient 708 in equation (2.12) is replaced by 607, giving rise to the Ilkovic equation [5]:

$$i_t = 607\ nD^{1/2}C^{o}m^{2/3}t^{1/6} \qquad (2.13)$$

Parameters such as n, D and C^o are characteristic of the solution being studied, and if these parameters are maintained constant, then the diffusion current can be expressed as:

$$i_d = \text{const.}m^{2/3}t^{1/6} \qquad (2.14)$$

The flow rate of mercury through the capillary is proportional to the height (h) of the mercury column when corrected for back pressure h_{corr}:

$$h_{corr} = h - 3.1/(mt)^{1/3} \qquad (2.15)$$

In addition, the flow rate is directly proportional to m and inversely proportional to t. Therefore:

$$i_d = \text{const.}h_{corr}^{2/3}h_{corr}^{-1/6} = \text{const.}h_{corr}^{1/2} \qquad (2.16)$$

This relationship between i_d and $h_{corr}^{1/2}$ is a criterion

commonly used to verify a diffusion-controlled limiting current [6].

2.1.2.3.2. Kinetic-controlled limiting currents

The limiting currents that are controlled by the rate of a chemical reaction occuring immediately adjacent to the electrode surface are referred to as kinetic currents. These chemical reactions may precede, follow or run parallel to the main electrode process.

2.1.2.3.2.1. Preceeding chemical reactions

This reaction type may be written as follows:

$$A \underset{k_b}{\overset{k_f}{\rightleftharpoons}} O$$

$$O + ne \rightleftharpoons R$$

where A is the electroinactive species, R the electrochemical reaction product and k_f and k_b are the forward and reverse rate constants. The equilibrium constant for the chemical reaction can therefore be written as:

$$K = k_f[O]/k_b[A] \qquad (2.17)$$

The limiting current is mostly kinetic in character [2] when the forward rate constant k_f is small, and the equilibrium concentration of O is negligible. In this case:

$$i_{lim} = i_k = 493nD^{1/2}m^{2/3}t^{2/3}(k_f/\ k_b)[A] \qquad (2.18)$$

However, if the equilibrium concentration of O is appreciable in the bulk solution, then the limiting current is the sum of the diffusion and kinetic current. Consequently:

$$i_{lim} = i_d + i_k \qquad (2.19)$$

To discover if the limiting current is kinetically controlled or otherwise, a plot of i_{lim} versus $h_{corr}^{1/2}$ is made. If the current is entirely kinetic in nature, then the limiting current will be independent of $h_{corr}^{1/2}$ [6].

2.1.2.3.2.2. Following chemical reaction

This reaction type can be represented as

$$O + ne \rightleftharpoons R$$

$$R \underset{k_b}{\overset{k_f}{\rightleftharpoons}} A$$

In this situation, the limiting current is independent of the

chemical reaction, and the limiting current is purely diffusion-controlled.

2.1.2.3.2.3. Chemical reactions occurring parallel to the electrode reaction

In this reaction type, the product of an electrode reaction may react with other species in solution to regenerate the original species:

$$O + ne \rightleftharpoons R$$
$$R + C \underset{k_b}{\overset{k_f}{\rightleftharpoons}} O$$

The above reaction is known as a catalytic process, where the oxidised form of the redox couple is regenerated by reaction of the reduced form of the species with species C, which is itself not reduced at the applied potential. When a negligible quantity of O is regenerated (i.e. when k_f is very small), the current will be diffusion controlled. However, when k_f increases, more of species O is produced through the catalytic process at the electrode than is diffusing from the bulk solution, and hence the catalytic current (i_c) is much greater than the diffusion current.

2.1.2.3.3. Adsorption-controlled limiting current

Many species dissolved in solution show a tendency to adsorb on the electrode surface, and this phenomenon can markedly affect the result of the electrochemical experiments. The electrode process may be represented as follows:

for reactant adsorption: $O_{soln} \rightleftharpoons O_{ads}$

$O_{ads} + ne \rightleftharpoons R_{soln}$

for product adsorption : $O_{soln} + ne \rightleftharpoons R_{soln}$

$R_{soln} \rightleftharpoons R_{ads}$

When the reactant species is adsorbed at the surface, then reduction of this species requires more energy than for the reduction of the solution species, due to the fact that the energy of adsorption must be overcome. As a result of this, at concentrations greater than full surface coverage, two waves may appear on the polarogram. The first is due to the reduction of the free electroactive species, whereas the second wave at more negative potentials is due to the reduction of the adsorbed species. In the case of product adsorption, however, less energy is required for reduction for $O_{soln} \longrightarrow R_{ads}$ than for $O_{soln} \longrightarrow R_{soln}$, so the adsorption wave occurs as a pre-wave to the main reduction wave.

The limiting adsorption current (i_a) is given by:

$$i_a = nFz0.85m^{2/3}t^{-1/3} \qquad (2.20)$$

where z is the maximum number of moles adsorbed per unit electrode surface.

2.1.2.4. Nature of the electrode process

Reversible or irreversible electrochemical processes are terms used to describe the nature of the electron transfer at the electrode surface. A reversible process, indicates the situation where the rate of electron transfer is fast enough to conform to thermodynamic predictions.
For the forward reaction, the current flowing is expressed as:

$$i = nFAk_fC^o_{(x=0)} \qquad (2.21)$$

The forward and backward rate constants can be written as follows [7]

$$k_f = k^0\exp[-\alpha nF/RT(E-E^o)] \qquad (2.22)$$

$$k_b = k^0\exp[(1-\alpha)/RTnF(E-E^o)] \qquad (2.23)$$

where k^0 is the heterogeneous rate constant of the electrode process at the standard potential (E^0), and α is the transfer coefficient (fraction of the applied potential influencing the

rate of reduction).

When substitution of equation (2.22) and (2.23) into (2.21) is done, the following equations result:

$$i_f = nFAC^0_{(x=0)}k^0\exp[-\alpha nF/RT(E-E^0)] \qquad (2.24)$$

$$i_b = nFAC^R_{(x=0)}k^0\exp[(1-\alpha)/RTnF(E-E^0)] \qquad (2.25)$$

The forward current (i_f) is positive and the backward current (i_b) is negative by convention. Under equilibrium conditions, $E = E^0$, and if $i_f = i_b$, equations (2.24) and (2.25) can be combined to give the well-known form of the Nernst equation:

$$E = E^0+(RT/nF)\ln([R]/[O]_{x=0})) \qquad (2.26)$$

where R and O are the oxidised and reduced forms respectively. Therefore a reversible electrode process is defined as one in which the concentration of the oxidised and reduced species at the electrode surface may be predicted by the Nernst equation.

Departures from reversible (Nernstian) behaviour are allowed given that the rate of the electron exchange process remains high, typically > 2×10^{-2} cm/sec in DC polarography. In these cases, a small net current flow in one direction can be maintained without large deviations from equilibrium concentrations, so that the Nernst equation is still applicable.

Electrochemical processes, in which kinetic rather

than thermodynamic laws determine the electrode surface concentrations of the species O and R, are said to be irreversible (non-Nernstian).

When one combines the Ilkovic and Nernst equations the following equation is obtained:

$$E_{DME} = E_{1/2}+(RT/nF)\ln(i/i_d-i) \qquad (2.27)$$

The above equation describes the shape of a polarographic wave for a reversible process with a diffusion-controlled limiting current. A plot of E_{DME} vs $\log_{10}(i/i_d-i)$ should be linear with a slope 59.1/n mV and an intercept on the axis of $E_{1/2}$ to indicate the reversibility of a DC polarographic process.

2.1.3. Cyclic Voltammetry

The technique of cyclic voltammetry was developed in 1938 by Matheson and Nichols [8], and since its introduction it has become perhaps the most effective and versatile electroanalytical technique for the mechanistic study of redox systems [9-13]. Its effectiveness results from its capability for rapidly observing the redox behaviour of electroactive species over a wide potential range. Once a redox couple has been located, it can be characterised from the potentials of peaks on the cyclic voltammogram and from changes caused by variation of the scan rate.

Cyclic voltammetry (CV) consists of cycling the potential of a working electrode in an unstirred solution and measuring the resulting current. The potential of the working electrode is controlled versus a reference electrode such as a saturated calomel electrode (SCE) or a silver/silver chloride (Ag/AgCl) electrode.

The repetitive triangular potential excitation signal for CV causes the potential of the working electrode to sweep back and forth between two designated potentials. The potential excitation that is applied across the electrode-solution interface in order to obtain a cyclic voltammogram is illustrated in Figure 2.2. Single or multiple scans may be used. Often there is little change between the first and successive scans; however the changes that do result are important as they can reveal information about reaction

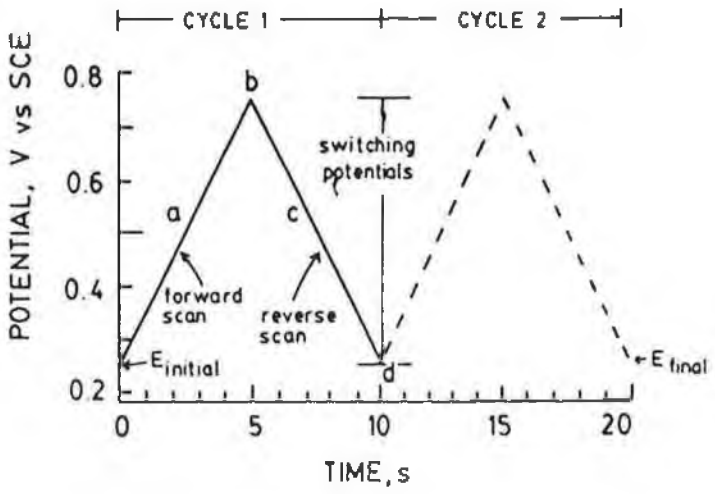

Figure 2.2. Typical potential-time excitation signal for cyclic voltammetry.

mechanisms [14].

To obtain a cyclic voltammogram, the current at the working electrode in an unstirred solution is measured during the potential scan. In Figure 2.3., a typical cyclic voltammogram for Fe^{2+} obtained at a carbon paste electrode using 1.0 M sulphuric acid as the supporting electrolyte is shown. In the forward scan, Fe^{3+} is electrochemically generated as indicated by the anodic current. In the reverse scan, the Fe^{3+} is reduced back to Fe^{2+} as indicated by the cathodic current. Therefore, CV is capable of rapidly generating a new species during the forward scan and then probing its fate on the reverse scan. This is a very important aspect of the technique.

The important parameters of a cyclic voltammogram are listed below:

(i) the cathodic (E_{pc}) and anodic (E_{pa}) peak potentials; and

(ii) the cathodic (i_{pc}) and anodic (i_{pa}) peak currents.

These parameters are labelled in Figure 2.3. One method for measuring i_p involves extrapolation of a baseline current. The establishment of a correct baseline is essential for the accurate measurement of peak currents. This is not always easy, particularly for more complicated systems. The second sweep generally causes the main problem since the baseline is not the same as the residual current obtained by an identical experiment in supporting electrolyte. Difficulty in obtaining

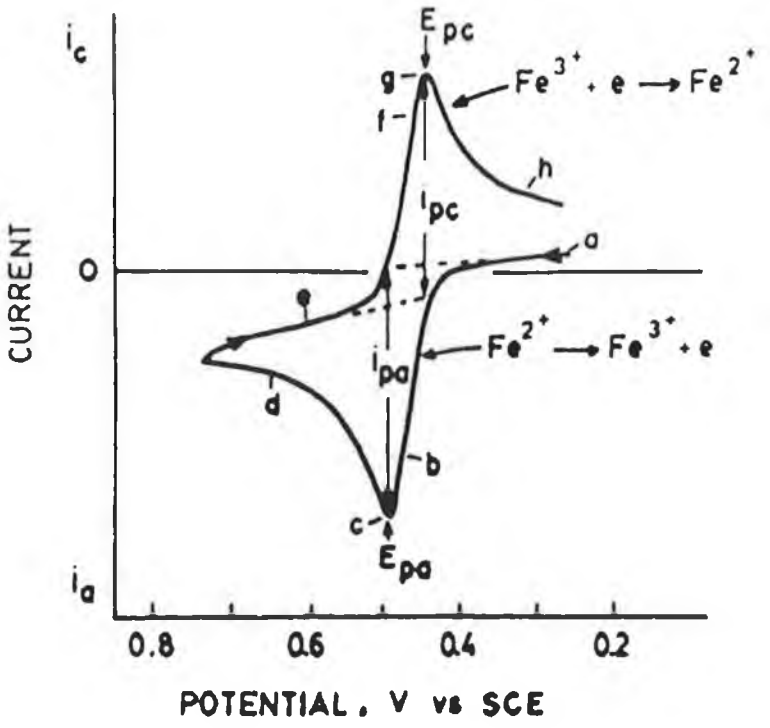

Figure 2.3. A typical cyclic voltammogram of Fe^{2+}/Fe^{3+} in 1 M sulphuric acid.

accurate peak currents has been suggested to be perhaps one of the biggest problems in CV [15].

Having established a correct baseline, the peak current measured depends on two steps:

(i) movement of the electroactive material to the working electrode; and

(ii) the rate of the electron transfer reaction.

The rate of electron transfer for a reduction process is a function of potential and is theoretically described as:

$$k_f = k^o \exp\ [-(\alpha nF/RT)(E-E^{o'})] \qquad (2.22)$$

where k^o is the standard heterogeneous electron transfer rate constant, α is the transfer coefficient, $E^{o'}$ is the formal reduction potential, n is the number of electrons transferred in the electrode process, F is the Faraday constant and R is the universal gas constant. The electron tranfer rate constant for the reverse process, k_b, is similarly controlled by the applied potential and is denoted by:

$$k_b = k^o \exp[((1-\alpha)nF/RT)(E-E^{o'})] \qquad (2.23)$$

When the electron transfer process is reversible, the difference between anodic and cathodic peak potentials is 59/n mV. This relationship may be used to evaluate n. Under

reversible conditions the electron transfer reaction at the electrode surface is fast enough to maintain the concentrations of the oxidised and reduced forms in equilibrium with each other. The equilibrium ratio for a given potential at the electrode surface is determined by the Nernst Equation:

$$E = E^{o'} + (RT/nF)\ln([R]/[O]_{x=o})) \qquad (2.26)$$

where O and R are the oxidised and reduced forms respectively and x is the distance from the electrode surface. It should be noted that the 59/n mV separation of peak potentials is independent of scan rate for a reversible couple, but is slightly dependent on switching potential and cycle number [16].

Electrochemical irreversibility is caused by slow electron exchange between the redox species and the working electrode. It is characterised by a separation of peak potentials that is greater than 59/n mV and is dependent on scan rate. At high scan rates, the electron transfer reaction may not be fast enough to maintain equilibrium conditions as the potential changes.

In cyclic voltammetry the peak current, i_p, is given by the following equation [14]:

$$i_p = k\, n^{3/2}\, A\, D^{1/2}\, C^o\, v^{1/2} \qquad (2.28)$$

where k is the Randles-Sevcik constant, A is the area of the

electrode, D is the diffusion coefficient, v is the scan rate and C^o is the concentration of the species in bulk solution. The linear dependence of i_{pc} and i_{pa} on $v^{1/2}$ is a further characteristic identifying a reversible system.

CV has become increasingly popular in all fields of chemistry as a means of studying redox states. The technique enables a wide potential range to be rapidly scanned for reducible or oxidisable species. This capability, together with the ability to use a variable time scale, make this one of the most versatile electroanalytical techniques available today. However, it must be said that its advantages lie mainly in qualitative rather than quantitative analysis. Quantitative measurements are best obtained using other techniques e.g. step, pulse or hydrodynamic techniques.

Perhaps the most useful aspect of CV is its application to the qualitative diagnosis of electrode reactions which are coupled to homogeneous chemical reactions [10-13].

2.1.4. PULSE POLAROGRAPHY

Pulse polarography has been developed from the need to suppress the capacitance current and therefore lower the detection limits of voltammetric measurements. Pulse polarography was first developed by Barker [17], arising from his work on square wave voltammetry. In this section, the theory and general features of pulse polarography are presented.

2.1.4.1. General features of pulse polarography

There are two important sources of current arising from pulse application:

(i) the faradaic current which is proportional to the concentration of the redox species in solution; and

(ii) the capacitance current needed to charge the electrode double layer.

The main idea behind the pulse technique is that the capacitance current which flows at an electrode in response to a potential pulse decays exponentially, while the faradaic current decays at a much slower rate. The current can then be measured at some time after the application of the pulse, which is long enough so that the capacitative current is negligible while the faradaic current is still appreciable. Therefore, the current which is measured, is almost a faradaic current and proportional to the concentration of the redox species.

The two main variants of pulse polarography are normal pulse polarography (NPP) and differential pulse polarography (DPP).

2.1.4.2. Normal pulse polarography (NPP)

In NPP, the electrode is held at a base potential, E_b, at which negligible electrolysis occurs for most of the life of each mercury drop from the DME. After a fixed time (which is measured from the birth of the drop), the potential is changed abruptly to a value E_n for a period of 50 msec in duration and the potential pulse is ended by a return to the base value E_b. The current is measured for the last 15-20 msec of the pulse duration. The drop is dislodged just after the pulse ends; then the whole cycle is repeated with successive drops, except that the step potential is made a few millivolts more positive or negative with each additional cycle. The output is a plot of sampled current vs step potential, and it takes the form shown in Figure 2.4. As a result of the delay that occurs between the application of the pulse and the sampling of the current, the contribution from the capacitance current is at a minimum, thus significantly improving the signal-to-noise ratio. This is because the capacitance current decays more rapidly than the faradaic current.

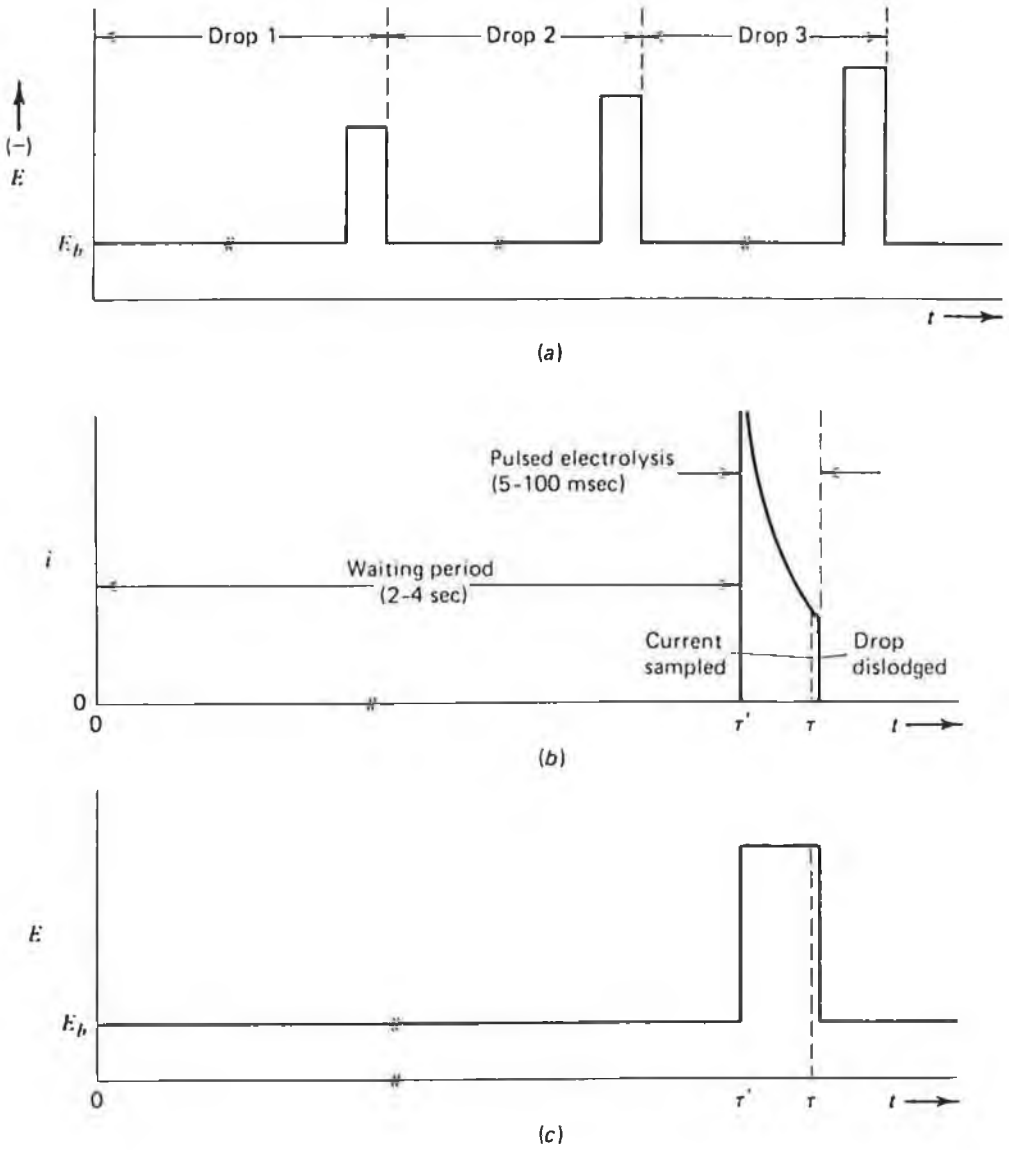

Figure 2.4. Sampling scheme for normal pulse polarography. (a) Potential program. (b) and (c) Current and potential during a single drop's lifetime.

2.1.4.3. Differential pulse polarography (DPP)

Better limits of detection than NPP can be obtained with small-amplitude pulse schemes as shown in Figure 2.5. The approach is similar to NPP, but several major differences are noted:

(i) the base potential applied during most of a drop's lifetime is not constant from drop to drop, but instead is changed steadily in small increments,

(ii) the pulse height is only 10-100 mV and is kept at a constant level with respect to the base potential, and two current measurements are taken during each drop's lifetime.

In DPP, pulses of fixed magnitude are superimposed on a linear DC potential ramp and applied to the electrode at a time just before the end of the drop. Therefore, at a fixed time period during the growth of each drop just before application of the pulse, the current flowing i_{dt1} is sampled. A small amplitude pulse (E<100 mV) is then superimposed on the voltage ramp (Figure 2.5.). The current flowing at the end of the pulse i_{dt2} is again sampled during a fixed time period after the application of the pulse. The difference between the two currents, Δi, = $i_{dt1}-i_{dt2}$, is the measured parameter. To obtain an expression for Δi, the following assumptions are made:

(i) no growth of the mercury drop occurs during the difference in sampling periods; and

(ii) the ratio of time interval between pulse

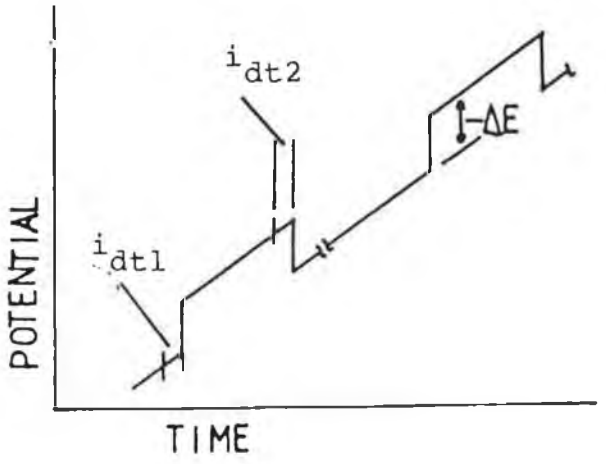

Figure 2.5. Waveform used in differential pulse polarography.

application and current measurement time during which the mercury drop has grown prior to pulse application, is small.

For a reversible electrode process the differential pulse current is obtained from the equation

$$i(E) = \varepsilon(\delta^2-1)i_d/(\delta^2+\varepsilon)(1+\varepsilon) \qquad (2.29)$$

where

$$\delta = \exp(-nF/RTE_2) \qquad (2.30)$$

and

$$\varepsilon = \exp((nF/RT)(E-E_{1/2})) \qquad (2.31)$$

The maximum value of $\Delta i(E)$, where $\Delta i(E) = i_p$, is found by differentiating equation 2.29:

$$i_p = i_d(\delta-1)/(\delta+1) \qquad (2.32)$$

Equation (2.32) shows that i_p is a linear function of concentration. However, catalytic and other perturbations of the electrode process, which result in i_d vs C plots being curved in DC polarography, have an analogous effect in both normal and differential pulse polarography with respect to i_{NPP} and i_p respectively [2].

For a reversible electrode process at a DME, the faradaic current measured in the differential pulse mode is:

$$i_f = i_{pulse} + i_{DC} \qquad (2.33)$$

where i_{pulse} is the pulse current. As indicated in equation (2.33), the faradaic current measured is the desired pulse current and a DC contribution due to the growth of the mercury drop. This DC faradaic contribution is exhibited by a shift in baseline. For reduction processes, the baseline following the peak is shifted upward, becoming quite pronounced at short drop times [18]. For analytical purposes, the peak current should be measured from the line extrapolated from the baseline before the peak.

As the concentration of the electroactive species is decreased, so the faradaic response decreases proportionally. Therefore, eventually the charging current masks the faradaic current. To overcome this limitation associated with the charging current, a stationary mercury drop electrode (SMDE) was introduced instead of the DME [19]. With the SMDE, the mercury drop grows quickly and remains constant until the drop is dislodged. The charging current in this case is significantly reduced and the limit of detection of DPP is improved.

The potential at which the current reaches it's maximum value is given by:

$$E_p = E_{1/2} - \Delta E/2 \qquad (2.34)$$

The value of E_p is shifted in a positive direction as the pulse amplitude is increased. Furthermore, the larger the value of ΔE, the larger the value of $(\Delta i)_{max}$. An increases in ΔE, however, increases the peak width, which decreases the overall resolution. In practice, values of ΔE between 10 and 100 mV are used. These offer the best compromise between adequate resolution and sensitivity.

2.1.5. Adsorptive stripping voltammetry

2.1.5.1. Introduction

In stripping analysis, the substance to be determined is preconcentrated at the working electrode prior to the actual measurement step. Most applications of this technique have centred around heavy metal analysis, which electrolytically deposit and form an amalgam with mercury. However, over the recent 10 years, there has been a large interest in the use of stripping analysis for the determination of biomacromolecules, drugs, organic and inorganic compounds that cannot be accumulated through electrolysis. Hence, an adsorptive accumulation (an alternative preconcentration step) has been used for these substances. The term "adsorptive stripping voltammetry" (AdSV) indicates an electroanalytical technique where the analyte is preconcentrated initially by adsorption at the working electrode, followed by voltammetric measurement of the surface bound species.

The amount of substance accumulated at the surface of the electrode may be affected by a number of parameters such as solvent, electrode material, potential, time, pH, ionic strength, mass transport and temperature [20]. Most adsorptive stripping procedures use the hanging mercury drop electrode (HMDE) for measuring reducible species, while carbon paste, wax impregnated graphite and platinum electrodes are used when

oxidisable analytes are of interest. The HMDE has many advantages over other working electrodes; it has self-cleaning properties, reproducible surface area and automatic control, and also offers lower detection limits (10^{-10} - 10^{-11} M) compared to those obtained at solid electrodes (10^{-8} - 10^{-9} M) due to lower background currents at mercury electrodes.

Basically, there are two main steps in the AdSV technique, which will be highlighted in the following sections.

2.1.5.2.1. Accumulation step

The low limits of detection using AdSV are attributible to the preconcentration that takes place during the accumulation step. This step is normally carried out under controlled potential conditions for a definite time and under reproducible mass transport (hydrodynamic) conditions in the solution. The species are deposited either in the form of:

(i) an amalgam or film on the surface of the mercury (drop or film);or

(ii) a film on a solid electrode.

2.1.5.2.2. Accumulation potential and time

The accumulation potential (E_{acc}) is applied to the working electrode to cause the analyte to deposit onto or

into the electrode material. The accumulation time (t_{acc}) must be carefully controlled; up to full surface coverage of the electrode, the longer the accumulation time, the greater the amount of analyte accumulated at the electrode during the stripping stage.

The accumulation step in stripping analysis is usually facilitated by convective transport of the analyte to the surface of the working electrode. This transport is achieved by electrode rotation or solution flow (in mercury film or solid electrodes), or by solution stirring (particularly for the HMDE working electrode). During the accumulation step, only a fraction of the given substance is deposited on the working electrode under reproducible conditions. If a constant current is maintained during the accumulation step, then the concentration of the analyte may be written with the application of Faraday's law. For the HMDE, the concentration in the drop, C_a, may be expressed by the following equation [21]:

$$C_a = 3it/4\pi r^3 nF \qquad (2.35)$$

where i is the cathodic or anodic current during the accumulation step, and r is the radius of the mercury drop. For a mercury film electrode (MFE) of thickness L and area A, the concentration in the film is given by:

$$C_a = it/ALnF \qquad (2.36)$$

The current flowing at any time i_t during the electrolysis step is given by the equation [22]:

$$i_t = 0.62nFAD^{2/3}w^{1/2}v^{1/6}C^0 \qquad (2.37)$$

where w is the rate of electrode rotation or solution stirring, v is the kinematic viscosity (defined as the viscosity divided by the density) [21], and C^0 is the bulk concentration of analyte at time t during accumulation.

2.1.5.2.3. The rest period

To allow formation of a uniform concentration of the analyte in the mercury, a rest period is used between the accumulation and stripping steps. At the end of the accumulation, the current drops to almost zero and a uniform concentration distribution is established quickly. This rest period also makes sure that the subsequent stripping step is performed in a quiescent solution. Also, during the rest period, electrodeposition helped by diffusion transport is continued. This results in the non-zero intercept in the peak current versus accumulation time plot.

2.1.5.3.4. The stripping step

This stage consists of anodic or cathodic scans depending on the character of the stripping process. The resultant voltammogram recorded during this step provides the analytical information of interest. The stripping current is proportional to the concentration of the analyte on or in the electrode, and hence to its concentration in the sample solution. The peak potentials also serve to identify the species of interest.

2.2. HIGH PERFORMANCE LIQUID CHROMATOGRAPHY

2.2.1. Introduction

Chromatography is essentially a physical method of separation, in which the components to be separated are distributed between two phases; one of these being a stationary phase and the other a mobile phase which percolates through or over the stationary phase [23]. The chromatographic process occurs as a result of repeated sorption/desorption processes during the movement of the sample components along the stationary phase, and the separation is due to the differences in the distribution constants of the individual components.

2.2.2. Features of chromatographic separation

There are two characteristic features of chromatographic separation [24]: a) differential migration of various compounds (solutes) in the original sample; and b) a spreading of the molecules of each solute along the column (band migration).

2.2.2.1. Differential migration

Differential migration refers to varying rates of movement of different compounds through the column, and is the basis of separation in chromatography; that is, without a

difference in rates of migration for two compounds, no separation would be possible.

Different migration rates in liquid chromatography (LC) is a result of equilibrium distribution of different compounds between the stationary phase and mobile phase and therefore is determined by experimental variables such as:

(i) mobile phase components;

(ii) stationary phase components;

(iii) separation temperatures

2.2.2.2. Band Spreading

The average migration rates of individual molecules of solutes are not similar. The different migration rates do not arise from the differences in the equilibrium distribution, but rather due to physical or rate processes. The processes leading to molecular spreading are dealt with below.

2.2.2.2.1. Eddy diffusion

This arises from the different flowstreams that the mobile phase follows between different particles within the column. Depending on the flowstreams sample molecules follow, the molecules may take different paths through the packed bed [25].

2.2.2.2.2. Mobile phase mass transfer

This refers to the different flow rates for different parts of a single flowstream between surrounding column particles. When liquid (mobile phase) flows close to a particle it moves very slowly, whereas mobile phase molecules in the centre of the flowstream move faster. Therefore, sample molecules near the column particles move slowly, whilst sample molecules in the centre of the flowstream move faster.

2.2.2.2.3. Stationary phase mass transfer

If the packing particles of a column are porous, the molecules of a sample diffuse into the pores and hence may penetrate the stationary phase or become attached in some fashion. In the former case, the molecules spend a longer time in the packing particle and therefore travel slower down the column. Those molecules that spend little time moving into and out of the stationary phase move further down the column.

2.2.2.2.4. Longitudinal diffusion

When the mobile phase is moving or even at rest, sample molecules tend to diffuse randomly in all directions.

This effect is only significant at low flow rates of mobile phase for small particle columns.

2.2.3. Retention in liquid chromatography

It is possible to derive equations for the quantitation of differential migration and band migration.
The average velocity within the column of a molecule of a solvent S is u (cm/sec) and a sample band X is u_x. From the previous section, the rate of movement of sample X through the column depends on R (the mole fraction of molecules of X in the mobile phase) and on the velocity of the mobile phase u through the equation:

$$u_x = uR \qquad (2.38)$$

When R = 0, no migration occurs and u_x is zero. Also, when the fraction of molecule X in the mobile phase is unity (R = 1), then the molecules move through the column at the same rate as mobile phase molecules i.e. $u_x = u$.

It is possible to express R in another fashion. The capacity factor k' is defined as the ratio of total moles of X in the stationary phase (n_s) to the total moles of X in the mobile phase (n_m), and may be written as follows:

$$k' = n_s/n_m \qquad (2.39)$$

As R describes the mole fraction of compound X that is present in mobile phase, the following equation can be derived from (2.39):

$$R = n_m/n_s + n_m \qquad (2.40)$$

Hence:

$$R = 1/(1 + k') \qquad (2.41)$$

and

$$u_x = u/(1 + k') \qquad (2.42)$$

It is now possible to relate the velocity of sample X (u_x) to retention time (t_r) and column length (L). Retention time is defined as the time that elapses from the moment the sample is introduced into the chromatographic system, to the point of maximum concentration of the eluted peak. Hence the time taken for compound X to move through a column of length L with a velocity u_x is:

$$t_r = L/u_x \qquad (2.43)$$

The time taken for an unretained compound to move through the column is given by:

$$t_o = L/u \qquad (2.44)$$

Combining equations (2.43) and (2.44), the retention time (t_r) may be expressed as;

$$t_r = ut_o/u_x \qquad (2.45)$$

On subsitution of this equation into equation(2.42) yields:

$$k' = (t_r - t_o)/t_o \qquad (2.46)$$

The value of k' relates where a compound elutes relative to unretained mobile phase molecules and is used to identify a peak.

Because t_r varies with flow rate, k' is sometimes expressed in terms of retention volume (V_r). Hence equation (2.46) can be written as:

$$k' = V_r - V_o/V_r \qquad (2.47)$$

where V_r = retention volume, which is the total volume of mobile phase required to elute the centre of a given peak, and V_o is the void volume (which is a measure of the internal volume of a HPLC system from injector to detector).

2.2.4. Efficiency of separation

The efficiency of a chromatographic column may be expressed by the number of theoretical plates, N, and is given by:

$$N = 16(t_r/w)^2 \qquad (2.48)$$

where t_r is the retention time of the peak and w is the base width of the peak.

N is nearly constant for different bands in a chromatogram for a given set of operating conditions.

The quantity N is also proportional to L (the column length), such that an increase in L results in an increase in N, and hence better separation. The proportionality of N and L can be written as:

$$N = L/H \qquad (2.49)$$

where H is the height equivalent of a theoretical plate (HETP).

2.2.5. Resolution

The aim of any chromatographic separation is adequate separation between the components of a sample mixture. Resolution (R) is a measure of the degree of separation [26] and may be defined as follows:

$$R = (t_b - t_a)/0.5(w_a + w_b) \qquad (2.53)$$

where t_a and t_b are retention times of compounds A and B

and w_a and w_b are their corresponding baseline peak widths.

It is possible also to equate R in terms of k' and N as follows:

$$R = \sqrt{N}/4(\alpha-1/\alpha)(k'/1+k') \quad (2.51)$$

where α is defined as the separation factor between adjacent peaks and is equal to the ratio of their k' values.

$$\alpha = k'_b/k'_a \quad (2.52)$$

From equation (2.51), resolution can be controlled by varying α, N, or k'.

2.3. ELECTROCHEMICAL DETECTION IN LIQUID CHROMATOGRAPHY

2.3.1. Introduction

The coupling of liquid chromatography with electrochemical detection (LCEC) offers a selective and sensitive tool for the determination of a wide variety of compounds of an easily oxidisable or reducible nature. Very low limits of detection have been achieved, in the order of 0.1 pmole for a number of oxidisable compounds. However, due to problems with dissolved oxygen and electrode stability, the practical limit of detection for easily reducible substances is at least 10-fold less.

Liquid chromatography (LC) and hydrodynamic voltammetry are in general very compatible techniques, and in combination yield important advantages for a number of trace determinations. The three major advantages are:

(i) selectivity;

(ii) low detection limits; and

(iii) low cost.

The use of LC for trace analysis requires a selective detector with a rapid response time, wide dynamic range and low active dead volume.

2.3.2. Fundamental Principles of Hydrodynamic Voltammetry

Hydrodynamic voltammetry involves the measurement of the current produced as the species undergoes an oxidation or reduction process at the electrode surface. In the case of amperometric detection, the working electrode is held at a fixed potential as the analyte flows past the electrode surface. The electrode is operated in the limiting current region for the eluted compounds (even though the concentration varies as the zones enter and leave the detector compartment).

2.3.3. Mass transport processes under hydrodynamic conditions

The most commonly used theory concerning the kinetics of heterogeneous chemical reactions taking place in a stirred solution has been developed by Nernst [27]. The Nernst theory states that there is a thin layer of static liquid immediately adjacent to the surface of the solid body. This is a layer through which diffusion of the reacting species takes place. Beyond this layer, called the diffusion layer of thickness d, the species is transported by convection. Inside the diffusion layer, the solution is assumed to be unstirred, and hence, the concentration distribution within the layer is thought to be linear.

On the basis of these assumptions, the flux of component taking part in the heterogeneous chemical reaction can be expressed as

$$j = DA((C^{O}-C)/d) \qquad (2.53)$$

where j is the mass flux, D is the diffusion coefficient, C^{O} is the concentration in the bulk solution, C is concentration at the electrode surface, and A is the surface area of the electrode.

However, experimental observations do not support Nernst's suppositions that the liquid is not stationary near the electrode surface and the concentration gradient is not linear. The Nernst relationship is still being used despite these limitations. From equation (2.53), it can be seen that every effect that decreases d (e.g., increase in flow rate, viscosity decrease,etc.) increases the mass flow. Even though this description is qualitatively correct, the relationship is not suitable for the quantitative description of the effect of these parameters. Equation 2.53 can be written as:

$$I = nFAD((C^{O}-C)/d) = k_{m}(C^{O}-C) \qquad (2.54)$$

The mass transfer coefficient, k_{m}, can be written as :

$$k_{m} = nFAD/d \qquad (2.55)$$

and can be calculated rigorously for certain cell geometries by

using various hydrodynamic equations, and limiting current equations for typical systems can be expressed [29].

Levich gave an exact treatment of the mass transport involving convection and diffusion [28]. Levich's theory fundamentally states that "the transport of a solute in a liquid is governed by two quite different mechanisms. First, there is molecular diffusion as a result of concentration differences; second, solute particles are entrained by the moving liquid and are transported with it. The combination of these two processes is called "convective diffusion of solute in a liquid". Either of these two strongly differing processes, convection and diffusion, can be predominant in one or another point in the liquid. However, in the vicinity of the solid surface, both processes have significant roles.

Generally, in addition to the convective diffusion, the migration of ions due to the effect of electrical attraction plays a role in an electrode process. Furthermore, the rate of a homogeneous chemical reaction may depend upon a heterogeneous chemical reaction in which it is involved. Therefore, the concentration distribution relating to a heterogeneous chemical reaction can be given as follows:

$$dc_i/dt = \nabla(D_i \nabla c_i) - V \nabla c_i + z_i F \nabla(u_i c_i \nabla \phi) + k_i \quad (2.56)$$

where D_i is the diffusion coefficient of species i, V is the

flow velocity, c_i is the concentration of species i, z is the number of charges transported by i, u_i is the ionic mobility, ϕ is the strength of the electric field and k_i is the rate of the homogeneous chemical reaction.

In equation (2.56), the first term relates to the concentration gradient of species i, and the second relates to the macroscopic flow velocity of the fluid and the concentration of i. The third term relates to the migration and the fourth one is the rate of the homogeneous chemical reaction.

2.4. GRAPHITE FURNACE ATOMIC ABSORPTION SPECTROMETRY

2.4.1. Introduction

Atomic absorption spectroscopy (AAS) is one of the most common analytical methods for the determination of elements. The term "atomic absorption" refers to the absorption of energy from a light source, with a consequent decrease in the radiation power transmitted through the flame or furnace. Measurement of this absorption gives rise to quantitative measurements. Because free atoms cannot undergo rotational or vibrational transitions as do molecules [30], only electronic transitions can take place when energy is absorbed or emitted. There are a variety of ways of obtaining free atoms and subsequent measurement of the radiation they absorb or emit. These include flame atomisation and electrothermal atomisation. Combustion flames, though cheap to produce, stable in operation, and depending on the gas mixture used (air-acetylene, maximum temperature 2200^{o}C, nitrous-oxide-acetylene, maximum temperature - 3200^{0}C) [30] able to produce a wide range of temperatures, nevertheless have certain disadvantages. The primary one is that the atomic vapour contains other highly reactive species, and therefore it is not possible to predict with certainty how a given mixture of elements may respond in terms of absorption. Many attempts have been made to produce the atomic vapour in a completely neutral or unreactive medium, hence the growth of electrical

methods to introduce the required amount of heat energy into the system. The use of a graphite furnace for generating atoms was first described by L'vov [31]. In most furnace techniques, the sample is raised to its atomisation temperature through the sequential steps of drying, ashing, and atomisation. Usually a fourth step, i.e. tube clean, is added in which any solid material remaining in the tube following atomisation is removed by volatilisation at the highest attainable temperature. When a low voltage is applied to the ends of the graphite tube, a current of several hundred amperes flows, resulting in a rapid temperature rise. Hence a power supply is used to provide a low voltage high power waveform, which can be controlled to give the required temperature for the required time for each of the steps noted above.

2.4.2. Atomiser material

An ideal atomiser should be constructed from a material which is chemically inert, has good thermal and electrical conductivity, and has low porosity and high melting point [32]. Graphite almost satisfies these conditions. It is made in a process in which carbon is heated resistively to about $3000^{0}C$ and at normal pressures it sublimes at about $3500^{0}C$; so this sets the upper limit for graphite atomisers. Graphite is oxidised at temperatures much lower than this in contact with air; hence, graphite atomisers

are always operated in an atmosphere of nitrogen or argon. However, normal graphite is porous and its porosity appears to increase after it has been maintained at high temperatures. Another disadvantage of graphite as an atomiser material is that some elements readily form stable carbides in contact with graphite at elevated temperatures. Pyrolytic graphite overcomes both of these problems to a large extent [33].

2.4.3. Selection of operating conditions

Each of the four stages i.e, drying, ashing, atomisation and tube clean must be carefully optimised to obtain the best results for any particular analysis.

2.4.3.1. Drying

During this phase the solvent is evaporated from the sample solution previously injected into the graphite tube. The step must be accomplished in a controlled manner such that there is a slow, even evaporation of the solvent from the matrix, leaving behind the dried solid sample. As an empirical rule, a setting of $105^{0}C$ is high enough for aqueous samples, and time necessarily varies according to the sample size.

2.4.3.2. Ashing and atomisation

When trace metals are to be determined in pure aqueous solutions, this phase has no significance. However, when trace metals are to be determined in varying amounts of matrix, the ashing stage is perhaps the most significant stage in the whole furnace programme. The success of the analysis depends on the correct selection of the ashing conditions. Proper thermal destruction of the matrix in a sample depends on the matrix itself. The use of too high an ashing temperature or time results in the loss of significant quantities of the analyte before the atomisation stage. The best method to determine the limits for both the ashing and atomisation stages lies in the construction of ash/atomise curves for the elements and matrices involved.

2.4.3.3. Ash/atomise curves

Having established the best drying temperature, the ashing stage is omitted, and an initial atomisation time and low temperature are set. A suitable volume is injected into the graphite tube and the complete furnace programme is carried out. The resulting peak height is plotted vs. temperature, and the atomisation temperature setting is increased before the next injection. A typical plot is shown in Figure 2.6. As the temperature is increased, so the peak height increases until a

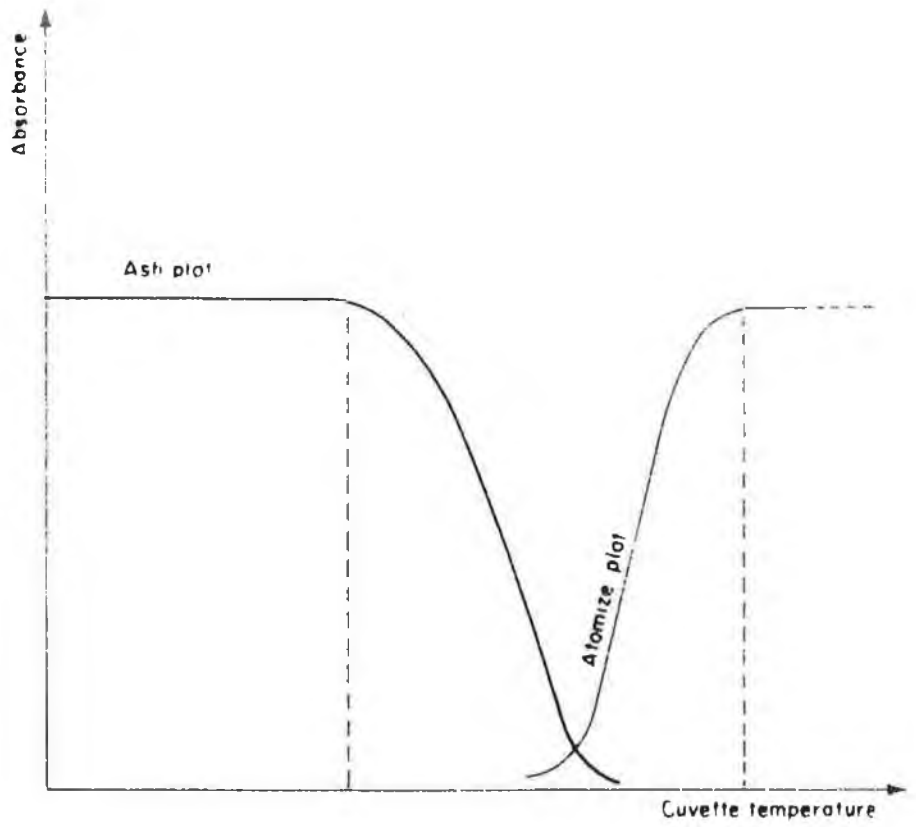

Figure 2.6. Typical ash/atomise curve

point is reached where the peak height does not increase. This point corresponds to the lowest temperature for complete atomisation.

Having selected the best atomisation temperature, a similar procedure is followed to optimise ashing conditions. A plot of peak height vs. temperature is a typical mirror image of the atomisation graph. The peak height remains constant until the point is reached where the analyte is lost and at this point the peak height decreases rapidly with increasing temperature. The ashing temperature is taken as the point $100^{0}C$ cooler than the turn-over point.

2.4.3.4. Tube clean

This temperature is normally set at several hundred degrees above the atomisation temperature, for about 5 sec. A matrix, such as blood or serum, leaves a deposit behind in the tube which may resist removal by any means other than physically brushing it out. Also with some elements, carbide or nitride formation occurs to give a memory effect. Therfore the tube must be clean for adequate analytical reproducibility.

2.4.3.5. Temperature programming

During the development of the furnace technique, it became clear that some sort of temperature programming was needed if reproducible results were to be obtained. A typical heating programme is depicted in Figure 2.7. The rate of rise of the tube temperature, together with residence time of each temperature, can be set and reproduced by controls. With this automatic feature, reproducibility can be maintained and settings repeated to match requirements of samples, according to their different physical and chemical characteristics.

Electrothermal atomisation, as outlined here, offers advantages over the flame approach. The first of these is where detection limits are sought which are below those given using a flame. As a rule, the reciprocal sensitivites given for the majority of elements by electrothermal atomisation are about 1000 times better than using a flame [32]. Secondly, electrothermal methods should be considered when the amount of sample is limited. The normal volume of solution taken for this technique is < 50 ul, compared with 0.5 ml necessary to obtain a reading using a flame. Thirdly, electrothermal atomisation can offer the possibility of analysing solid samples without dissolution [32]. However, this statement should be interpreted with some caution as solid sampling presents a number of problems that do not occur in solution methods.

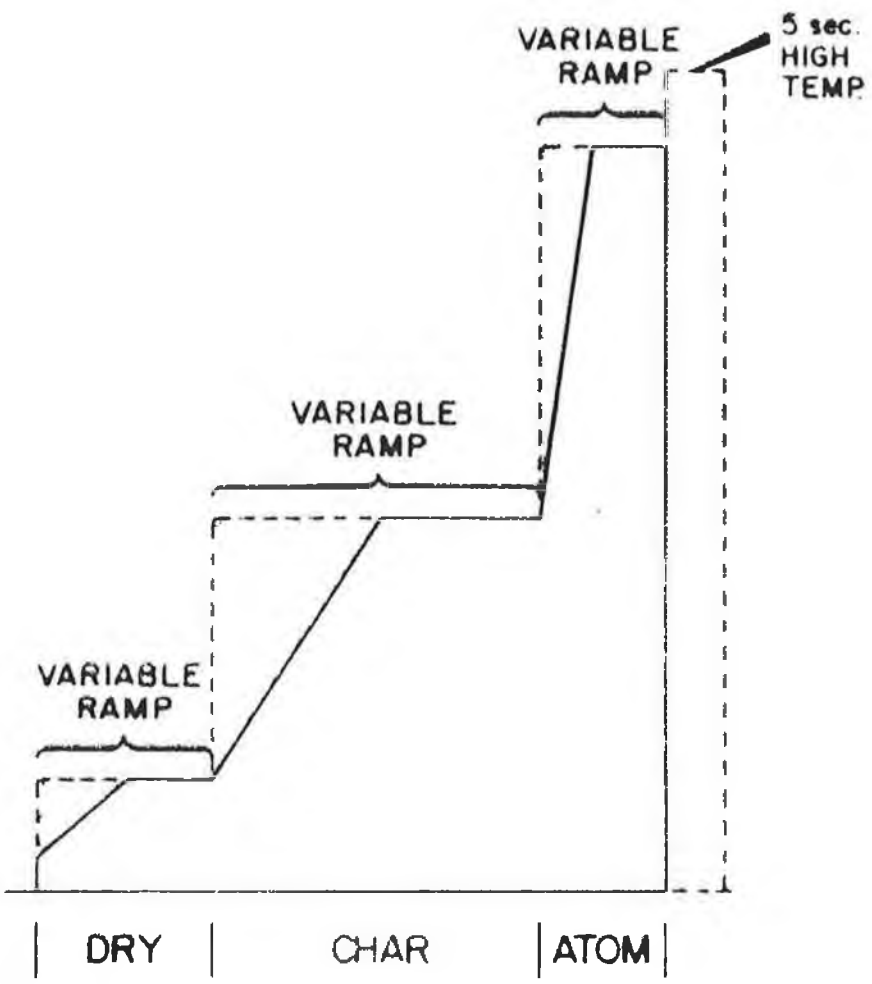

Figure 2.7. Diagram of temperature or ramp programming of the furnace. The four stages of heating are shown as steps.

2.5. REFERENCES

1. Moloy J.T., J. Chem. Educ.,1983,60,285.
2. Bond A.M., Modern Polarographic Methods in Analytical Chemistry., (Marcel Dekker Inc; New York, 1980).
3. Ilkovic D., J. Chim. Phys.,1938,35,129.
4. Ilkovic D., Collect. Chem. Commun.,1934,6,498.
5. Heyrovsky J., and Kuta J., Principles of Polarography., Academic Press, New York, 1960).
6. Zuman P., and Heyrovsky J., Practical Polarography., (Academic Press, New York, 1969) pp 19-40.
7. Crow D.R., Polarography of Metal Complexes., (Academic Press, New York, 1969).
8. Matheson L.A., and Nichols N., Trans. Electrochem. Soc., 1938,73,193.
9. Nicholson R.S., and Shain I., Anal. Chem., 1964,36,706.
10. Evans D.H., Acc. Chem. Ress., 1977,10,3131.
11. Heineman W.R., and Kissinger P.T., Am. Lab., 1982,14,29.
12. Evans D.H., O'Connell K.M., Peterson R.A., and Kelly M.J., J. Chem. Educ., 1983,60,290.
13. Kissinger P.T., and Heineman W.R., J. Chem. Educ., 1983,60,702.
14. Cauquis G., and Parker V.D., Organic Electrochemistry., (Marcel Dekker Inc. New York, 1973).
15. Adams R.N., Electrochemistry at Solid Electrodes., (Marcel Dekker Inc; New York, 1969).
16. Bard A.J., and Faulkner L.R., Electrochemical Methods.,

Fundamentals and Applications., (Wiley, New York,1980)

17. Barker G.C., Z. Anal. Chem., 1960,173,79.

18. Bond A.M., and Grabark B.S., Anal. Chim. Acta.,1977, 88,227.

19. Peterson W.M., Amer.Lab., 1979, 11,69.

20. Wang J., Amer.Lab., p41,(1985).

21. Wang J., Stripping Analysis: Principles, Instrumentation and Application., (VCH Publishers Inc. Deerfield Beach, Florida, 1985).

22. Copeland T.R., and Skogerbor R.K., Anal. Chem., 1974, 46,1257A.

23. Poole C.M., and Schuette S.A., Contemporary Practice of Chromatography., (Elsevier, 1984).

24. Snyder L.R; and Kirkland J.J., Introduction to Modern Liquid Chromatography., (J.Wiley and Sons, Chichester, 1979).

25. Hamilton R.J., and Sewell P.A., Introduction to High Performance Liquid Chromatography., (Chapman and Hall, London, 1977), pp. 12-36.

26. Knox J.H.,(editor); High Performance Liquid Chromatography., (Edinburgh University Press, Edinburgh 1978), pp. 5-19.

27. Nerst W., Z. Phys. Chem., (Leipzig), 1904,47,52.

28. Levich V.G., Physiochemical Hydrodynamics., (Prentice Hall, Englewood Cliffs,N.J; 1962.

29. Stulik K., and Pacakova V., Electroanalytical measurements in flowing liquids., (Ellis Horwood Publ. Chichester.)

30. Bauer H.H; Christian G.D; and O'Reilly I.E; Instrumental Analysis; (Allyn and Bacon Inc.)

31. L'vov B.V; Spectrochim. Acta; 1961,17,761.

32. Price W.J; Spectrochemical Analysis by Atomic Absorption; (Publ. Heyden.)

33. L'vov B.V; Spectrochim. Acta; 1970,24B,53.

CHAPTER THREE

HIGH PERFORMANCE LIQUID CHROMATOGRAPHY OF CISPLATIN AND ITS HYDROLYSIS PRODUCTS

3.1. INTRODUCTION

The history and clinical background of cis-dichlorodiammineplatinum(II) (cisplatin) has already been outlined in Chapter 1. The particular structure and physiochemical properties of cisplatin have presented particular problems in the development of analytical procedures which provide the necessary selectivity and sensitivity for the determination of the intact drug in biological fluids. The analytical methods may be conveniently divided into non-selective methods, which detect only the platinum metal, and selective methods, which are capable of detecting the intact compound. The methods which rely on the non-selective determination of platinum include X-ray fluorescence (XRF), proton induced X-ray emission (PIXE), inductively coupled plasma (ICP), flameless atomic absorption spectrometry (FAAS) and high performance liquid chromatography (HPLC) with pre-column derivatisation. This chapter will deal with HPLC techniques in both non-selective and selective modes for the determination of cisplatin, and also look at the use of alumina as a stationary phase for the separation of cisplatin and its hydrolysis products.

3.1.1. Non-selective methods

One of the most useful methods for the determination of platinum in biological samples involves derivatisation with

diethyldithiocarbamate (DDTC), to yield a complex with a single chromophore in the UV region of the spectrum. The complex can be extracted into chloroform and separated by normal phase [1] or reversed-phase [2] modes of HPLC. This reaction was originally adapted simultaneously by Bannister et al. [1] and Borch et al. [2] for the determination of platinum excreted into urine. This method, which has a detection limit of 3 ng/ml, was adapted subsequently for the analysis of plasma ultrafiltrate [3]. Andrews et al. [3] were then able to determine cisplatin in plasma ultrafiltrate following derivatisation with DDTC, with quantitation carried out using a nickel chloride internal standard. The chromatographic separation was achieved using reversed-phase HPLC on a C_{18} radial compression column. The complex eluted with methanol/water (4/1) at a flow rate of 1.5 ml/min, and was detected at 254 nm. The limit of detection was 0.1 ug/ml cisplatin in the ultrafiltrate. This approach for the determination of cisplatin was validated by comparison with graphite furnace atomic absorption spectrometric (GFAAS) determinations in duplicate samples.

3.1.2. Selective methods

A great deal of effort has been directed towards the development of selective methods for the determination of cisplatin and its analogues in biological fluids. Most of the literature has dealt with the analysis of cisplatin, and the

methods of choice have been largely based on HPLC. However, HPLC of cisplatin is not particularly straightforward, due to difficulty in detection and poor chromatographic properties.

Although cisplatin is a neutral molecule, it may be retained on cationic stationary phases such as Partisil 10 SAX [4,5]. An alternative to using chemically bonded stationary phases [4,5] is to use solvent generated phases [6-9], in which the cationic surfactant hexadecyltrimethylammonium bromide (HTAB), is physically adsorbed onto the surface of silica gel or alkylsilylsilicas. The advantage of these types of stationary phase is that they can be operated with purely aqueous mobile phases which are compatible with the electrochemical detectors as described by Bannister et al. [10], and the post-column reaction detectors as described by Marsh et al. [9]. These solvent generated systems have also been used for the chromatography of other platinum(II) and platinum(IV) complexes in addition to cisplatin [6-9].

Riley et al. [6] tried to identify the sites of interaction on a cationic stationary phase (Partisil 10 SAX), as there appears to be three potential sites on this phase for interaction of cisplatin; namely

(i) quaternary ammonium groups;

(ii) silanol moieties; and

(iii) hydrocarbon groups.

They looked at the effect of methanol on the retention of cisplatin on this column and compared it to a hydrophobic stationary phase (μ Bondapak C_{18}) and silica gel (Partisil

5). The retention of cisplatin on a bonded anion-exchange column increased with increasing methanol concentration, whilst cisplatin was poorly retained and its retention decreased slightly with increasing methanol concentration in the other two columns. These results suggest that the drug is retained on Partisil 10 SAX primarily as a result of interactions with the bonded quaternary ammonium groups and that these interactions are strengthened by the presence of methanol in the mobile phase. These interactions are believed to occur via ion-dipole interactions of the neutral drug and cationic groups on the stationary phase. The poor retention of cisplatin on silica indicate that dispersion forces arising from dipole interactions play a minor role in the retention of cisplatin on Partisil 10 SAX and similarly, the results obtained on the hydrophobic stationary phase indicates that solvophobic interactions of cisplatin with the hydrocarbon moieties of Partisil 10 SAX are relatively unimportant. Hincal et al. [5] coupled strong anion- and strong cation-exchange columns to permit retention of both cisplatin and the positively charged hydrolysis products. However, this method was used as a stability indicating assay for cisplatin in formulations and not as a bioassay. Riley et al. [8] applied the separation of platinum complexes on solvent generated anion-exchangers to the analysis of cisplatin in urine using automated column switching, whereas Kitz et al. [11] utilised the retention of cisplatin on ion-exchangers, by coupling a strong cation-exchanger (pre-column) and a strong anion-exchanger

(analytical column) for the determination of cisplatin in plasma and urine with UV detection and column switching.

It should also be noted that Parsons et al. [12], used a reversed-phase column modified by alkylsulphonic acids for the chromatography of hydrolysis products from cisplatin in fresh and aged solutions. This chapter also presents results using ion-pair chromatography with electrochemical detection for the determination of cisplatin and hydrolysis products [13]. Daley-Yates and M^{c}Brien used sodium dodecylsulphate as an ion-pair reagent for the separation of platinum species [14].

Cisplatin has a low solubility in organic solvents and is not readily extracted from biological fluids. Therefore, bioanalysis of intact cisplatin or its analogs nearly involves direct injection of the biological fluid (plasma or urine). However, this does place a large strain on the ability of the detection system to differentiate between analyte and the potentially interfering endogenous compounds. Several detection systems have been used for the on-line detection of platinum-containing drugs and include UV absorption [1,8, 11,15], UV absorption following post-column derivatisation [9], and reductive electrochemistry [12,16-18]. In addition to on-line techniques, fraction collection and determination of the fractions by GFAAS has also been used in combination with HPLC for the determination of cisplatin in plasma ultrafiltrate [15] and urine [8].

Direct UV detection [7,11] provides limits of detection of about 1 μg/ml at 280 nm and about 20 ng/ml at 210

nm. Untreated urine cannot be injected into a mobile phase of greater than 60% aqueous methanol, due to the precipitation of inorganic salts. Cisplatin can be analysed in urine with direct UV detection at 280 nm using a solvent generated anion exchange system. But, in this case, automated column switching is required to separate the drug from endogenous substances [8]. Kitz et al. [11] have described a sensitive HPLC method with direct UV detection at 210 nm for the analysis of intact cisplatin in urine and plasma follwing column switching.

On reviewing the literature, the method of choice for the determination of intact cisplatin appears to be HPLC with either electrochemical detection [10,12,16-18] or UV detection following post-column derivatisation [9]. Both methods require minimal pre-treatment of urine or plasma ultrafiltrate and result in detection limits of 25-50 ng/ml. The use of electrochemical detection of cisplatin in the reductive mode was described initially by Bannister [10], who applied polarographic detection following HPLC separation of cisplatin. The column eluent was passed into an electrochemical detector consisting of a dropping mercury electrode (DME) operated at 0.00 V (vs Ag/AgCl). The use of a very low operating potential allows the selective detection of cisplatin, eliminating those components of urine which interfere when UV detection is used. The disadvantages of this system are:

(i) oxygen must be eliminated from the system by rigorous purging with nitrogen,

(ii) the temperamental nature of the system,

(iii) the dependency of relative response on the nature of the ligands co-ordinated with Pt.

Polarographic detection of cisplatin achieved limits of detection of 70 ng/ml in urine and plasma. This was improved later by others [17,18] who used the more convenient glassy carbon electrode detector.

The post-column reaction detection system described by Marsh et al. [9] is perhaps an alternative to electrochemical detection. In this system, separation was achieved on a solvent generated anion-exchanger and the platinum-containing species are selectively derivatised to give highly UV-absorbing species before they enter the spectrometer. The detection system is based on the prior observations of Hussain et al. [19], that a strongly UV absorbing species is produced when cisplatin is reacted with bisulphite ions. In order for this reaction to be reproducible, the platinum complexes must first be reacted with potassium dichromate before derivatisation with bisulphite. The nature of the complex or complexes formed in the reactor, and the precise role played by the dichromate ions are unknown. Nevertheless, the reaction detector has an excellent linear, dynamic range, resulting in detection limits of 40 ng/ml in biological fluids (comparible to those limits obtained by HPLC with electrochemical detection).

3.2. THE USE OF AN ALUMINA STATIONARY PHASE IN HPLC

The use of alumina as a stationary phase material in modern liquid chromatography has not been widely reported over the past ten years. In classical adsorption chromatography it must compete with silica, and both materials have been largely superceded by chemically modified silicas.

Like silica, alumina can be considered as a typical polar adsorbent, and most separations proceed in the same way on the two oxides. However, where silica is only active through its surface hydroxyl groups, alumina possesses two alternative possibilities for interaction with solutes. The acidic sites of alumina adsorb basic solutes through nucleophilic interactions, and the same sites may also form charge transfer complexes with typical electron donors such as aromatic solutes [20]. On the other hand, acidic solutes may interact with basic sites on the alumina surface through the transfer of a proton leading to chemisorption. In general, alumina interacts strongly with polarised molecules.

3.2.1. Ion-exchange properties of alumina

Alumina acts as a typical ion-exchanger, but is also amphoteric in nature, so that its ion-exchange properties are strongly pH-dependent. This amphoteric character can be explained by the presence of two distinct types of hydroxyl

groups on the alumina surface (Figure 3.1.). From this it can be seen that there are hydroxyl groups chemisorbed onto acidic sites (Al atoms), whilst there are protons chemisorbed onto oxygen atoms. Therefore, when neutral alumina is washed with NaOH, the chemisorbed protons will be neutralised and replaced by sodium ions. These Na^+ ions can exchange with other cations and are responsible for the cation-exchange properties of alkaline alumina at higher pH's. However, when the alkaline alumina is washed with HCl, the protons of the acid give rise to two effects:

(i) they desorb the hydroxyl groups, which are then replaced by Cl^- ions to give rise to the anion-exchange properties of acidic alumina; and

(ii) the protons also replace the Na^+ ions attached to the oxygen atoms.

So, as a result of these washings, alumina exhibits cation and anion-exchange properties over fairly broad pH ranges.

However, it is possible to define a pH where the net charge on the surface is zero i.e. the zero point charge (ZPC). Generally, at pH values below the ZPC, alumina can be used as an anion-exchanger where the net charge on the column is positive, and at pH values higher than ZPC, alumina exhibits cation-exchange properties where the net charge is negative. The ZPC of alumina depends on the nature of the buffer ions used; for example, in the presence of acetate ions the ZPC = 6.5, for citrate ions it is 3.5, for borate ions it is 8.3, for

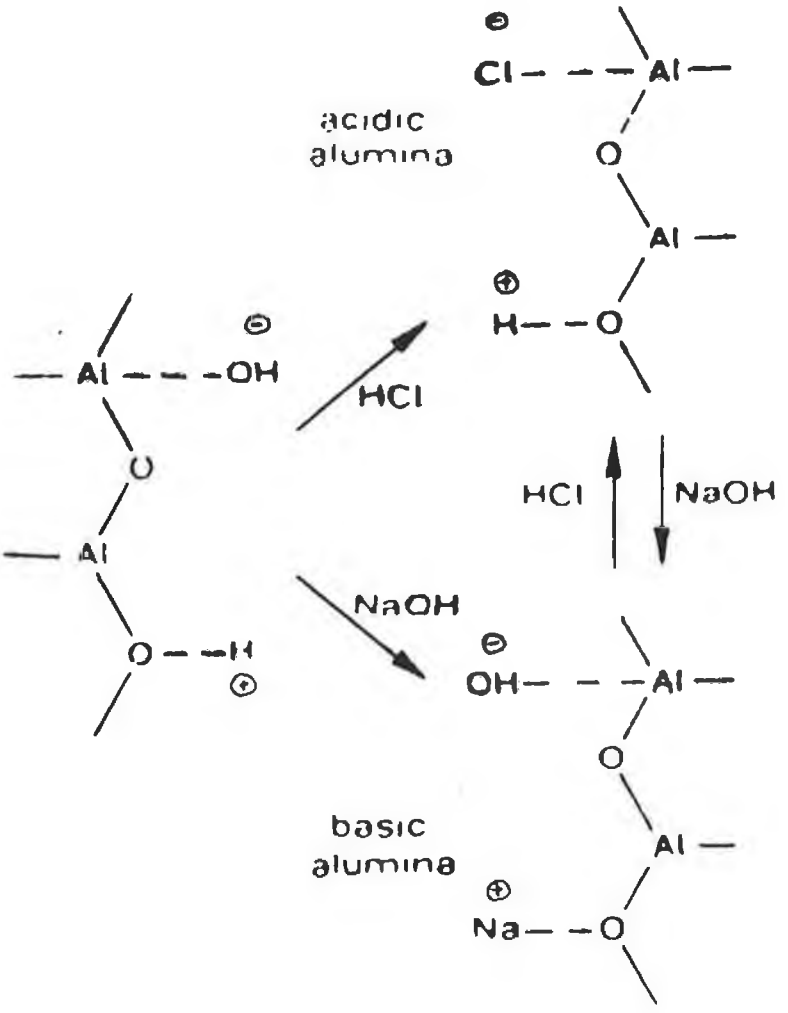

Figure 3.1. Surface behaviour of alumina in basic and acidic media.

carbonate ions it is 9.2 and for phosphate ions it is 6.5 [21]. So, selectivity using the alumina column can be manipulated by judicious choice of the pH of the mobile phase.

3.2.2. Applications of alumina stationary phase

Most of the literature on alumina has concentrated on the separation of basic compounds. For instance, Lingeman et al. [21] investigated both alumina and silica for the separation of some basic solutes, especially quaternary ammonium compounds. This study also involved the investigation of the retention behaviour of amines and quaternary ammonium ions as a function of the type and concentration of organic modifier, pH and type and concentration of the competing ion and buffer components in the mobile phase.

The separation of proteins is one of the most challenging areas in liquid chromatography and has received a lot of attention in the literature over recent years. Various new materials have been developed over the decade, mostly directed towards ion-exchange and size exclusion chromatography. However, in this context, alumina presents an attractive alternative, as both mechanisms can be combined. In the separation of proteins, the concept of ZPC has a close parallel in the definition of the isoelectric point (pI) of a protein, where the net charge of the protein is zero. So for pH > pI, the net charge of the protein is negative,and for pH <

pI, the charge on the protein is positive. Therefore the relative values of the ZPC of alumina and the pI of the protein are important for ion-exchange separation using the alumina column. Laurent et al. [22] used this stationary phase for the separation of some standard proteins, such as bovine serum albumin, ovalbumin, myoglobin, trypsinogen, lysozyme and chymotrypsinogen at pH 9 (phosphate buffer).

3.3. EXPERIMENTAL

3.3.1. Materials

Cisplatin was obtained from Sigma; samples of the formulated drug Neoplatin (containing saline, mannitol and cisplatin) were obtained as a gift from University College Dublin (Pharmacology Department), having previously been donated by the Bristol Myers Company. All solutions were prepared in water obtained by passing distilled water through a Milli-Q water purification system. Solutions prepared in saline were prepared in 0.15 M NaCl.

The mobile phase composition used throughout the study involving the C_{18} column was 10 mM sodium acetate, pH 4.6, which was 5 mM in octanesulphonic acid. The mobile phase was first degassed using an ultrasonic bath and finally deoxygenated with helium for 20 min.

The mobile phase composition used for separation involving alumina was in the main 0.05 M phosphate buffer, prepared using disodium hydrogen phosphate and dihydrogen sodium phosphate, and adjusting the pH accordingly. Methanol, acetonitrile and tetraethylammonium bromide (TEABr) were all of analytical grade. All mobile phases were filtered initially and degassed for 20 min.

3.3.2. Apparatus

The system used for the detection of the cisplatin species at the mercury (Hg) electrode was a Princeton Applied Research Corporation (PARC) Model 174A polarographic analyser, interfaced with a PARC model 303A static mercury drop electrode (SMDE). A large drop was used routinely throughout this investigation. The cell was modified with a PARC Model 310 flow adapter for liquid chromatographic detection. The chromatographic system consisted of a Waters RR/066 solvent delivery system with a Waters U6K injection port in conjunction with a guard column containing Waters C_{18} Corasil (37.50 um) material and a Waters analytical column (15 cm x 3.9 cm) packed with a Nucleosil 10 C_{18} stationary phase. Chromatograms were recorded on a Philips PM 8251A chart recorder using a chart speed of 300 mm/hr. The mobile phase was continuously purged with helium to minimise the interference due to dissolved oxygen.

For separations on the alumina column, the chromatographic system consisted of an ACS Model 353 ternary solvent system with a Rheodyne 7125 injector (20 μl injection loop) in conjunction with a guard column containing alumina packing material obtained from Waters and a Techsphere 5 alumina (15 cm x 4.6 mm) analytical column. The UV detector was a Shimadzu SPD -6A UV spectrophotometric detector connected to

a Philps PM 8252 dual pen recorder. Chromatograms were recorded using a chart speed of 300 mm/hr. The wavelengths used to detect cisplatin were 205 or 220 nm depending on the transparency of the buffer.

3.3.3. Methods

For the HPLC investigations using the Hg detector, 1 mg/ml stock solutions of both formulated and non-formulated cisplatin were prepared by dissolving an appropriate amount of each drug in either 0.15 M NaCl or deionised water. In the alumina study, 1 mM stock solutions of cisplatin were prepared in both 0.15 M and deionised water. Blank solutions of both water and NaCl were injected during both studies. In the stability study of cisplatin using the alumina column, samples of cisplatin in both NaCl and water were injected every hour over a period of time.

3.4. HIGH PERFORMANCE LIQUID CHROMATOGRAPHY WITH ELECTROCHEMICAL DETECTION FOR THE DETERMINATION OF CISPLATIN AND ITS HYDROLYSIS PRODUCTS

3.4.1. Optimisation of mobile phase conditions

A large part of this study involved the optimisation of chromatographic conditions for the separation of cisplatin and possible products. Based on the work of Parsons and Leroy [12], the use of 10 mM sodium acetate, pH 4.6, containing heptanesulphonic acid as a modifier, had been suggested as the optimum mobile phase for the separation of cisplatin and its hydrolysis products. During the early studies, the use of similar mobile phases containing both pentanesulphonic acid and octanesulphonic acid as modifiers were investigated. The use of the latter gave slight improvement with respect to resolution and sensitivity of the chromatograms for chloride, cisplatin and possible hydrolysis products. If no modifiers were used in the mobile phase, chromatograms showed a single broad peak with a shoulder. Retention times were not affected by increasing the concentration of the ion-pair reagents investigated. It was found, however, that the concentration of octanesulphonic acid in the mobile phase had to be greater than 4 mM before cisplatin was resolved from any other species. Increasing the concentration of octanesulphonic acid in the mobile phase above this level had no effect upon the retention time of cisplatin. For all subsequent investigations, the mobile phase was made 5

mM in octanesuphonic acid. The optimum flow rate was found to be 1.0 ml/min. A typical chromatogram using the conditions outlined previously is shown in Figure 3.2. At lower flow rates, the resolution was decreased from that shown in Figure 3.2, whereas at higher flow rates, the peaks eluted close to the solvent front.

3.4.2. Optimisation of parameters affecting electrochemical detection at a mercury electrode

This part of the study involved investigation of the use of three different current sampling schemes, i.e. sampled DC, normal pulse and differential pulse modes which were applied from a constant potential applied to the HMDE. Sampled DC detection involves consideration of the applied potential only. On setting the initial potential, the current is measured (sampled) for a short period of time at the end of the drop time set on the instrument. However, in normal pulse and differential pulse modes, two potentials are considered; that is, the initial applied potential and the potential reached on application of the pulse. With careful selection of these values, the half-wave potentials of the reaction of interest can be positioned between the two potential settings. In the normal pulse mode, the current is measured at the end of the

pulse, whilst in the differential pulse mode, the current is measured before and at the end of the applied pulse, and it is the difference in the current that is recorded. Compared to sampled DC and normal pulse, the differential pulse mode offers an improvement in selectivity and lower limits of detection, and was thus used throughout these studies.

As can be seen from Figure 3.2., depending on the concentration of cisplatin solution injected, a maximum of three peaks (with a shoulder on the third) were detected. In order to identify these peaks, the following approach was taken. When chloride ions were injected solely onto the column, the first peak at t_R= 3.0 min was the only one detected (peak 1). When a solution of cisplatin in water was prepared and immediately injected onto the column, only peak 3 (i.e at t_R= 4.0 min) was detected. The second peak at t_R= 3.6 min and the shoulder on the third peak appeared at high concentrations of cisplatin (>100 μg/ml),and also in solutions that had been left to stand for a few days. Hence, it would appear that these are both due to the formation of hydrolysis products, in accordance with the findings of Parsons and Leroy [12].

It was observed that at concentrations < 100 μg/ml, the chromatogram showed only two well defined peaks with retention times of 3.0 and 4.0 min, which have already been shown to be chloride and cisplatin respectively.

Chromatovoltammetric curves were then constructed in order to determine the optimum applied potential that would give the highest sensitivity for the determination of

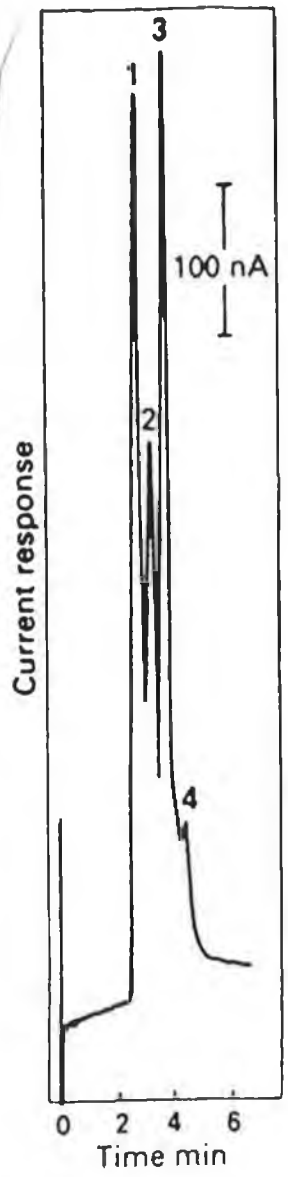

Figure 3.2. HPLC trace of an aged solution of 1 mg/ml of cisplatin, using an HMDE as detector;applied potential, +0.05 V vs Ag/AgCl.(1) sodium chloride; (2) hydrolysis product of cisplatin; (3) cisplatin; and (4) hydrolysis product of cisplatin.

cisplatin, in addition to chloride and hydrolysis products. These curves were constructed by plotting the current for each peak as a function of the initial applied potential in the range 0.00 V to + 0.20 V (versus Ag/AgCl). These applied potentials were increased in a step-wise manner (20 mV) over a series of injections. The resulting chromatovoltammetric curves are shown in Figure 3.3., from which the optimum potential for detection of the platinum species at the mercury electrode can be seen to be + 0.05 V (versus Ag/AgCl).

Using an applied potential of + 0.05 V, linear calibration graphs were obtained for the three peaks. Linear regression analysis of the data obtained for the the cisplatin peak shows that the current was related to the concentration by the equation: $I = 0.470C + 0.084$ ($r = 0.99$). The limit of detection of cisplatin at the Hg working electrode, based on a signal to nose ratio of 3:1, was found to be approximately 5 µg/ml.

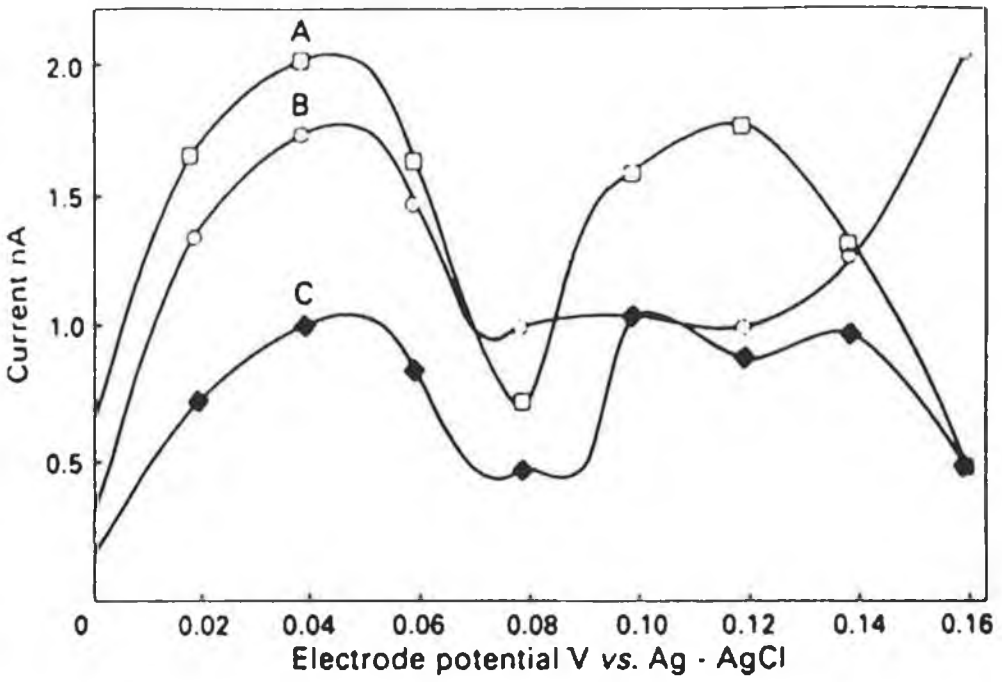

Figure 3.3. Chromatovoltammetric curve obtained for an aged solution of 1 mg/ml of cisplatin at an HMDE; potential range, 0.00 to +0.16 V vs Ag/AgCl. (A) cisplatin; (B) sodium chloride; and (C) hydrolysis product of cisplatin.

3.5. THE APPLICATION OF A NON-MODIFIED POLAR STATIONARY PHASE (ALUMINA) IN COMBINATION WITH AQUEOUS SOLVENT MIXTURES FOR THE SEPARATION OF CISPLATIN AND ITS HYDROLYSIS PRODUCTS

In this investigation, the retention behaviour of cisplatin and its hydrolysis products (Chapter One, Figure 1.2) were studied as a function of pH and concentration of buffer components in mobile phase, type and concentration of organic modifier and also concentration of competing -ion, tetraethyammonium bromide (TEABr). On optimisation of chromatographic conditions, the alumina stationary phase was applied to monitor the stability of cisplatin prepared both in water and saline.

3.5.1. Effect of concentration of buffer in mobile phase

Aluminium oxide shows anion-exchange properties at pH values below the zero point charge (ZPC) and cation-exchange behaviour above this pH value. Hence for the analysis of positively charged compounds, the pH of the mobile phase should be higher than the ZPC. A phosphate buffer was chosen in this study to allow investigations over a wide pH range. The ZPC of alumina using phosphate is 6.5 [21].

The ion-exchange capacity of alumina in respect of cisplatin and its hydrolysis products was initially monitored using a series of eluents of different concentrations of

sodium dihydrogen phosphate in the range 0.01 - 0.1 M. During the separation of cisplatin using the alumina column, four major peaks were observed as shown in Figure 3.5. The effect of varying the concentration of the buffer on these 4 peaks is shown in Figure 3.6. These peaks have been identified as 1) Cl^-, 2) cisplatin and the hydrolysis products A and B. Over the concentration range studied, there was little change in the retention of the parent drug, whilst there is a small decrease in the retention of Cl^-. A decrease in the concentration of buffer gave rise to a large increase in retention times for both hydrolysis products. However, using a buffer concentration of 0.1 M did not resolve peaks A and B successfully, and a mobile phase of 0.01 M phosphate buffer revealed tailing of peak B. It was decided to use a concentration of 0.05 M phosphate buffer for the separation of cisplatin and its hydrolysis products in subsequent studies.

3.5.2. Effect of pH

In aqueous solutions, cisplatin undergoes slow hydrolysis. Chloride is removed from the coordination sphere of the Pt(II) ion and replaced by a water or hydroxide ion. So, at neutral pH's, several hydrolysis products may be present in solution (Figure 1.2.). A study of the retention behaviour of cisplatin and its hydrolysis products over a pH range between 4.5 and 11.0 was carried out, using a mobile phase of 0.05 M

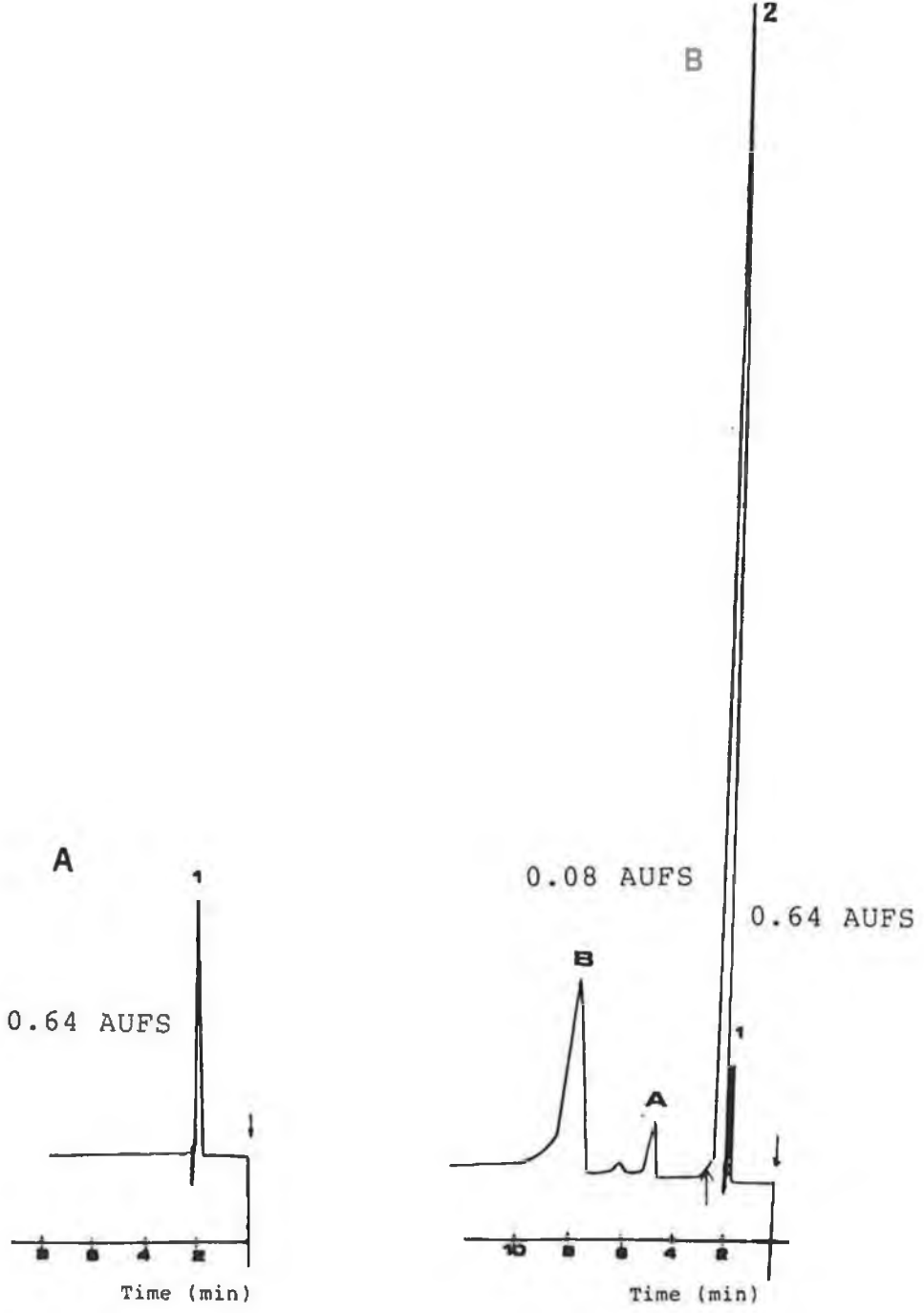

Figure 3.5. Typical chromatograms of (a) 0.15 M NaCl (b) 1 mM cisplatin in water. Stationary phase, alumina column. Mobile phase, phosphate buffer, 0.05 M, pH 5.5. Flow rate 1 ml/min. UV detection using 205 nm. (1) Cl^-, (2) cisplatin, and hydrolysis products A and B of cisplatin.

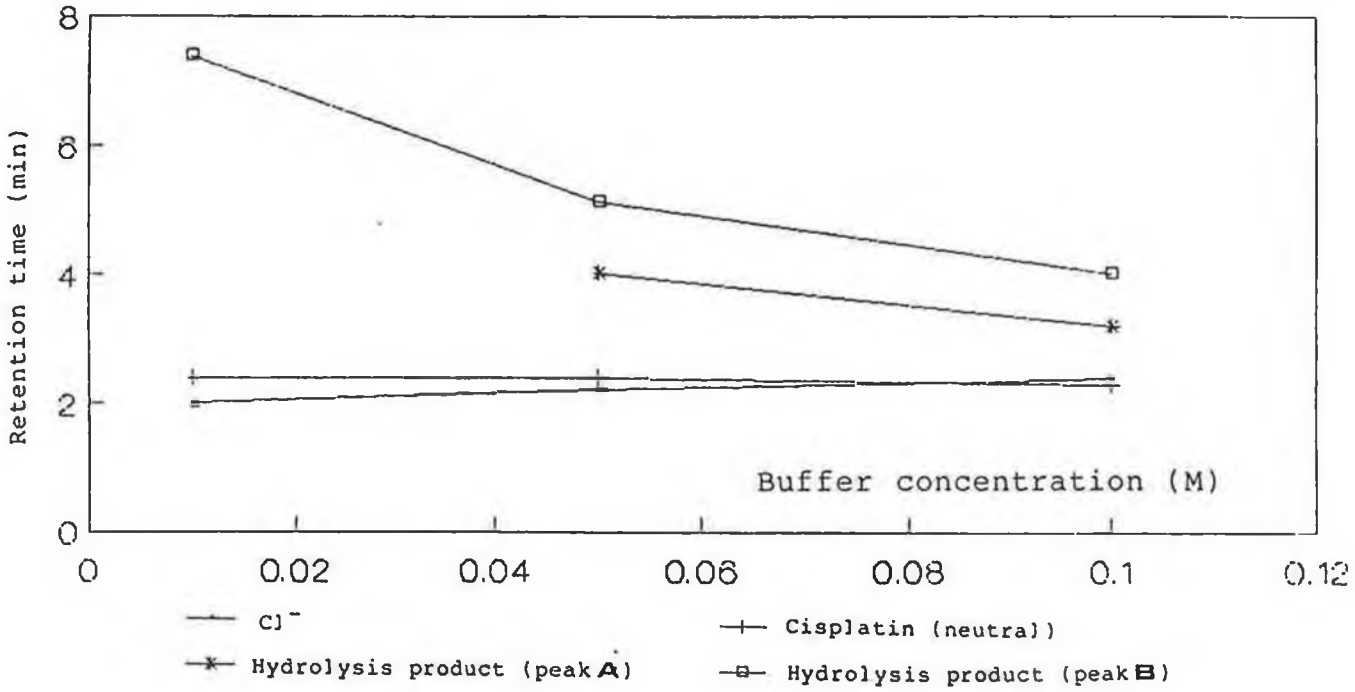

Figure 3.6. Effect of buffer concentration on the retention of cisplatin, hydrolysis products and Cl^- ions. Mobile phase, sodium dihydrogen phosphate at various concentrations. Flow rate 1 ml/min.

phosphate buffer. The behaviour of the four species over this pH range is shown in Figure 3.7.

The retention behaviour of peaks 1 and 2, i.e. chloride and cisplatin, are virtually unaffected by the change in pH. The fact that the neutral molecule and anions are hardly retained, is in agreement with the assumption that the most important interactions on the aluminium oxide surface are electrostatic in nature [21]. This observation also indicates that the interaction between the active sites on the alumina surface and the neutral cisplatin molecule are minimal compared to the interactions previously reported on strong anion/cation-exchangers that have chemically bonded [4,5] or have solvent generated ion exchange properties [6-9]. The neutral drug in fact elutes close to the solvent front (Figure 3.5.) with a retention time of 2.4 min. Therefore, the non-modified alumina stationary phase in conjunction with aqueous mobile phases, does not lend itself as a successful model for the separation of cisplatin, especially in biological matrices, as most of the endogenous (and therefore potentially interfering) components of such matrices, also tend to elute with similar retention times to that of the neutral drug.

On the other hand, Figure 3.7. does indicate that the retention of the possible hydrolysis products i.e peaks A and B, are affected by changes in pH. Peak B was always the predominant species of the two over the pH range studied. Figure 3.7. shows an increase in retention of peak B on increasing the pH from 4.5 to 6.5. Above this pH, however, a

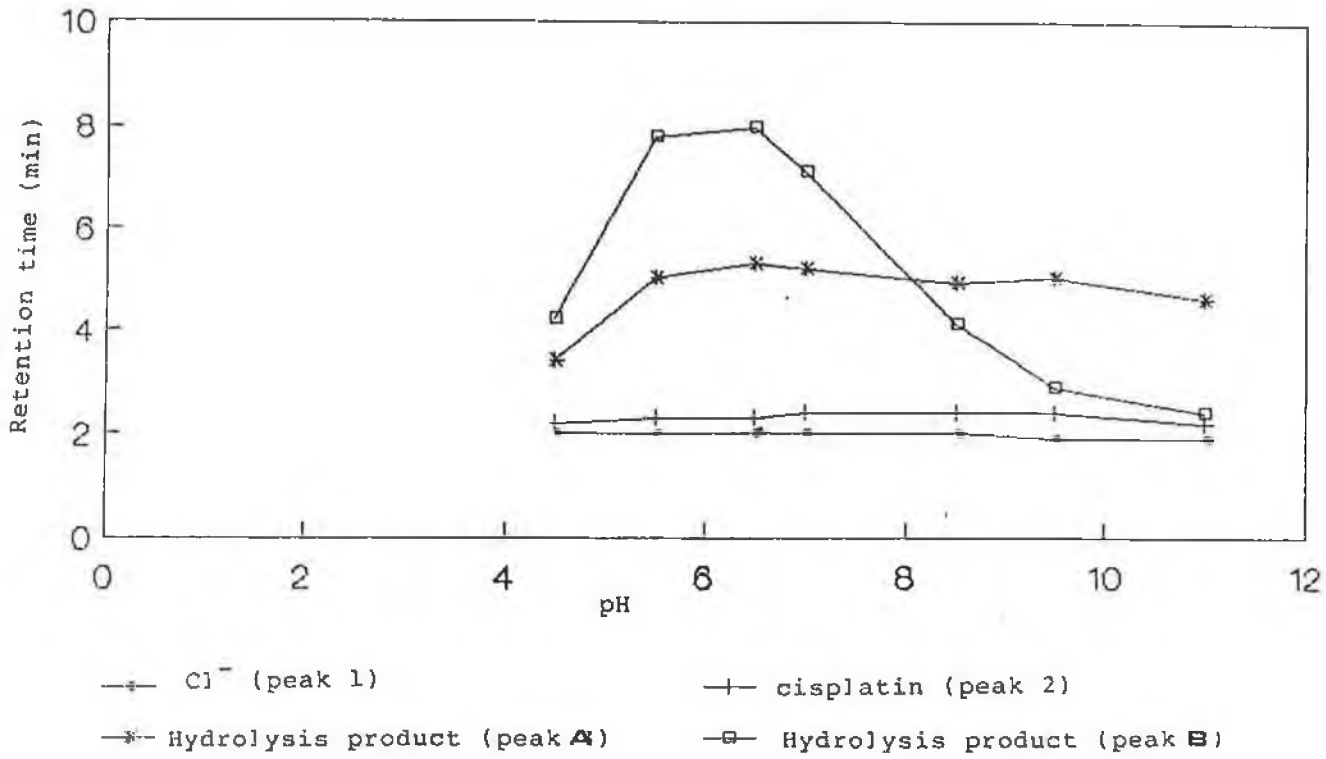

Figure 3.7. Effect of pH on the retention of cisplatin, hydrolysis products A and B and Cl^- ions. Mobile phase, 0.05 M phosphate buffer; Flow rate 1 ml/min.

decrease in retention of this species on the alumina was found. Similar behaviour in retention was also observed for peak A, although the decrease in retention was not as dramatic as that noted for peak B. This decrease in retention at high pH's for both hydrolyis products, can perhaps be attributed to the reduced degree of protonation of these species at high pH values.

At pH's lower than the ZPC, i.e 6.5, there was a decrease in retention time for the hydrolysis products. This behaviour is perhaps to be expected since the column is positively charged at pH values below the ZPC. Hence, due to electrostatic repulsion, these cationic species would be expected to elute quickly.

At pH values between 5 and 6.5, a maximum retention of the two positively charged species was observed. This behaviour would tend to suggest that the distinct regions of anionic-and cationic-exchange behaviour of the alumina column as reported in the literature, may not be as clear-cut as previously thought. These results would suggest that there is an overlap of these areas of ionic character. Using a mobile phase of pH values between 5 and 6.5 seems to give rise to a column whose ionic behaviour is neither strongly anionic or completely neutral in character, compared to the nature of the column using mobile phases of low pH. Therefore, based on this supposition, one can perhaps tentatively try to identify the hydrolysis species. The species that has the shorter retention time, i.e peak A, may perhaps be the doubly positively charged

species, eluting earlier than the singly charged species (peak B), due to electrostatic repulsion between the doubly charged species and the moderately positively charged column at pH values between pH values of 5 and 6.5. Also peak B is always larger in magnitude than peak A, which also suggests that peak B is indeed the positively charged mono-aquo hydrolysis product, and this behaviour is in agreement with the literature that has shown that the mono-aquo species is the predominant hydrolysis product of cisplatin (Chapter One, Section 1.2.1.). Due to the high quality of chromatographic separation and resolution of the hydrolysis species, a mobile phase of 0.05 M phosphate buffer, pH 5.5, was chosen to separate cisplatin and its hydrolysis products.

3.5.3. EFFECT OF ORGANIC MODIFIER

The effect of organic modifiers such as methanol and acetonitrile on the retention and selectivity of the separation of cisplatin and its hydrolysis products is shown in Figures 3.8. a and b. As already noted in section 3.5.2. in the absence of any organic modifier, the system had adequate selectivity to permit the separation of the hydrolysis products; however, it did not successfully permit the separation of the neutral drug. Clearly, the addition of either methanol or acetonitrile does not affect the poor retention characteristics of cisplatin and the Cl^- ions. [At this stage of the experimental procedure,

aged solutions of cisplatin were being used, and this accounts for the third hydrolysis product noted in the chromatographic separation (peak C) and subsequently monitored throughout the following procedures]. Increases in methanol concentrations led to a slow increase in retention for peak B and sharper increase in retention for peaks A and C. The use of acetonitrile revealed slower increases in retention for peaks A and C, whilst there was again longer elution of peak A with increasing acetonitrile concentrations. However, methanol concentrations of >40% resulted in poor resolution of peaks A and C, and with the use of acetonitrile, inadequate base-line resolution of all three degradation products resulted.

Clearly, in the alumina system, the addition of organic modifiers such as methanol and acetonitrile does not improve resolution of the different hydrolysis products; and in fact, it results in poorer chromatography compared to the separation and resolution that can be achieved with water-rich eluents. In general, the shape and base-line resolution of the chromatographic peaks was not better when organic/aqueous solvent mixtures were used as eluents, and analysis time was also dramatically increased.

3.5.4. Effect of competing-ion

The influence of different concentrations of the competing ion, tetraethylammonium bromide (TEABr), was then

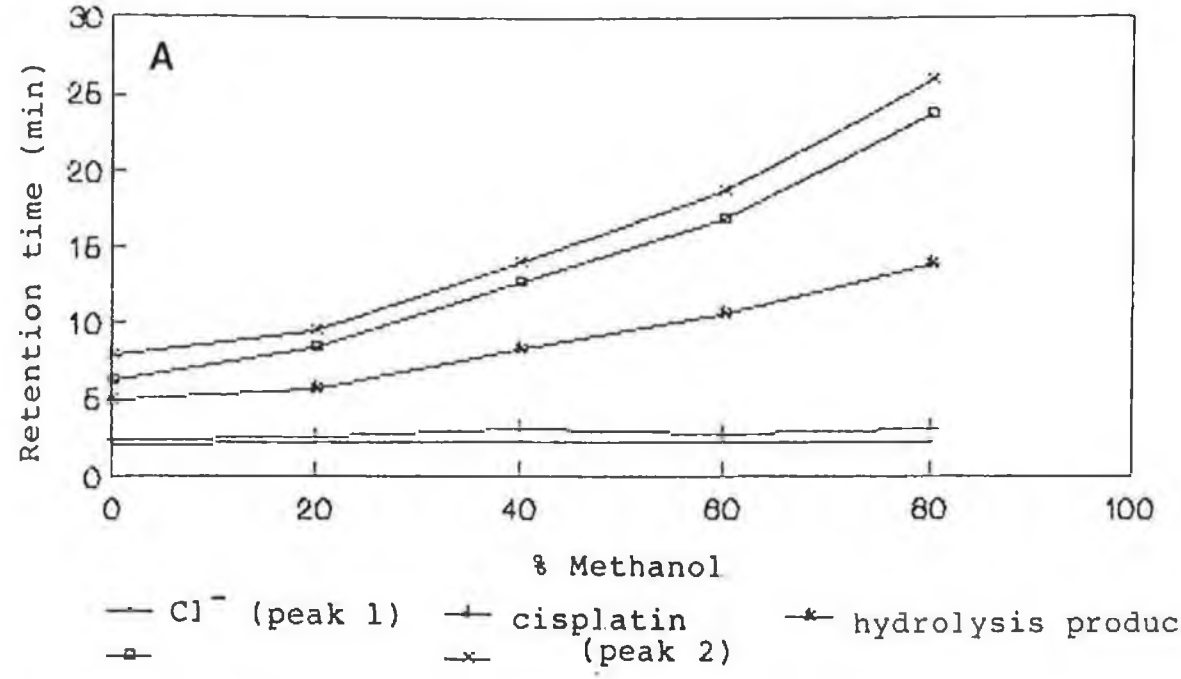

Figure 3.8a. Effect of methanol on addition to aqueous mobile phase on retention behaviour of cisplatin, hydrolysis products, and Cl^- ions. Mobile phase, phosphate buffer, 0.05 M, pH 5.5; Flow rate 1 ml/min.

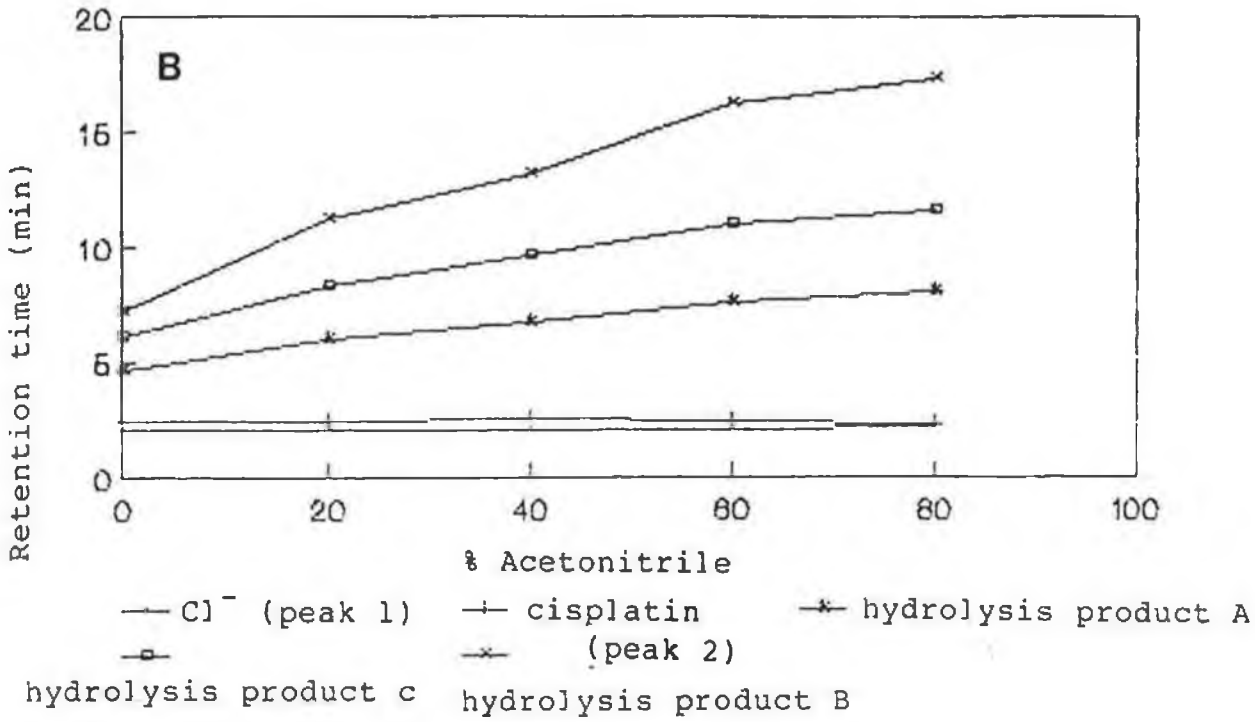

Figure 3.8b. Effect of acetonitrile on addition to aqueous mobile phase on the retention behaviour of cisplatin, hydrolysis products, and Cl^- ions.
Mobile phase, phosphate buffer, 0.05 M pH 5.5; Flow rate 1 ml/min.

studied, in order to see if this would affect (primarily) the retention of the neutral drug.

However, increasing the concentration of TEABr had no influence on the retardation of either Cl^- or the neutral compound (Figure 3.9.). On the other hand, the increased concentration of this long chained competing-ion did influence the retention behaviour of the three hydrolysis products. The solute cations compete with TEA^+ ions in the eluent for the active sites on the alumina surface. It would appear that the smaller solute ions are displaced by the larger TEA^+ ions, resulting in a slight decrease in retention times for the three hydrolysis products. The use of TEABr required a change of wavelength from 205 nm to 220 nm to monitor the products (due to decreased transparency of the mobile phase on the addition of TEABr). The overall chromatographic shape of these species, in particular peak C, was poorer compared to the chromatography obtained using a purely aqueous mobile phase.

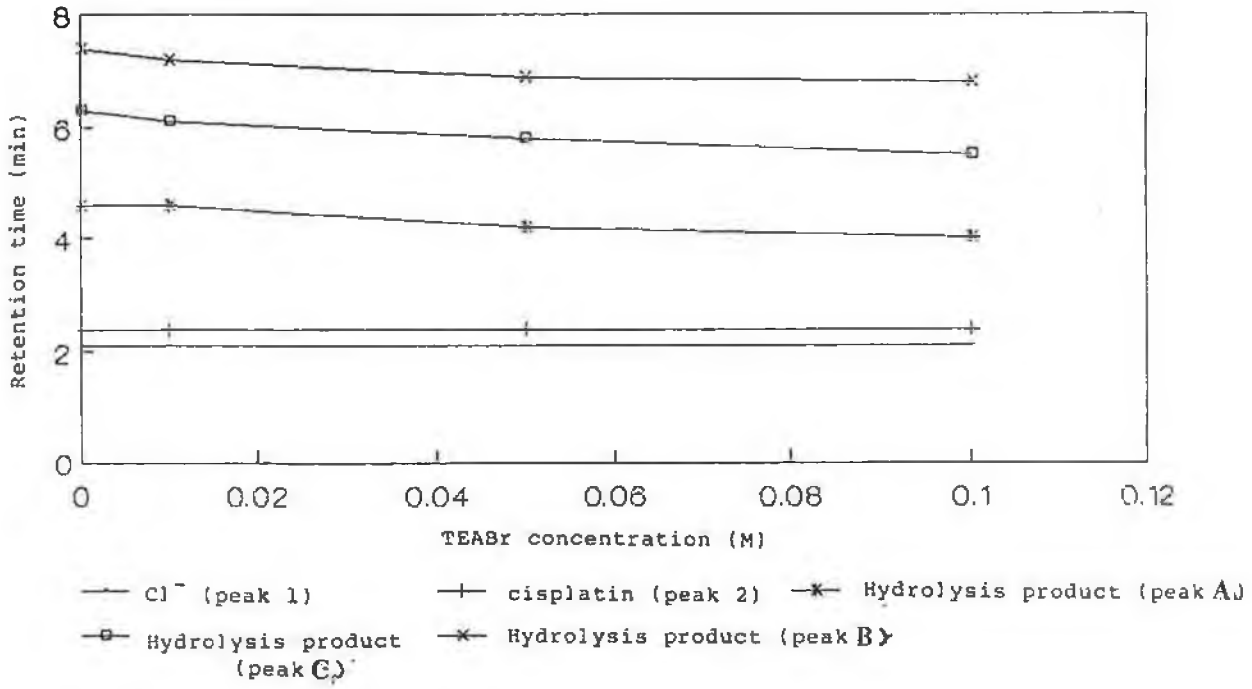

Figure 3.9. Effect of concentration of the competing-ion TEABr on addition to mobile phase of 0.05 M phosphate buffer, pH 5.5.

3.5.5. CONCLUSION

The following points may be drawn from the chromatographic separation of cisplatin and its degradation products, using the non-modified alumina column as the stationary phase.

(i) Alumina is an amphoteric ion-exchanger which acts as a cation-exchanger in basic eluents and as a anionic-exchanger in acidic pH.

(ii) However, the transition from one mechanism to the other seems to be gradual, and not as clear-cut as perhaps suggested in the literature.

(iii) The pH of the eluent should be chosen in such a way that the solute ions are fully protonated, and so that the alumina surface possesses ion-exchange capacity.

(iv) At neutral pH's and below, cisplatin becomes hydrolysed to form positively charged degradation products.

(v) Neutral molecules and anions are hardly retained on this system hence, cisplatin (neutral) and Cl^- ions (from hydrolysis and NaCl) were not retained. This behaviour is in agreement with the assumption that the principal interactions on the alumina surface are electrostatic in nature [22].

(vi) The above observation also indicates that the interactions between the active sites on the alumina surface and neutral cisplatin are ineffective, compared to the

interactions reported using strong cation/anion exchange columns that are chemically bonded or solvent generated ion-exchange columns, where the drug is retained via ion-dipole interactions of the drug and surface quaternary ammonium groups [4-9].

(vii) At pH's > 7 (where the column behaves as a cationic exchanger), the hydrolysis products are not fully protonated, and this may explain the decreases in retention of the products at high pH's.

(viii At pH's < 5, a decrease in retention of the products was observed, due to the electrostatic repulsion between these positively charged species and the positively charged sites on the column.

(ix) In addition to pH, the concentration of a hydrophobic long chained competing-ion (TEABr) and the influence of the addition of organic modifiers (methanol and acetonitrile) were examined. The competing-ion and the organic modifiers did influence the retention behavior of the cationic products on this system, but had little or no influence on the resolution of these species. In general, the chromatography was not enhanced on the addition of any of the above components.

(x) An aqueous eluent of phosphate buffer 0.05 M, pH 5.5, successfully and selectively separated the major hydrolysis products of the antineoplastic agent cisplatin. The separation being superior to that reported by Hincal et al. [5].

The above system was then applied to monitor the stability of the drug in both aqueous and saline solutions.

3.5.6. The application of a non-modified stationary phase with aqueous mobile phases to monitor the degradation of cisplatin to cationic species in both aqueous and saline solutions.

The alumina stationary phase, using an aqueous mobile phase, proved to be a useful method in monitoring the disappearance of cisplatin from aqueous solutions. In this system, the chromatography is unambigious and one can isolate Cl^- ions and cisplatin (neutral), if not quite from the solvent front, from the decomposition products. Typical chromatograms are shown in Figures 3.10. a and b, and 3.11.a and b, for 1 mM solutions of cisplatin dissolved in both water and saline. Peaks 1 and 2 are the Cl^- ion and the neutral drug respectively, whilst peaks A and B are the major hydrolysis products, and peak C an unidentified hydrolysis product.

The fate of the drug in both solutions can be seen graphically in Figures 3.12. and 3.13., where the decrease of the drug and increase of the hydrolysis products and Cl^- ion in terms of peak height is shown over a period of time. The larger increase in Cl^- noted in saline conditions is due to the initial large concentration of Cl^-. Initially, it can be seen that there is a larger degree of hydrolysis of cisplatin in water compared to the drug dissolved in saline; whilst hydrolysis products A and B increase in size under aqueous conditions compared to saline conditions. The peak height of peak C does not change over the experimental time scale.

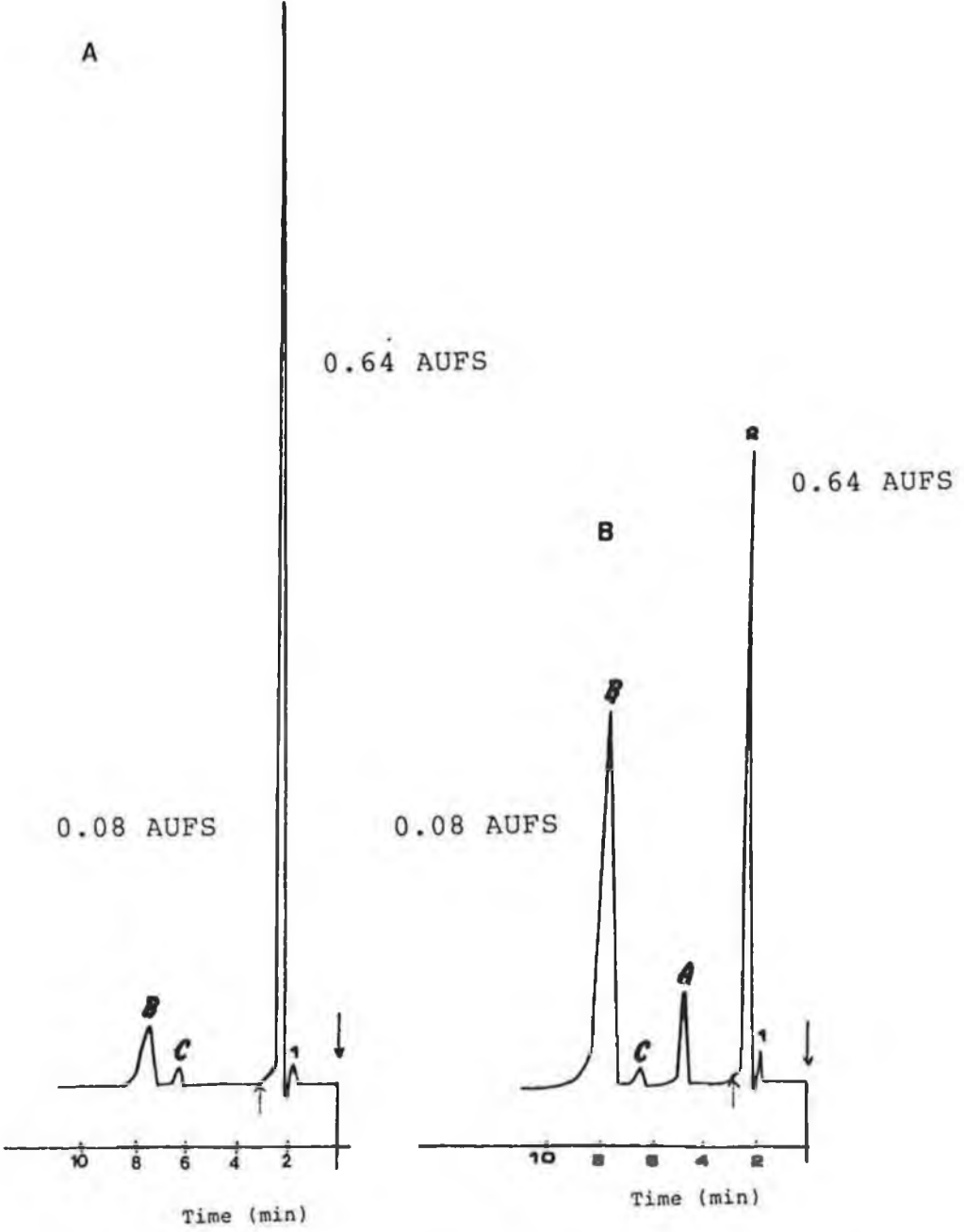

Figure 3.10. Typical chromatograms of 1 mM solution of cisplatin dissolved in water.

(a) cisplatin at time = 0

(b) cisplatin at time = 8 hours.

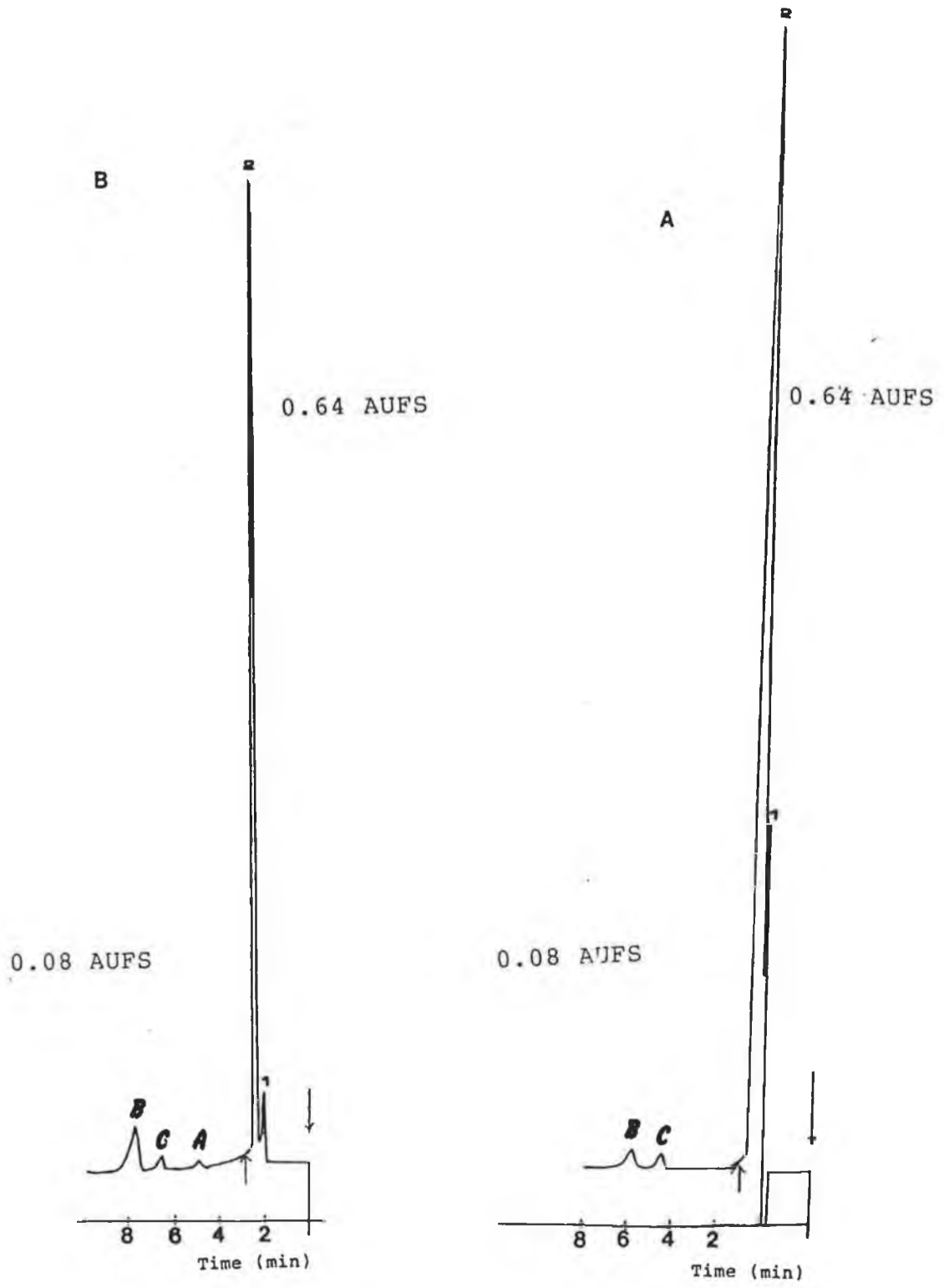

Figure 3.11. Typical chromatograms of 1 mM solution of cisplatin dissolved in saline (0.15 M NaCl).

(a) cisplatin at time = 0

(b) cisplatin at time = 8 hours.

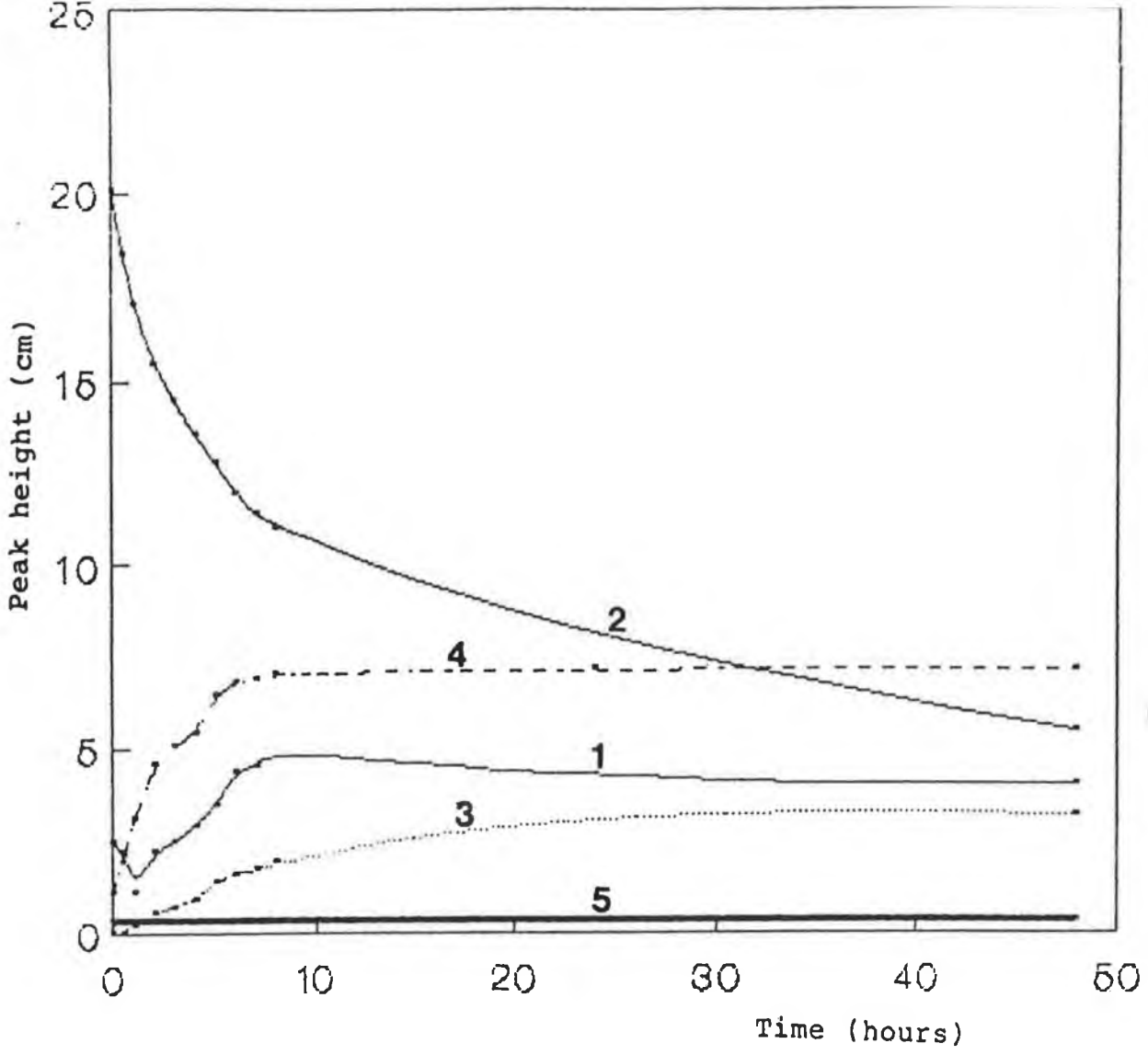

1) peak 1 (Cl^-), 2) peak 2 (cisplatin), 3) hydrolysis product A
4) hydrolysis product B, 5) hydrolysis product C

Figure 3.12. Fate of cisplatin, hydrolysis products, and Cl^- ions over a period of time when the drug was dissolved in water.

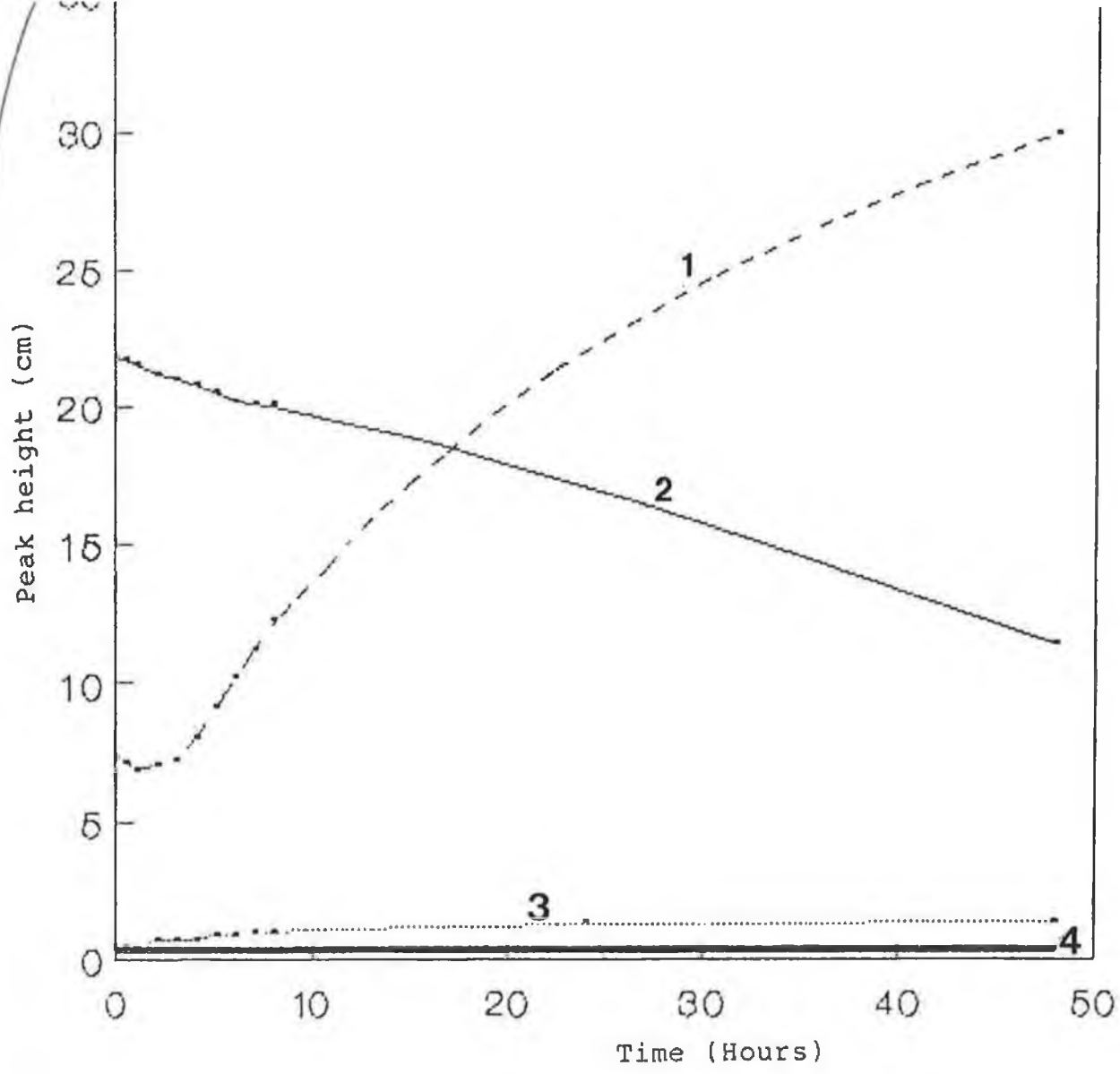

1) peak 1 (Cl^-), 2) peak 2 (cisplatin) 3) hydrolysis product B, 4) hydrolysis product C

Figure 3.13. Fate of cisplatin, hydrolysis products, and, Cl^- ions over a period of time, when the drug was dissolved in saline.

When the loss of cisplatin in water was monitored, it was observed that there was an initial rapid loss of the drug, and after 40 hours the system appeared to reach equilibrium, with a significant fraction of the drug still remaining intact. Figure 3.14, shows plots of percentage cisplatin remaining vs. time, for solutions of cisplatin prepared both in water and saline. For the hydrolysis of cisplatin in water it was observed that there is an initial rapid loss of the drug, i.e. 10% in a 1/2 hour and over 55% loss after 8 hours. Accompanying this disappearance of cisplatin was an increase in the height of peak B. This peak appeared on immediate injection of the drug, and increased linearly in height up to 2 hours after preparation. A second major peak (peak A) was noted 1 hour after preparation, and had previouly been identified as another hydrolysis product. A complete identification of these peaks results was made from comparison of the spectra of peak 2 (cisplatin) and peaks 3 and 4. The spectra of all 3 three peaks were almost similar,except that there is a shift in maximum absorption at 220 nm (cisplatin) to lower wavelengths for peaks A and B. The shift may be due to protonation of the cisplatin molecule; so these spectral patterns would suggest that peaks A and B are the protonated species of the parent molecule. These results, along with the interpretation of retention behaviour of these peaks (Section 3.5.2.) reinforces the identification that peak A is due to the doubly charged di-aquo species (III) and B is due to the singly charged mono-aquo species (II).

When the data in Figure 3.14. was plotted as the ln of

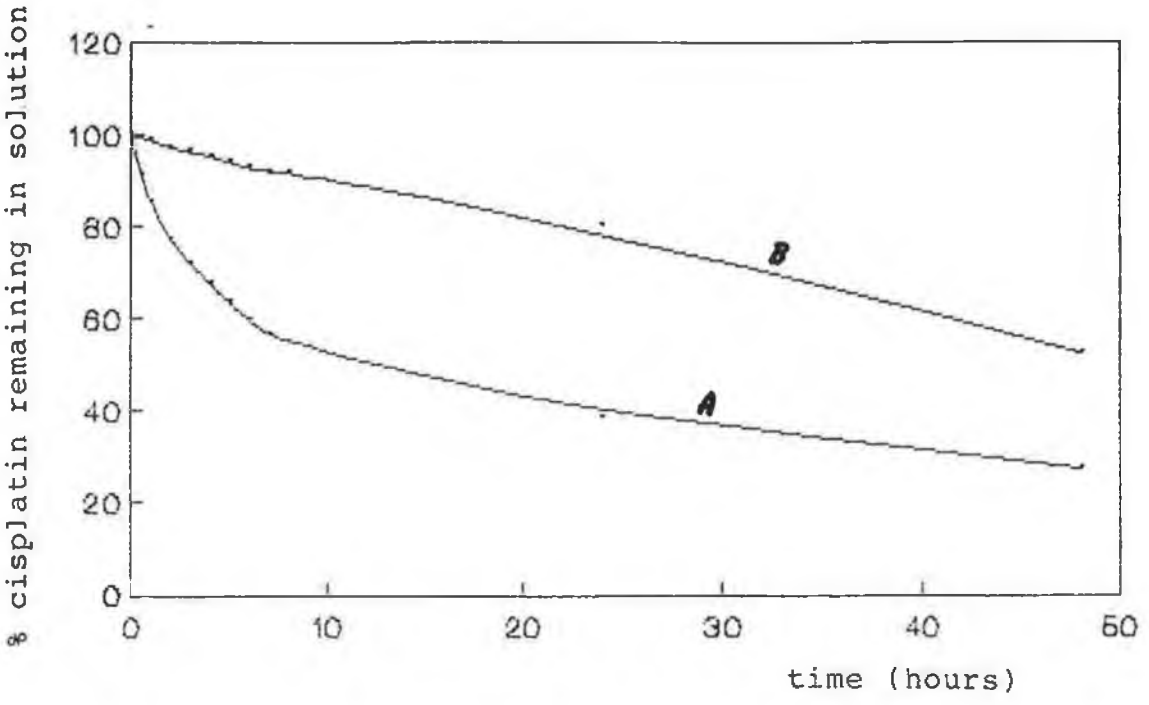

Figure 3.14. Plot of % cisplatin remaining in both aqueous (A) and saline (B) solutions as function of time, for an initial concentration of 1 mM cisplatin.

cisplatin remaining vs time, linearity was observed up to about 8 hours (Figure 3.15.), suggesting that the reaction was first order.

Most of the literature (Chapter One, Section 1.2.2) reports that the rate of loss of cisplatin follows the stepwise replacement of chloride, as shown below;

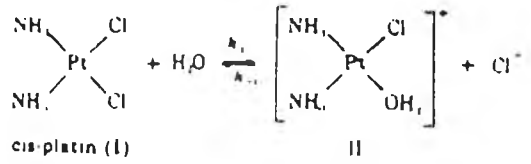

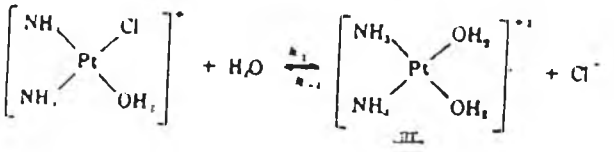

From the above equations, the addition of chloride to aqueous solutions of cisplatin would be expected to stabilise cisplatin by shifting the aquation equilibrium to the left. The experimental data is in agreement with this (see Figures 3.12 and 3.13.). There was a 10% loss of the drug after 8 hours in saline compared to the 10% loss after 1/2 hour when the drug was dissolved in water. The hydrolysis species do not increase to any significant extent in saline, and the peak at 4.8 min (peak A) is not observed at all over the experimental time scale.

However, the first aquation reaction suggests that the reaction

should not obey simple first order kinetics since the reverse reaction is a second order process. These processes are in agreement with the experimental data, as the rate of disappearance of (I) does not equal the rate of appearance of (II). From consideration of the second aquation reaction one showed that the disappearance of (II) leads to the appearance of (III), the di-aquo species (peak A) which is observed in the chromatograms. In this case, when cisplatin was dissolved in water, the reaction kinetics in first reaction are pushed to the right.

However, the equilibrium constant for the displacement of the second chloride ligand is small (K_2 = 1.1×10^{-4} M) relative to that for the displacement of the first chloride ligand (K_1 = 3.63×10^{-3} M) [23]. Therefore it has been assumed only the first aquation reaction as being significant in determining the rate loss of cisplatin. Therefore, the rate of loss of cisplatin at any time can be expressed as:

$$-d[I]/dt = k_1[I] - k_{-1}[II][Cl^-]$$

Assuming k_{-1} is negligible (as there are Cl^- ions present) Figure 3.15 gives a rate constant of 2.13×10^{-5} s^{-1}. This experimental result is a little lower than the values of Martin et al [24] of 2.5×10^{-5} s^{-1}, and 2.47×10^{-5} s^{-1} obtained by Hincal et al. [5]. The fact that this experiment was not carefully controlled with respect to temperature (i.e.

the HPLC system and solutions were not thermostated to 25°C as in [5]), and also there was a certain ambiguity in the location of t=0 (as at least 30 min were required to dissolve the drug completely), may account for the deviation from published results.

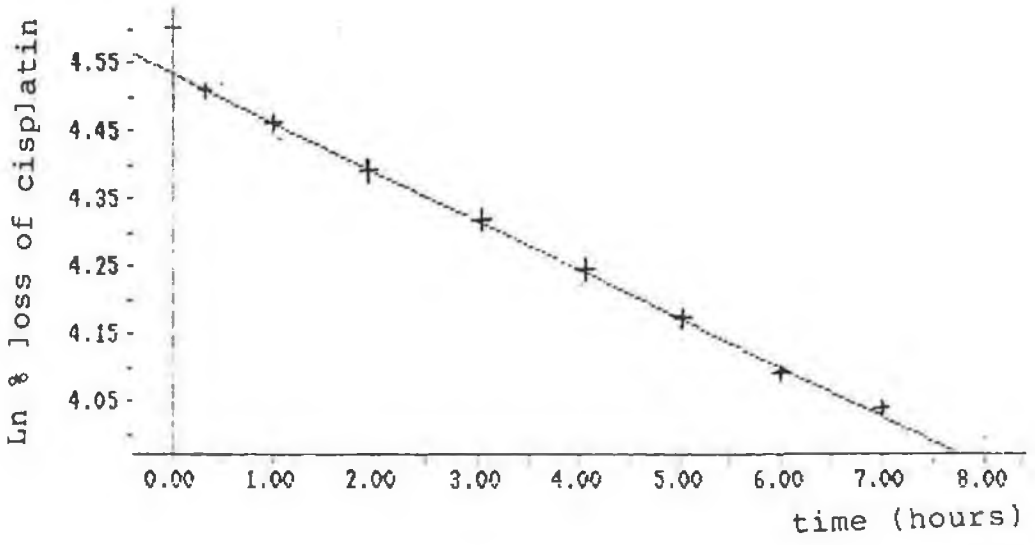

Figure 3.15. Ln plot for loss of cisplatin in water from the data presented in Figure 3.14.

3.6. REFERENCES

1. Bannister S.J., Sternson L.A., and Repta A.J., J. Chromatogr., 1979,173,333.
2. Borch R.F., Markovitz J.H.,and Pleasants M.E., Anal Letts., 1979,12(138),917.
3. Andrews P.A., Wung W.E., Howell S.B., Anal Biochem., 1984,143,46.
4. Chang Y., Sternson L.A.,and Repta A.J., Anal Letts., 1978,11,449.
5. Hincal A.A., Long D.F., and Repta A.J., J. Par. Drug Assoc., 1979,33,108.
6. Riley C.M., Sternson L.A., and Repta A.J., J. Chromatogr., 1981,217,405.
7. Riley C.M., Sternson L.A., and Repta A.J., J. Chromatogr., 1981,219,235.
8. Riley C.M., Sternson L.A., Repta A.J., and Siegler R.W., J Chromatogr.,1982,229,373.
9. Marsh K.C., Sternson L.A., and Repta A.J., Anal. Chem.,1984,56,491.
10. Bannister S.J., Sternson L.A., and Repta A.J., J. Chromatogr.,1983,273,301.
11. Kitz R., Hayakawa K., and Miyazaki M., Biomed. Chromatogr.,1989,3,pp.
12. Parsons P.J., and Leroy A.F., J. Chromatogr.,1986,378,395.
13. O'Dea P., Shearan P., Dunne S., and Smyth M.R., Analyst,1988,113,1791.

14. Daley-Yates P.T., and M^{C}Brien D.C.H., Biochem. Pharmacol., 1983,32,181.

15. Long D.F., Repta A.J., and Sternson L.A., Int. J. Pharm.,1980,6,167.

16. Parsons P.J., Morrison P.F., and Leroy A.F., J. Chromatogr., 1987,385,323.

17. Krull I.S., Ding X-D., Selavka C., and Hochberg F., J. Chromatogr. Sci.,1983,21, pp.

18. Ding X-D., and Krull I.S., J. Liq. Chromatogr.,1983,6(12), 2173.

19. Hussain A.A., Haddadin M., and Iga K., J. Pharm. Sci.,1980,60,364.

20. Laurent C.J.C.M., Billiet H.A.H., and de Galan L., Chromatographia,1983,17,253.

21. Lingeman H.A., Van Munster H.A., Beynen J.H., Underberg W.J.M., and Hulshoff A., J.Chromatogr.,1986,352,261.

22. Laurent C.J.C.M., Billiet H.A.H., de Galan L., Buylenhuys F.A., and Van der Marden F.P.B., J Chromatogr.,1984,287,45.

23. Long D.F., and Repta A.J., Biopharm. Drug Disposition,1981,2,1.

24. Martin D.S., and Reishus J.W., J. Am. Chem. Soc.,1961,83,2457.

CHAPTER FOUR

ELECTROANALYTICAL STUDIES OF BIOLOGICALLY IMPORTANT DISULPHIDE-CONTAINING MOLECULES, AND THEIR INTERACTIONS WITH CISPLATIN

4.1. INTRODUCTION

Despite the widespread clinical application of cisplatin, its behaviour in biological systems is not fully understood. As already outlined in Chapter One, the concentration of the intact drug appears to fall rapidly following intravenous infusion of the drug. This slow elimination has been attributed to redistribution and extensive protein binding. These biotransformation products have not been successfully isolated. However, there are some indications that reactions with divalent sulphur-containing species such as cystine, methionine, peptides and proteins containing these amino acid are taking place [1,2].

In aqueous media, the two labile Cl^- groups of cisplatin can dissociate and hydrolysis products can be formed (see Chapter One, Figure 1.2.). It is these species that are believed to be the reactive forms of cisplatin that produce covalent attachments to DNA (the target within the cell). Also, it is the hydrolysed forms of cisplatin that can react with the species outlined above. The protein-bound cisplatin appears to have little activity [3], whilst it has also been indicated that direct reaction of cisplatin with sulphur-containing components within the cell also results in non-cytotoxic products.

In order to more fully understand the nature of protein-drug binding, the use of AdSV has been investigated to study the interactions of cisplatin with human serum albumin (HSA) and with one of its constituent "building blocks", the amino acid cystine. Cystine (Figure 4.1.) plays an important role in the structure of some proteins (Figure 4.2.), and it also contains disulphide groups, which have been implicated in cisplatin binding [1,2]. As the electrochemical reduction of proteins has been attributed to a large extent to the reduction of disulphide groups, the significance of the AdSV behaviour becomes important in trying to establish both the electrochemical behaviour of proteins and amino acids, and drug- protein/amino acid binding, by the comparison of voltammograms from both types of disulphide-containing molecules.

The following sections take a look at some of the elctroanalytical techniques which have used to determine some proteins and amino acids containing disulphide links.

4.1.1. Electrochemical behaviour of proteins containing disulphide/thiol groups

In principle, simple disulphides give rise to cathodic waves at the dropping mercury electrode (DME), which are due to their reduction to the corresponding thiol:

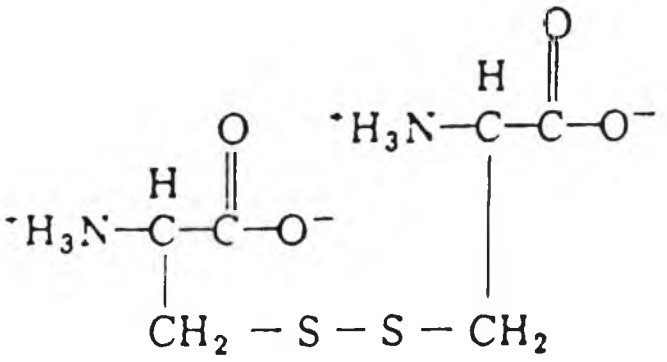

Figure 4.1. Structure of the amino acid, cystine, shown here in its zwitterionic form.

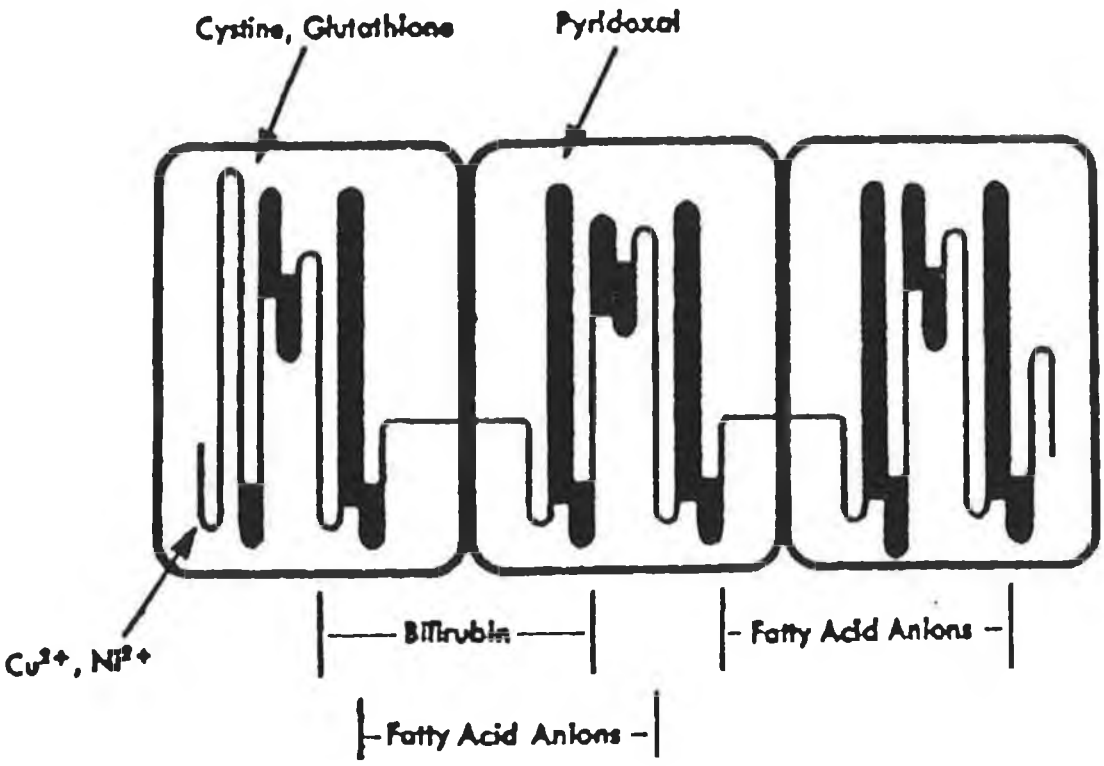

Figure 4.2. Conformation and binding sites of albumin.

$$R - S - S - R + 2e^- + 2H^+ \longrightarrow 2RSH$$

However, it has been noted that polarisation time and the type of electrode used may be responsible for the number of reducible disulphide groups in proteins. For example, when using the DME, it has been found that only 2 disulphide bridges of insulin are reduced at -0.60 V vs SCE [5], whereas in the investigation of albumin [4] only 4 out of the 17 bridges were found to be reduced. However, when the hanging mercury drop electrode (HMDE) was used, 3 disulphide bridges in insulin and 9 in albumin were reduced. A study which investigated the use of 8 M urea to denature albumin showed similar results [4], perhaps indicating that slow surface denaturation possibly occurs to some extent at the HMDE, whilst this doesn't appear to happen at the DME.

Bovine serum albumin (BSA) and human serum albumin (HSA) are proteins in the form of a single polypeptide chain of molecular mass 69,000. BSA is crosslinked by 17 disulphide bonds [4]. The molecule also contains one free sulfhydryl group.

The reduction of the disulphide links in HSA by β mercaptoethylamine hydrochloride was examined by Markus and Kharush [6]. This study looked at the reduction in the presence and absence of sodium dodecyl sulphate (SDS), which acts as a denaturing agent. SDS causes the unfolding of the protein molecule, so that all the disulphide bonds become accessible to reduction, whereas only one bond was reduced when

the experiment was carried out in the absence of SDS. Kolthoff and co-workers [7] used a rotating mercury pool electrode to carry out amperometic titrations of the -S-S- groups of both native and BSA denatured with silver nitrate in the presence of sulphite. Leach et al.[8] noted that BSA was not electrochemically reducible directly at a mercury pool in the pH range 2.9 - 9.0 at potentials of between -1.2 and -2.0 V vs SCE; but when β-mercaptoethanol was used, 15 -S-S- bonds were reduced when the potential was held at -1.2 V vs SCE. Behr et al. [9] found that the adsorption of BSA onto the HMDE blocked the reduction of cadmium ions at low pH's but not at pH 7.0, which they ascribed to a change in the charge of BSA with increased pH.

Polarographic studies were carried out looking at the reduction of the disulphide bonds of insulin, ribonuclease chymotrypsin, trypsin, haemoglobin and BSA, by Weitzman and Cecil [10] using the DME. These disulphide containing proteins all gave rise to a single cathodic wave at pH 1.0 which was shown to involve the reduction of some of the groups, whilst at pH 7.1 and 9.2, a second cathodic wave was observed for some of the proteins. This second wave appeared after the first wave had reached its limiting value, and was also shown to involve the reducton of -S-S- groups. AC polarography has been used to study the reduction processes of disulphide bonds and free Zn(II) in several types of insulin preparations [11].

Stankovich and Bard [4] examined the electroreduction of bovine serum albumin (BSA) in solutions of

pH 7.4 at the hanging mercury drop electrode by double potential step chronocoulometry as well as by cyclic voltametry at a mercury pool electrode by controlled potential coulometry. They proposed a mechanism involving the reduction of an adsorbed monolayer of BSA in which at short time periods, 3 or 4 disulphide bonds were reduced. When the product remains adsorbed for large time periods, all the disulphide bonds (17) are reduced resulting in an insoluble product which cannot be re-oxidised.

4.1.2. Electroanalysis of proteins containing disulphide/ thiol groups

The early 1980's saw an increase in the use of electroanalytical techniques to determine trace levels of serum proteins and albumin. For instance, Hertl developed a differential pulse polarographic assay for serum protein [12]. He found that both human serum and HSA showed a differential pulse polarographic wave at -0.60 V. When solutions were sufficiently dilute, i.e. < 7.0 μg/ml at neutral pH's, the polarographic response was linearly related to solution concentrations, whereas at high pH values, (pH 12.6) a near-linear response to 70 μg/ml was obtained (at the expense of slow sample equilibration time). Forsman [13] has investigated the use of stripping voltammetry for the determination of some well known disulphide-containing proteins and peptides such as

insulin, ribonuclease, oxytocin etc. His study showed that for most of the proteins (except insulin), stripping voltammetry in the presence of excess copper(II) resulted in detection limits of $2x10^{-9}$ M.

More recently, Smyth and co-workers [14,15] were able to utilise adsorptive stripping voltammetry to study the behaviour of HSA and BSA. The adsorptive stripping voltammetric behaviour of both proteins were optimised with respect to accumulation potential, accumulation time and scan rate, giving limits of detection of $2.9x10^{-8}$ M (HSA) and $2x10^{-9}$ to $1.5x10^{-8}$ M (BSA). Trace measurements of trypsin and chymotrypsin using the same techniques were carried out by Wang and co-workers [16]. The adsorbed proteins yielded well defined waves at -0.30 V vs Ag/AgCl giving rise to limits of detection of $3x10^{-7}$ M.

A new analytical method, based on the adsorptive preconcentration of biomacromolecules on an electrode, the transfer of the adsorbed layer into a new medium (containing background electrolyte), and subsequent voltammmetric analysis has recently been proposed by Palecek and Postbieglova [17] for the analysis of some proteins, lipids and polysaccharides. This technique made it possible to carry out the voltammetric analysis of large biomolecules adsorbed from media not suitable for conventional voltammetric analysis.

Since it has been widely assumed that the

electrochemical behaviour of these proteins is due to the presence of disulphide/thiol moieties, many workers have studied the amino acids cystine and cysteine (both containing sulphur groups).

Stankovich and Bard [18] studied the electroreduction of cystine and the oxidation of cysteine with respect to pH at the HMDE by cyclic voltammetry and at a mercury pool using coulometry. The mechanism proposed for the reduction of cystine involved the reduction of an adsorbed monolayer of cystine to form solution phase cysteine. Mercury electrodes have been used by Bond et al. [19] to compare the behaviour of homocysteine (a product of methionine metabolism not normally detectable in human tissue fluids), cysteine, and the disulphides cystine and homocystine. The former two molecules are closely related in structure, and the resulting polarograms indicated that they have similar limiting currents per unit concentration and shape, as well as similar $E_{1/2}$ values of -0.125 V. Differential pulse polarography of homocysteine showed limits of detection of approximately 10^{-6} M, whilst differential pulse cathodic stripping voltammetry yielded detection limits of 10^{-9} M. Unlike the thiols, there was a difference noted in the electrochemical reduction of the disulphides ($E_{1/2}$ cystine - 0.455 V, homocystine - 0.650 V). Work has recently been published describing a method for the determination of cystine and cysteine in sea water and fresh water again using CSV. In the presence of added copper (II) ions, a limit of detection of 0.1 nM was obtained [20]. Kuzel

[21] in 1973 was able to use polarographic techniques to quantitatively determine cystine excreted in the urine as a result of cystinuria, using a sulphite-nickel electrolyte solution

Other electrode types have been sucessfully used in the determination of sulphydryl compound. Hitchman and Nyasulu [22] used copper electrodes (which were cathodically treated before analysis) for the direct potentiometric determination of a number of proteins, L-cysteine and L-histidine, whilst the use of chemically modified electrodes, made by incorporating cobalt phthalocyanine (CoPC) into conventional carbon paste electrodes, were shown to catalyse the electrooxidation of cysteine, homocysteine, and N-acetylcysteine. When used as the working electrode in amperometric detection following HPLC, limits of detection for the above were of the order of 2.7 pmole.

4.1.3. Electroanalytical studies of antigen-antibody interactions

It was as far back as the early 1950's when polarographic techniques were investigated to see if they could be used to monitor immunological reactions. Breyer and Radcliff [23], using an azoprotein as the antigen, carried out experiments that showed on the addition of specific and non-specific sera, the polarographic wave of the azoprotein

varied, i.e. on addition of the specific antiserum to the azoprotein, a sharp decrease in the wave was observed, whereas when non-specific serum was added, only a decrease due to the diluent effect was seen. Kano and co-workers [24] then studied the Brdicka currents of human immunoglobin G (IgG) and sheep anti-human IgG. These currents (polarographic catalytic hydrogen evolution currents produced by proteins in the presence of a cobalt salt) were studied by direct current and differential pulse polarographic methods. For a mixture of IgG and anti-IgG, the currents were smaller than the sum of currents due to IgG and anti-IgG in separate solutions; the difference being attributed to complex formation between IgG and anti-Ig G. Using differential pulse polarography, limits of detection of 10^{-10} M of antigen (or antibody) were obtained.

Adsorptive stripping voltammetry has also proved successful in monitoring immunological reactions. Smyth and co-workers [14,25] have used this technique to follow the voltammetric behaviour HSA and anti-HSA as well as IgG and anti-IgG, and monitored the interaction of these molecules. Limits of detection for HSA were 2.9×10^{-8} M, whilst linear calilration curves were obtained for both IgG and anti-IgG in the range $1x10^{-9}$ - $1x10^{-7}$ M and $1x10^{-9}$ - $1x10^{-8}$ M respectively.

Chemically modified electrodes have also been investigated to monitor antigen-antibody reactions. Yamamoto et al. [26] investigated the immunological reaction of human chorionicgonadatropin (hCG) in a potentiometric

investigation using a cyanogen bromide-treated electrode coated with the corresponding anti-serum. It was found that the potential of the modified electrode shifted in the positive direction upon contact with a solution of hCG, and the rate of the reaction at the interface between electrode and solution was the order of 10^4 mol^{-1} s^{-1} in diethyl barbiturate buffer.

4.2. EXPERIMENTAL

4.2.1. Materials

All materials used were of analytical grade and solutions were prepared in water obtained by passing distilled water through a Milli-Q water purification system. Throughout the electrochemical studies, a 0.1 M phosphate buffer (pH 7.4) was prepared using disodium hydrogen phosphate and sodium dihydrogen phosphate. Cystine was obtained from BDH Chemical Ltd and cisplatin was obtained from Sigma. Stock solutions of both cystine and cisplatin were prepared in water.

4.2.2. Apparatus

All voltammograms were obtained using a Princeton Applied Corporation (PARC) Model 264A Polarographic Analyser combined with a PARC Model 303 magnetic stirrer and an Omnigraphic Model 2000 x-y recorder.

4.2.3. Procedures

Before each investigation, the electrolyte was purged with nitrogen for 8 min. Following the addition of analyte to the cell, the electrolyte was further purged for 2

min. After this step, the potential relating to the accumulation potential (E_{acc}) was applied to the cell for the required accumulation time (t_{acc}), with continous stirring. The solution was then maintained at rest during the equilibration period of 30 s. A differential pulse scan was then initiated using an initial potential (E_{acc}) and scanning to -1.00 V. During most of the studies, a scan rate of 10 mV/s, pulse amplitude of 50 mV and a large drop was used. The adsorptive stripping cycle was repeated using a new drop.

4.3. ELECTROANALYTICAL STUDIES OF THE DISULPHIDE-CONTAINING AMINO ACID, CYSTINE

4.3.1. Cyclic voltammetry of cystine

A typical cyclic voltammogram for a 4.0×10^{-5} M solution of cystine in phosphate buffer, pH 7.4, using an initial potential of +0.20 V (without accumulation), is shown in Figure 4.3. Cystine gives rise to two reduction peaks at -0.15 V (peak A) and -0.49 V (peak B), and an anodic peak in the reverse scan at -0.45 V. The main cathodic peak at -0.49 V peak B, shows a linear dependence on scan rate, v, for v = 50-500 mV/s (Figure 4.4.) and together with its morphology, seems to indicate an adsorption-controlled process. According to Stankovich and Bard [18] and Kolthoff and Barnum [37], and together with this experimental evidence, the process corresponds to the reduction of cystine to cysteine, according to the following mechanism:

$$RSSR + 2H^+ + 2e^- \longrightarrow 2RSH$$

The oxidation wave that appears on the reverse scan is not directly related with cystine itself. It has a shape corresponding to that of a diffusion process and the peak current $i_{p,a}$ is linear with $v^{1/2}$. Kolthoff and Barnum [37] did not find an anodic polarographic process with cystine. However they did find such an anodic process for cysteine. By

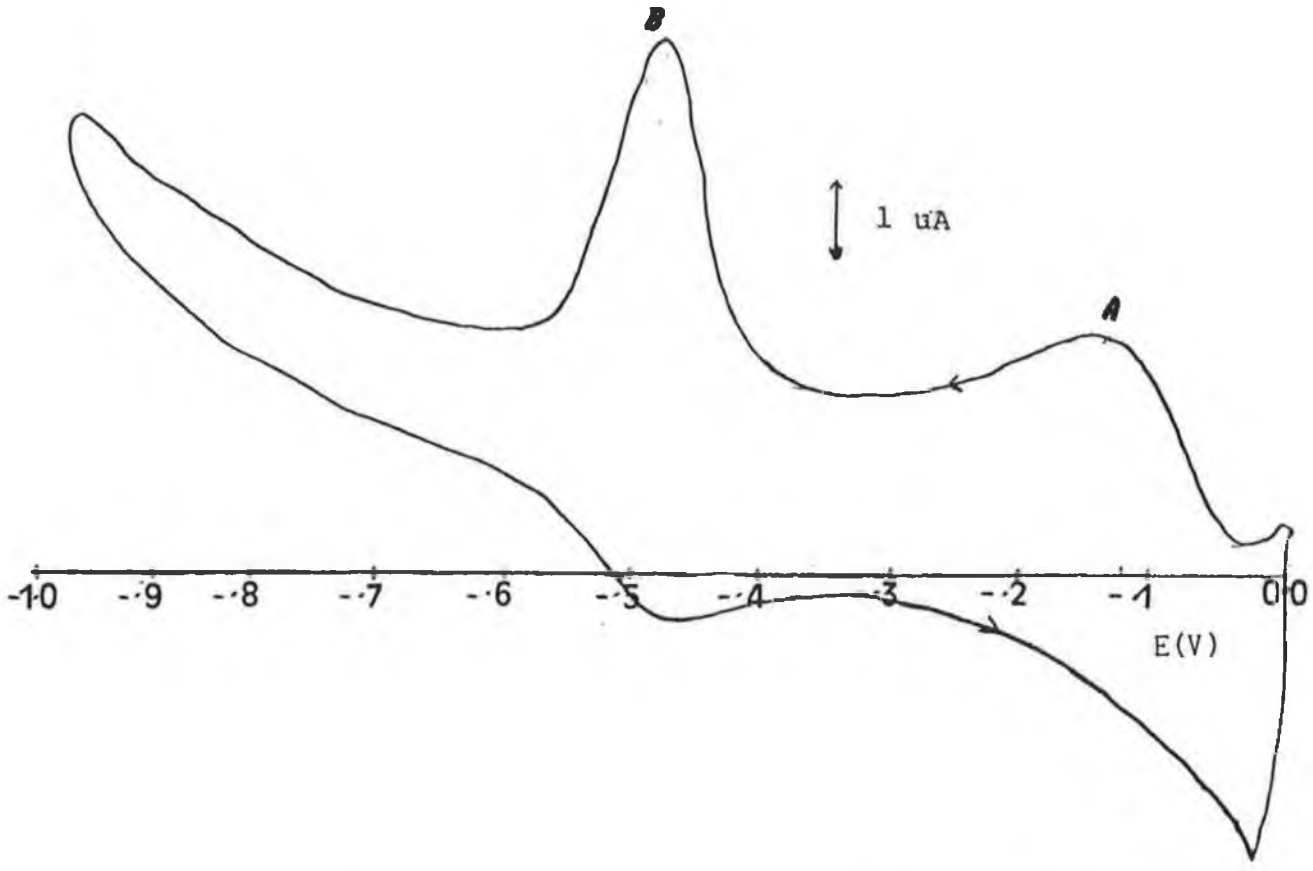

Figure 4.3. Cyclic voltammetry of 4.0×10^{-5} M cystine in phosphate buffer, pH 7.4, in an unstirred solution. Scan rate 500 mV/s.

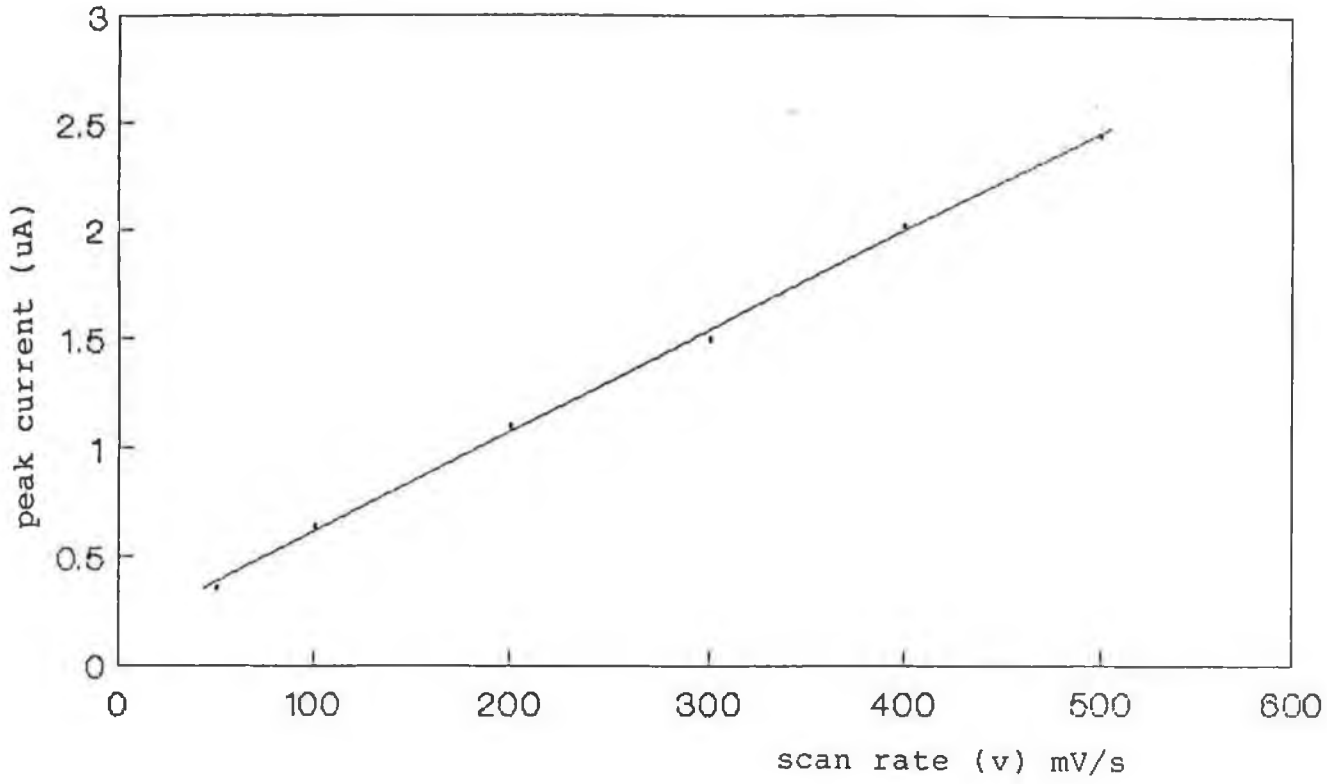

Figure 4.4. Dependence of cathodic peak current ($i_{p,c}$) on scan rate (v), for a 4×10^{-5} M cystine solution in phosphate buffer, pH 7.4.

comparison with their experimental findings, the anodic process here can be ascribed to the oxidation of cysteine, arising from the reduction of cystine. Peak A at E_p = -0.15 V, also has a shape corresponding to a diffusion-controlled process. This peak can be attributed to the reduction of R-S-Hg-S-R species, the mechanism of which is outlined in detail later.

Subsequent repetitive scans yielded lower peak currents for all three processes compared to those of the first trace. This change in repetitive cycling would appear to indicate that both the reduced and oxidised forms of this amino acid are not very strongly adsorbed, as other molecules containing -S-S- links are [13]. It does however show similar adsorption behaviour to BSA [12] on repetitive CV scans. This decrease in current is more than likely due to the depletion of the layer of species adjacent to the electrode surface.

4.3.2. Adsorptive stripping voltammetric behaviour of cystine

The AdSV behaviour of cystine was examined, paying particular attention to the effect of accumulation potential (E_{acc}), accumulation time (t_{acc}), drop size, scan rate and pulse amplitude, plus the effect of concentration of the amino acid.

The effect of accumulation time on the AdSV behaviour of a 10^{-7} M solution of cystine is shown in Figure 4.5. Two peaks were noted at -0.35 V (peak A) and -0.55 V (peak B). The peak currents for peak A were larger than for peak B (Figure 4.5.), when there was no (or only a very small) accumulation time used. This dependence of current on t_{acc} for both peaks is represented graphically in Figure 4.6. Peak A shows a linear increase up to 50 s; however, above this time, a plateau region was observed in the plot. A well defined linear increase in current with increasing t_{acc} was observed for peak B. However, at times > 500 s, linearity was not adhered to. This behaviour may be attributed to:

(i) saturation of Hg electrode with cystine; and/or

(ii) adsorption equilibrium being obtained.

The effect of stirring (i.e. mass transport) during the preconcentration period was also examined. For example, with solution stirring, both stripping peaks were between 85 -88-fold larger than the corresponding peaks in a quiescent solution (Figure 4.7.)

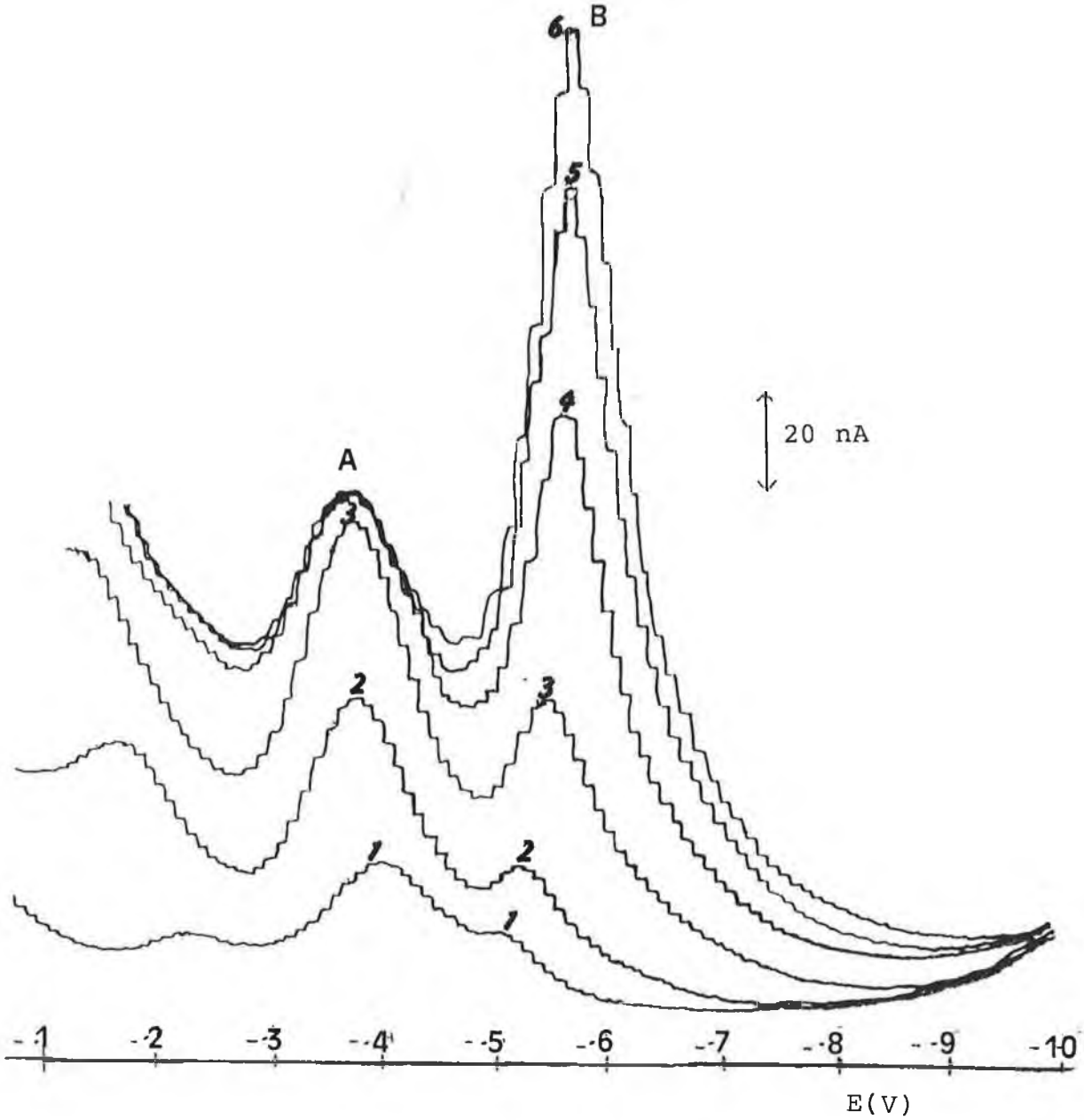

Figure 4.5. AdSV behaviour of 1.0×10^{-7} M cystine at various t_{acc} between 0 – 180 s, using an E_{acc} of + 0.10 mV/s, pulse amplitude 50 mV and large drop. t_{acc}: (1) 000 s, (2) 20 s, (3) 60 s, (4) 100 s, (5) 140 s, (6) 180 s.

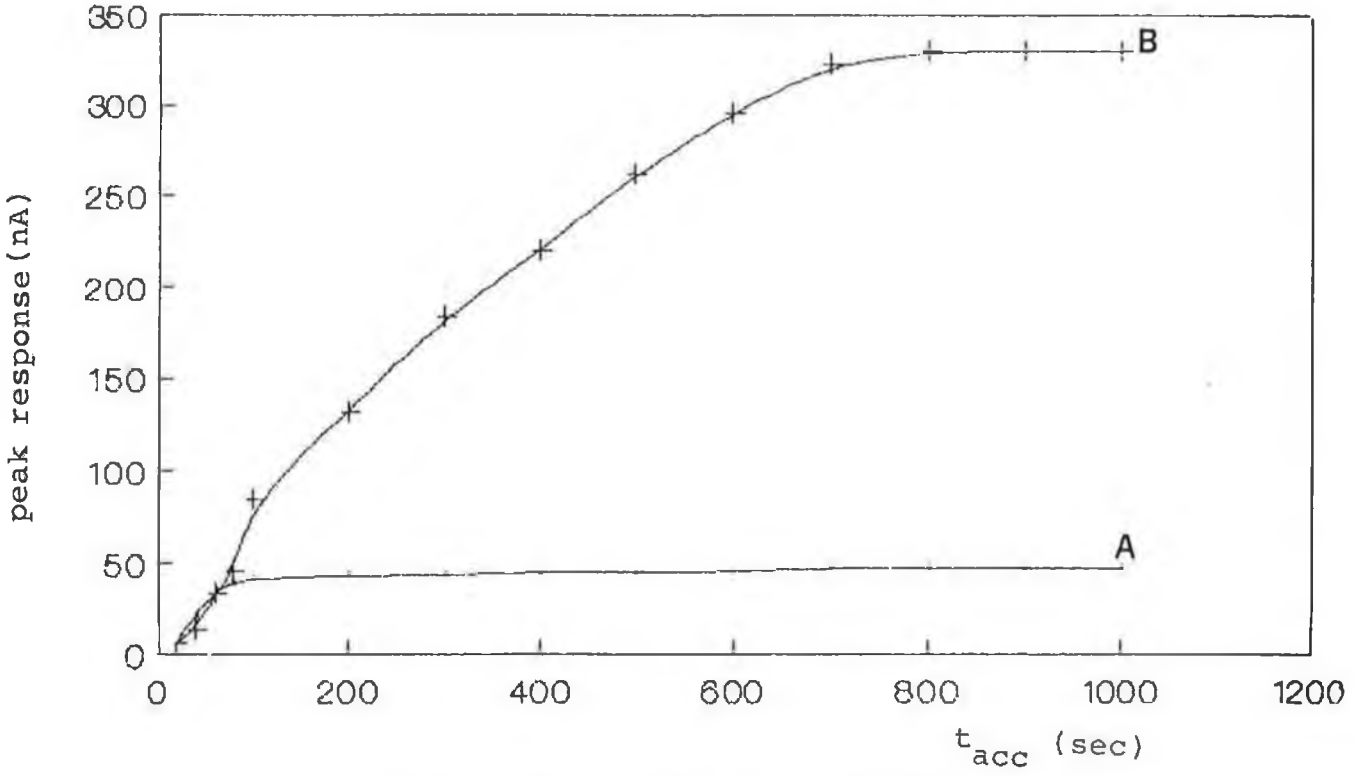

Figure 4.6. Dependence of peak currents for peaks A and B with t_{acc} (concentration of cystine, 10^{-7} M).

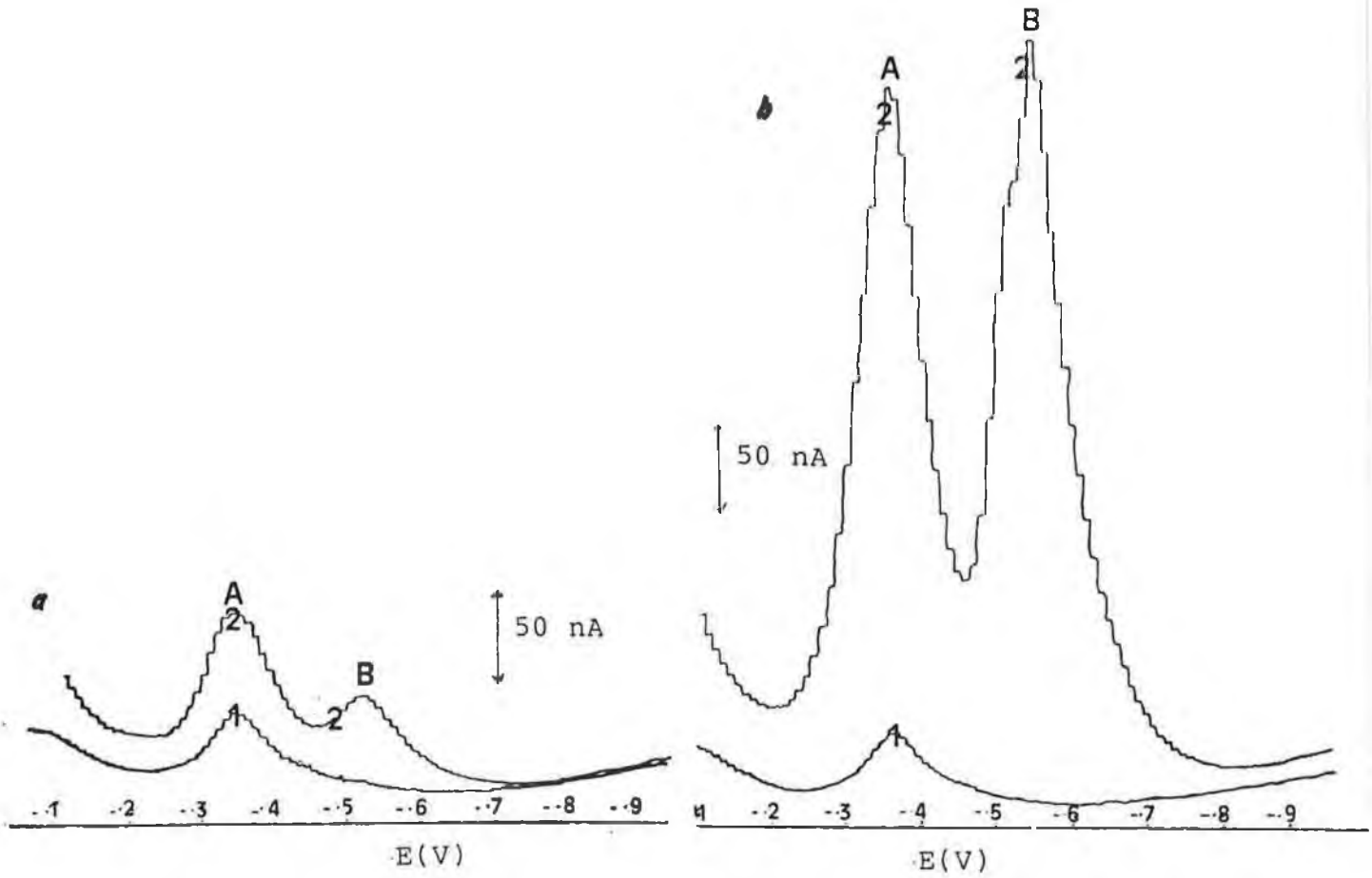

Figure 4.7a. AdSV behaviour of 4 x 10^{-7} M cystine in a quiescent solution.
(1) t_{acc} 0 s, (2) t_{acc} 200 s.
E_{acc} +0.20 V, scan rate 10 mV/s, pulse amplitude 50 mV.

Figure 4.7b. AdSV behaviour of 4 x 10^{-7} M cystine in a stirred solution.
(1) t_{acc} 0 s, (2) t_{acc} 200 s.
Conditions as in Figure 4.7a.

The two peaks noted for the adsorption and subsequent reduction of cystine showed varying behaviour with respect to accumulation potential. The dependence of the peak currents for both peaks A and B, over the potential range +0.3 - -0.20 V, is shown in Figure 4.8. Both peaks exhibited a similar behaviour over the potential range +0.30 V to +0.10 V, where a maximum current was obtained for both peaks for an E_{acc} of +0.20 V. This was subsequently chosen as the optimum potential to monitor the behaviour of the amino acid. However, at potentials more negative than +0.10 V, peak A was not clearly observed, whilst peak B showed a decrease in current at potentials more negative than +0.10 V.

This variation in current of cystine with variation of E_{acc}, together with the information gathered from the CV experiments allows the nature of these two peaks to be ascribed. Peak B appears to have all the characteristics of an adsorbed species. Its CV behaviour and peak potential is similar to that published by Stankovich and Bard [18], and its AdSV behaviour is rather similar to those waves found at similar potentials for cystine [37] and for the disulphide-containing proteins HSA [14], BSA [15] and IgG [25]. The peak at -0.56 V as already outlined can therefore be ascribed to the reduction of cystine to cysteine according to the reaction:

$$RSSR + 2H^+ + 2e^- \longrightarrow 2RSH_{ads}$$

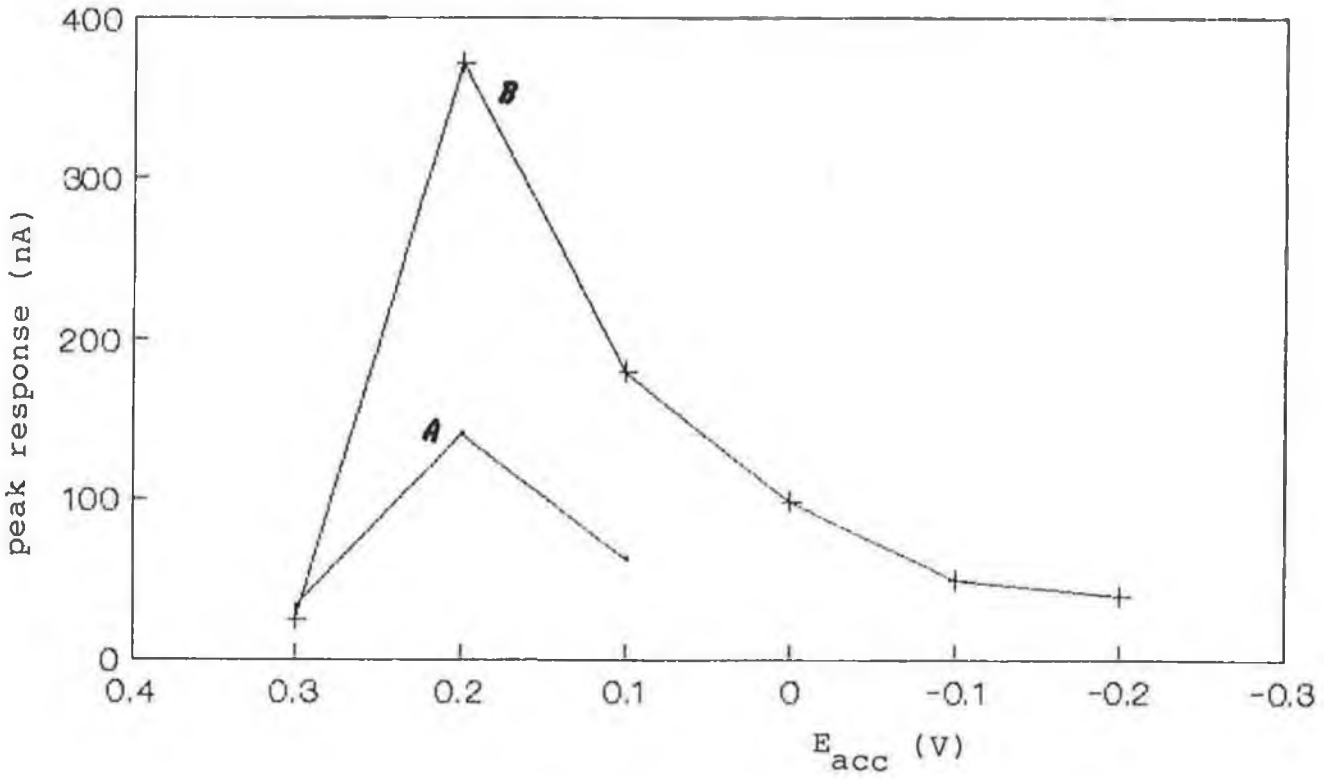

Figure 4.8. Dependence of peak currents for peaks A and B of cystine with E_{acc}.

The nature of peak A is more complex. Peak A was found only when accumulation was carried out at positive potentials. During this accumulation, there appears to be an equilibrium between the bulk solution concentration of cystine and that of the adsorbed species at the electrode surface. The mechanism ascribed for peak A (in agreement with work published for the reduction of thiuram disulphides and diphenyl disulphides [38]), suggests the addition of mercury across the disulphide linkage:

$$R\text{-}S\text{-}S\text{-}R \xrightarrow{Hg} R\text{-}S\text{-}Hg\text{-}S\text{-}R$$

and the subsequent reduction of this mercury salt to cysteine:

$$R\text{-}S\text{-}Hg\text{-}S\text{-}R + 2e^- + 2H^+ \longrightarrow 2RSH + Hg$$

From the experimental evidence, the equilibrium process may be expressed as follows:

$$RSSR_{soln} \rightleftharpoons RSHgSR_{ads}$$

The formation of this mercurous cysteinate seems to be concentration dependent of the bulk cystine solution, and this equilibrium appears to be reached very quickly (see plateau region for peak A in Figure 4.6.). The higher the bulk solution concentration of cystine, the higher the mercury salt formation, hence the greater the magnitude of response (compare

Figures 4.5. and 4.7a and b. The formation of this mercurous cysteinate only occurs in the presence of Hg(II) ions, as noted from the fact that peak A is seen only during accumulation at positive potentials. The wave noted during CV experiments -at 0.15 V, which showed linearity with $v^{1/2}$, corresponds more than likely to peak A using AdSV. Hence peak A is diffusion controlled, whilst peak B suggests an adsorption controlled behaviour.

The AdSV behaviour of peak B of cystine was then evaluated with respect to drop size, scan rate and pulse amplitude. These results are collated in Table 4.1., and from this it should be noted that the optimum conditions for the determination of cystine are: E_{acc} +0.20 V, pulse amplitude 50 mV, scan rate 10 mV/s and "large " drop size. Under these conditions, a calibration curve was obtained for the determination of cystine, using an accumulation time of 200 s. The plot was linear over the range 5×10^{-8} M - 8×10^{-7} M. These results compare favorably with those obtained by van den Berg et al [20], who used cathodic stripping voltammetry to determine cystine and cysteine in sea-water, in the presence of Cu(II). Using an accumulation period of 4 min, limits of detection were of the order 1×10^{-8} M. The technique reported here has improved on the sensitivity for cystine determination compared to that reported by Kutzel [21], who applied a polarographic method using a sulphite-nickel electrolyte, to determine cystine in urine. The reproducibility of this technique held for cystine concentrations between 1 - 6 mM.

t_{acc}	E_{acc}	drop size	scan rate (mV/s)	$-E_p(A)$ (V)	$I_p(A)$ (nA)	$-E_p(B)$ (V)	$I_p(B)$ (nA)
20	+0.10	1	10	-0.35	7.8	-0.54	5.9
40	+0.10	1	10	-0.35	21.5	-0.54	13.7
60	+0.10	1	10	-0.35	35.3	-0.54	33.5
80	+0.10	1	10	-0.35	39.2	-0.54	45.3
100	+0.10	1	10	-0.35	41.2	-0.54	84.6
200	+0.10	1	10	-0.35	43.1	-0.54	131.8
300	+0.10	1	10	-0.35	43.1	-0.54	220.4
400	+0.10	1	10	-0.35	45	-0.54	261.5
500	+0.10	1	10	-0.35	45	-0.54	295.3
600	+0.10	1	10	-0.35	45	-0.54	322.8
700	+0.10	1	10	-0.35	47	-0.54	301.1
80	+0.10	1	10	-0.35	47	-0.54	301.1
200	+0.05	1	10	-0.35	-	-0.54	91.8
200	+0.10	1	10	-0.35	62	-0.54	179.60
200	+0.20	1	10	-0.35	141	-0.54	371
200	+0.30	1	10	-0.35	32.6	-0.54	24.5
200	+0.00	1	10	-0.35	-	-0.54	97.95
200	-0.10	1	10	-0.35	-	-0.54	48.97
200	-0.20	1	10	-0.35	-	-0.54	38.7
200	+0.20	1	10	-0.35	242.8	-0.54	316
200	+0.20	m	10	-0.35	148.9	-0.54	191.8
200	+0.20	s	10	-0.35	124	-0.54	144.8
200	+0.20	1	2	-0.35	132.6	-0.54	126.8
200	+0.20	1	5	-0.35	242.8	-0.54	330.6
200	+0.20	1	10	-0.35	295.9	-0.54	459
200	+0.20	1	20	-0.35	269	-0.54	451

Table 4.1. Influence of accumulation time (t_{acc}), accumulation potential (E_{acc}), drop size and scan rate on peak current of peak A ($i_{p(A)}$) and peak B ($i_{p(B)}$).

4.4. INTERACTIONS OF CISPLATIN WITH BIOLOGICALLY SIGNIFICANT DISULPHIDE-CONTAINING MOLECULES

4.4.1. AdSV behaviour of HSA in the presence of cisplatin

The typical voltammetric behaviour of HSA (2.5 x 10^{-7} M), in 0.1 M phosphate buffer, pH 7.4, using an accumulation time of 300 s is shown in Figure 4.9. The voltammograms were recorded using a negative going scan. Two peaks were noted; peak A' at -0.44 V and peak B' at -0.56 V. The behaviour observed is in accordance with that reported by Rodriquez et al. [14]. However, on the addition of the antineoplastic agent, cisplatin, the currents for both these peaks decreased (Figure 4.10.). The decrease in peak B' was linear with respect to cisplatin concentrations < 1 x 10^{-8} M, whilst peak A' decreased in a non-linear manner. A slight increase in current was also noted at about -0.68 V, when cisplatin concentrations > than 1 x 10^{-8} M cisplatin were added to HSA. This wave was not observed when HSA was present only in the cell. The substantial decrease of stripping current for peak B' may be attributed to the inaccessability of the disulphide linkages of the protein for reduction at the electrode surface, due to cisplatin binding.

Following these experimental observations, it was decided to investigate the use of AdSV to monitor the interaction of HSA with cisplatin, using the observed decrease in current for HSA (by monitoring peak B') upon the addition of

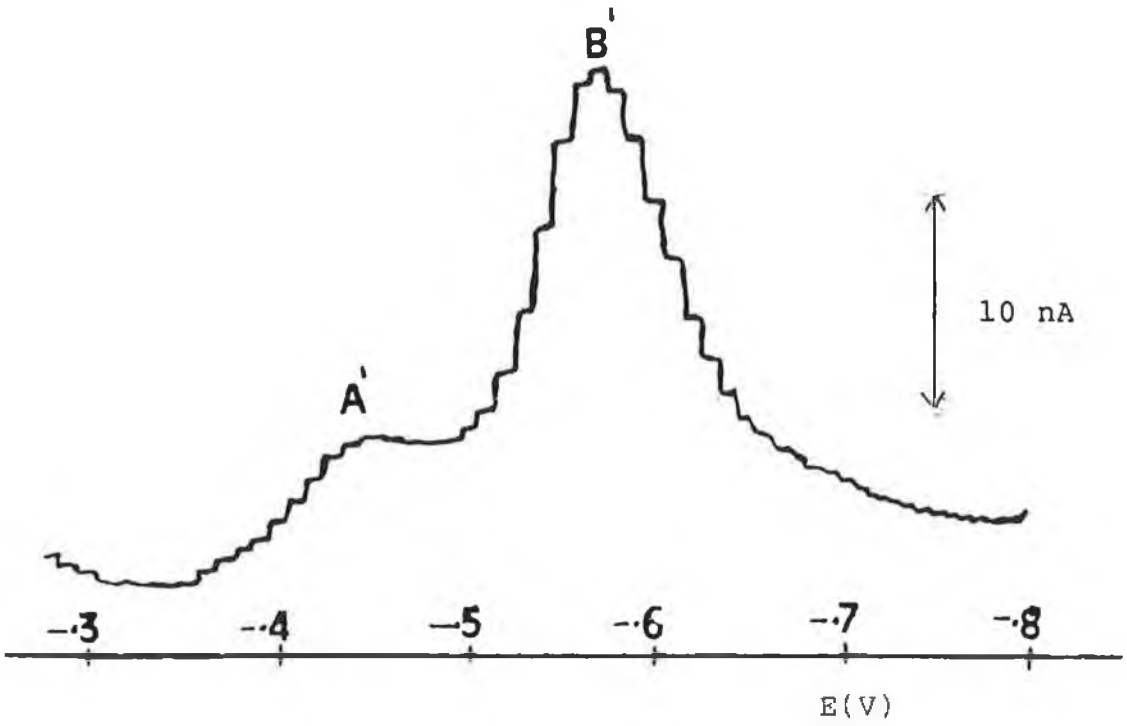

Figure 4.9. Typical AdSV behaviour of 2.5×10^{-7} M human serum albumin (HSA), in phosphate buffer, pH 7.4, using t_{acc} 300 s, E_{acc} +0.20 V, scan rate 10 mV/s, pulse amplitude 50 mV.

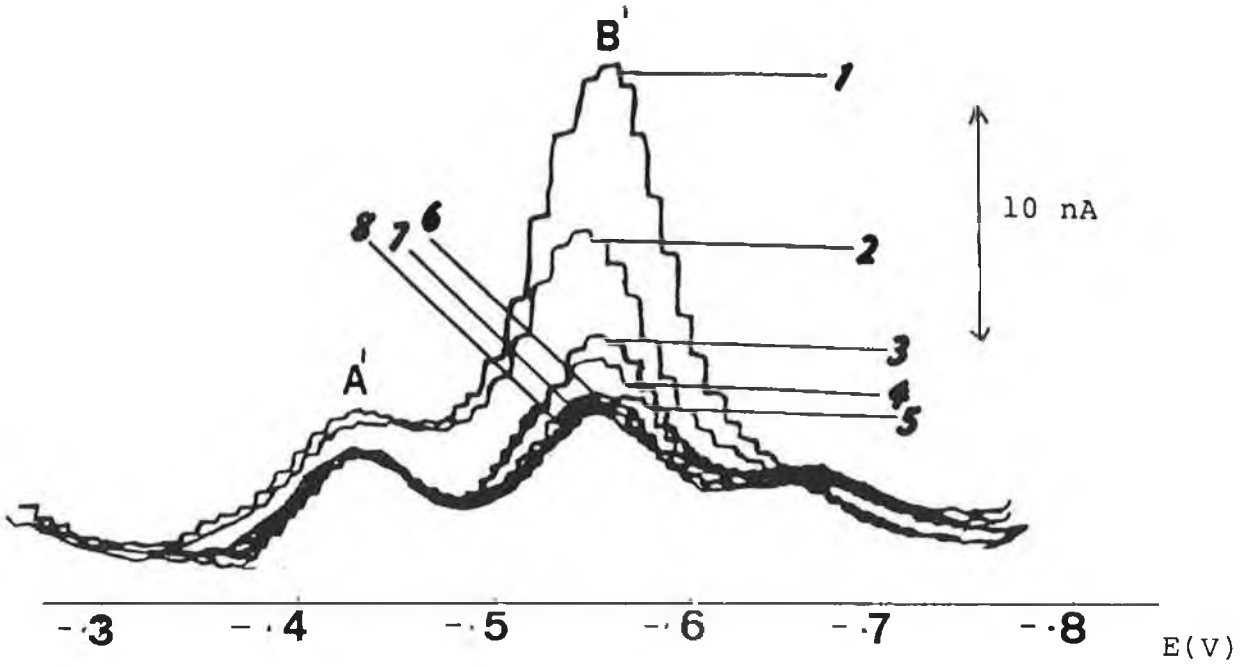

Figure 4.10. AdSV behaviour of HSA in the presence of cisplatin.

(1) HSA 2.5 x 10^{-7} M, (2) (1) + 0.5 x 10^{-8} M cisplatin (3) (1) + 1 x 10^{-8} M cisplatin, (4) (1) + 1.5 x 10^{-8} M cisplatin, (5) (1) + 2 x 10^{-8} M cisplatin, (6) (1) + 2.5 x 10^{-8} M cisplatin, (7) (1) + 3 x 10^{-8} M cisplatin, (8) (1) + 3.5 x 10^{-8} M cisplatin.

E_{acc} +0.10 V; t_{acc} 300 s; scan rate 10 mV/s, pulse amplitude 50 mV.

the drug.

The use of electrochemical techniques to study drug-albumin interactions are not new. Squella et al. [27] monitored the binding of HSA with chlordiazepoxide using alternating current (AC) polarography, whilst Livertoux and Bessiere [28] monitored the interactions of flurazepam and diazepam with HSA using both DPP and AC polarography. The binding characteristics of albumin with cadmium [29], azo dyes [30-33], vanadium [34] and molybdate ions [35] have also been evaluated using polarographic techniques. However, the use of AdSV is perhaps a new approach to monitor the interactions of proteins and drugs. Rodriquez et al [36] have used this technique to monitor the interaction of IgG with diazepam and flurazepam. The mathematical approach taken by Squella et al. [27] has been adapted to evaluate our experimental results, where the binding studies were investigated by increasing the cisplatin concentration at a fixed HSA concentration, as shown in Figure 4.10.

The currents for albumin in the presence and absence of cisplatin may be denoted as I_p and $I_{p,o}$, respectively, and c, c_b and c_f, are the concentration of the total, bound and free albumin, where:

$$c = c_f + c_b \qquad (4.1)$$

Then:

$$I_p/I_{p,o} = [c_f + kc_b]/c \qquad (4.2)$$

where k is the fractional coefficient, and is the value of $I_p/I_{p,o}$ when a sufficient excess of cisplatin has been added to interact with all the HSA and cisplatin. Graphically, the value may be obtained by extrapolation:

$$\lim_{c_f \longrightarrow 0} I_p/I_{p,o} = k \qquad (4.3)$$

The addition of gradually increasing amounts of cisplatin results in the reduction of the peak B'of HSA until it attains a constant value. The effect of increasing cisplatin concentration on this peak current ratio is shown in Figure 4.11. From this graph one can obtain a fractional coefficent for the HSA-cisplatin system, at pH 7.4, of k = 0.32. The fractional coefficients reported for the chlordiazepoxide-HSA system [27] are similar to that reported here. This would suggest that there is strong interaction of cisplatin with HSA.

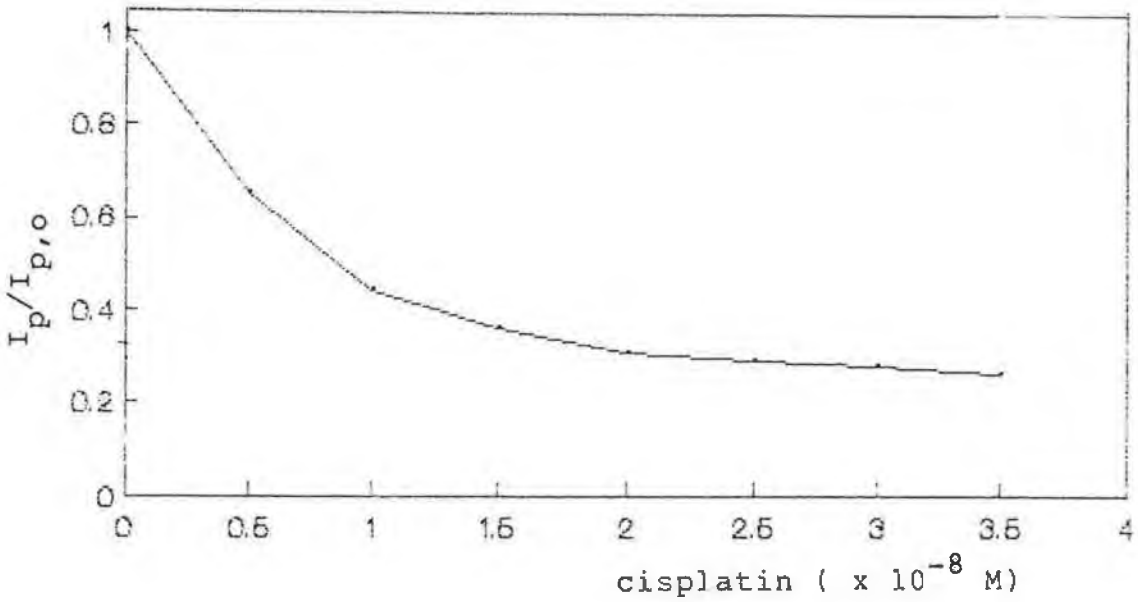

Figure 4.11. Dependence of $I_p/I_{p,o}$ on cisplatin concentration at a fixed HSA concentration of 2 x 10^{-7} M, in phosphate buffer, pH 7.4.

The behaviour of HSA in the presence of cisplatin, monitored by the decrease in the current for peak B', shows similarities to those studies previously devised to determine the interaction of HSA with benzodiazepine drugs [28,36] (these drugs have shown to exhibit high binding affinities for albumin). Riley et al.[2] were able to assess cisplatin reactivity with peptides and proteins using HPLC. On incubation of HSA with cisplatin they found that this protein had at least one or more reactive sites that are readily accessible to cisplatin. Therefore by comparison, the experimental results presented here suggest that cisplatin also has a high affinity for HSA, similar to that reported for the benzodiazepine drugs [36].

A means of expressing this binding affinity between HSA and drug is by an expression of binding constants and binding sites. One of the most common methods to determine these parameters from experimental data, is the use of the Scatchard plot [27,28,36,39]. However, this method was not applicable to the HSA-cisplatin system reported here, as this plot requires the measurement of the concentration of ligand bound to protein, at a series of values of concentration of free ligand in solution, containing a fixed total protein concentration. In order to obtain more reliable data it will be necessary in the future to utilise another technique such as HPLC, to separate free and bound cisplatin. One way of doing this might involve the use of an alumina column (see Chapter Three).

4.4.2. AdSV behaviour of cystine in the presence of cisplatin

The experimental evidence reported in Section 4.4.1. is rather ambiguous when it comes to trying to interpret the interaction between the protein and the drug. It was decided therefore to take the study a step further and investigate the affinity of the drug for cystine, the amino acid containing disulphide bonds in its structure, and which plays an important role in maintaining the tertiary structure of HSA.

The AdSV behaviour of cystine has already been outlined in Section 4.3., and using those conditions already optimised, 2 peaks were noted at -0.37 V (peak A) and at -0.52 V (peak B) for a 2 x 10^{-6} M cystine solution. Gradual increments of a 10^{-5} M solution of cisplatin were then added to the cell already containing cystine, and Figure 4.12. shows the resultant voltammetric peaks for cystine upon the addition of cisplatin. The current response observed for both peaks is similar to that noted for the addition of cisplatin to HSA, although the observed current decrease with increasing drug concentrations for both peaks appears linear compared to the behaviour noted for peak A' and B'in HSA. The mechanism proposed for the AdSV behaviour of cystine, suggests that peak B is due to the reduction of cystine to give cysteine. Thus it would appear that the interaction of cisplatin with cystine occurs at these disulphide groups. It is these bonds that are

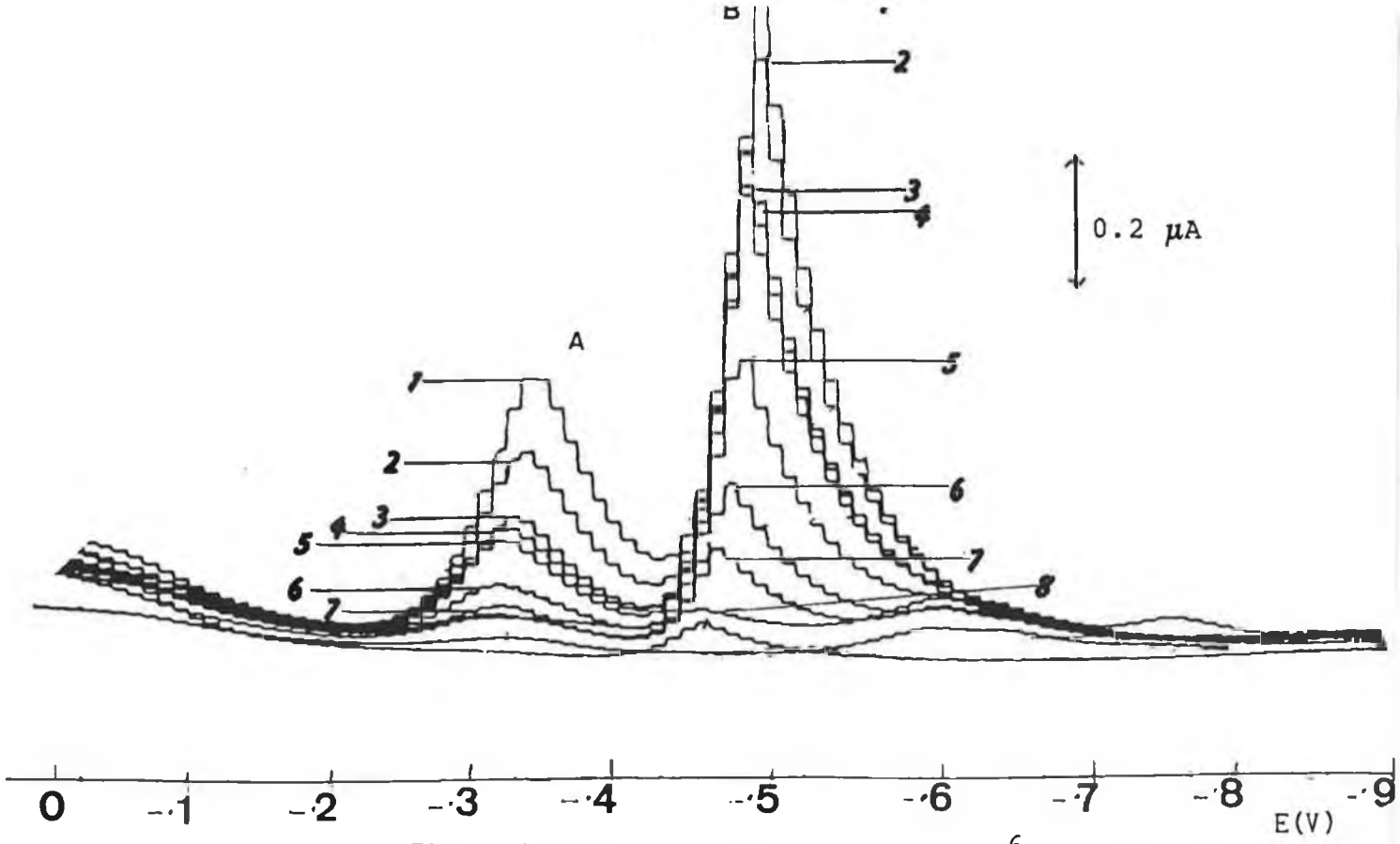

Figure 4.12. AdSV of 2.0 x 10^{-6} M of cystine in the presence (1) cystine 2 x 10^{-6} M, (2) (1) + 1 x 10^{-8} M cisplatin, (3) (1) + 2 x 10^{-8}M cisplatin, (4) (1) + 3 x 10^{-8} M cisplatin, (5) (1) + 4 x 10^{-8} M cisplatin, (6) (1) + 5 x 10^{-8} cisplatin, (7) (1) + 6 x 10^{-8} M cisplatin, (8) (1) + 7 x 10^{-8} M cisplatin.

E_{acc} = 0.10 V, t_{acc} 100s, scan rate 10 mV/s pulse amplitude 50 mV.

responsible for the electrochemical activity of the amino acid, and hence binding of drug to these bonds results in the decrease in currents for the original cystine waves.

The degree of interaction of drug to the amino acid was influenced by concentration of the added drug, where at concentrations > 10^{-7} M cisplatin, the cystine peaks are virtually eliminated. Studies were also undertaken to look at the effect of incubation times on the interactions of cisplatin and cystine, and also the degree of interaction of a freshly prepared sample of cisplatin compared to that of an aged sample. The experimental results suggest that the degree of interaction in the cystine/cisplatin system was greatly influenced by the incubation time allowed. The cell was thermostatted at 37^{0}C and the cystine-cisplatin mixture allowed to react over a 1 hour period. Under these conditions, there was an 80% decrease in the original peak current for peak B of cystine. It was then decided to monitor what happened within the system over certain time intervals. There are a few points to note from the voltammograms shown in Figure 4.13. The accumulation potential was held at 0.00 V, hence the non-appearance of peak A (see Section 4.3.2.). On running the voltammograms every 10 min, during incubation at 37^{0}C, there was a shift to slightly more positive potentials for peak B from -0.53 V to -0.45 V after a 70 min incubation period. There is also the appearance of a new wave at -0.61 V, which becomes more defined with longer incubation times. From

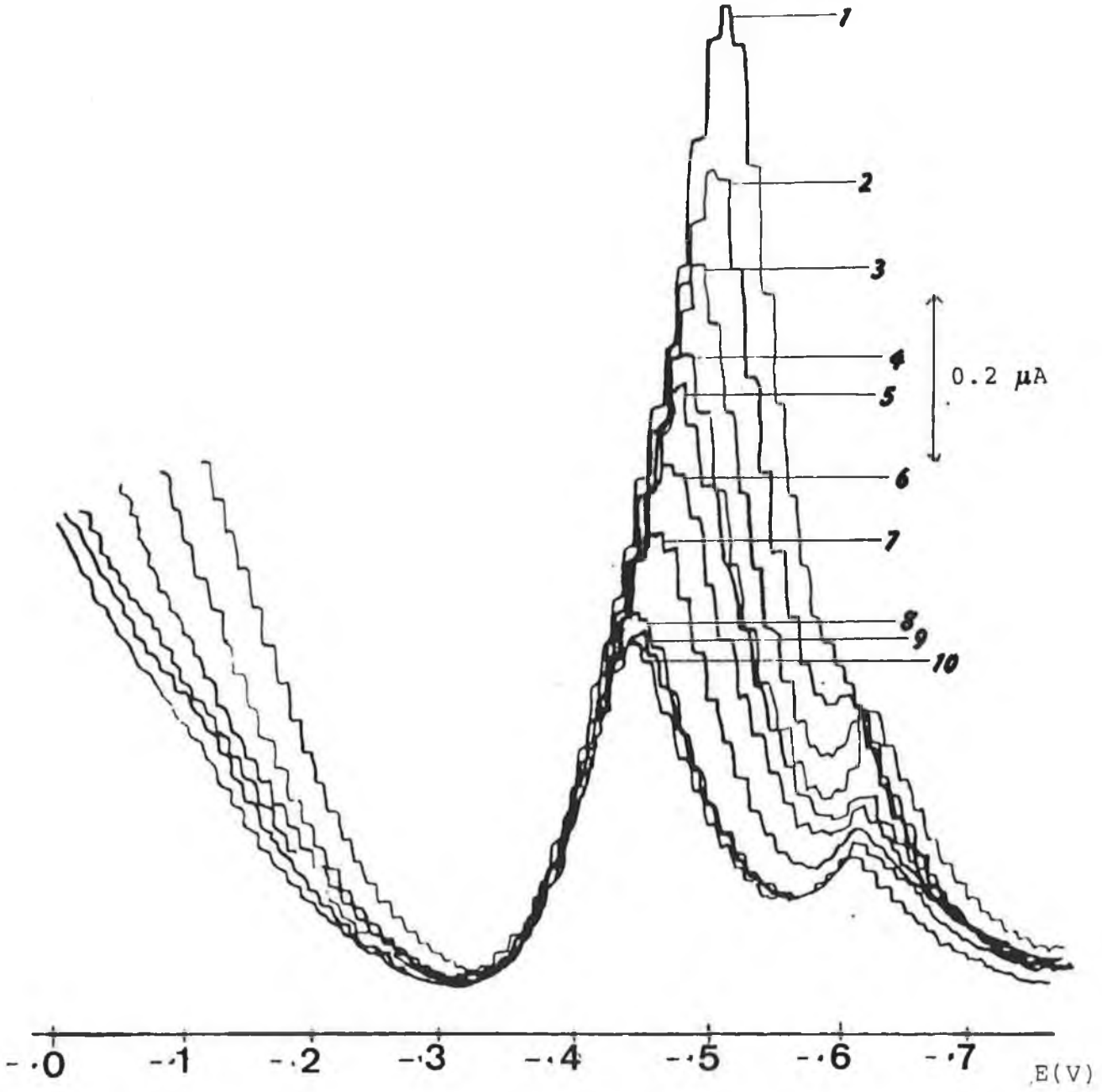

Figure 4.13 Effect of incubation at 37^{0}C of cystine-cisplatin system, over a period of time (80 min).
(1) cystine 2 x 10^{-5} M,
(2) addition of 1 x 10^{-8} M cisplatin
(3) – (10), scans of the cystine-cisplatin system taken every 10 min.

the overall experimental results it would appear that interactions between cystine and cisplatin are concentration dependent and are influenced by the temperature and length of incubation time at this temperature. Physiological conditions, such as those used here i.e., 37^0C and pH 7.4, reveal perhaps stable and favourable interaction conditions for interaction between the drug and amino acid, as noted in the shift to positive potentials and the new wave.

The affinity for cisplatin to cystine was also followed with respect to the age of the interacting drug where the degree of interaction of fresh and aged samples of cisplatin with cystine were compared. The results revealed that freshly prepared samples of cisplatin gave rise to smaller decreases in peak current of the original cystine peak, whilst interactions of an aged solution of the drug with the amino acid resulted in a larger decrease in the peak currents of peak B (Figure 4.14.). This behaviour may perhaps be attributed to the presence of the positively charged hydrolysis products of cisplatin, i.e, the mono-aquo and di-aquo species, which result from the degradation of the drug due to ageing, and have been suggested in the literature to bind particularly well across molecules containing disulphide groups [1,2].

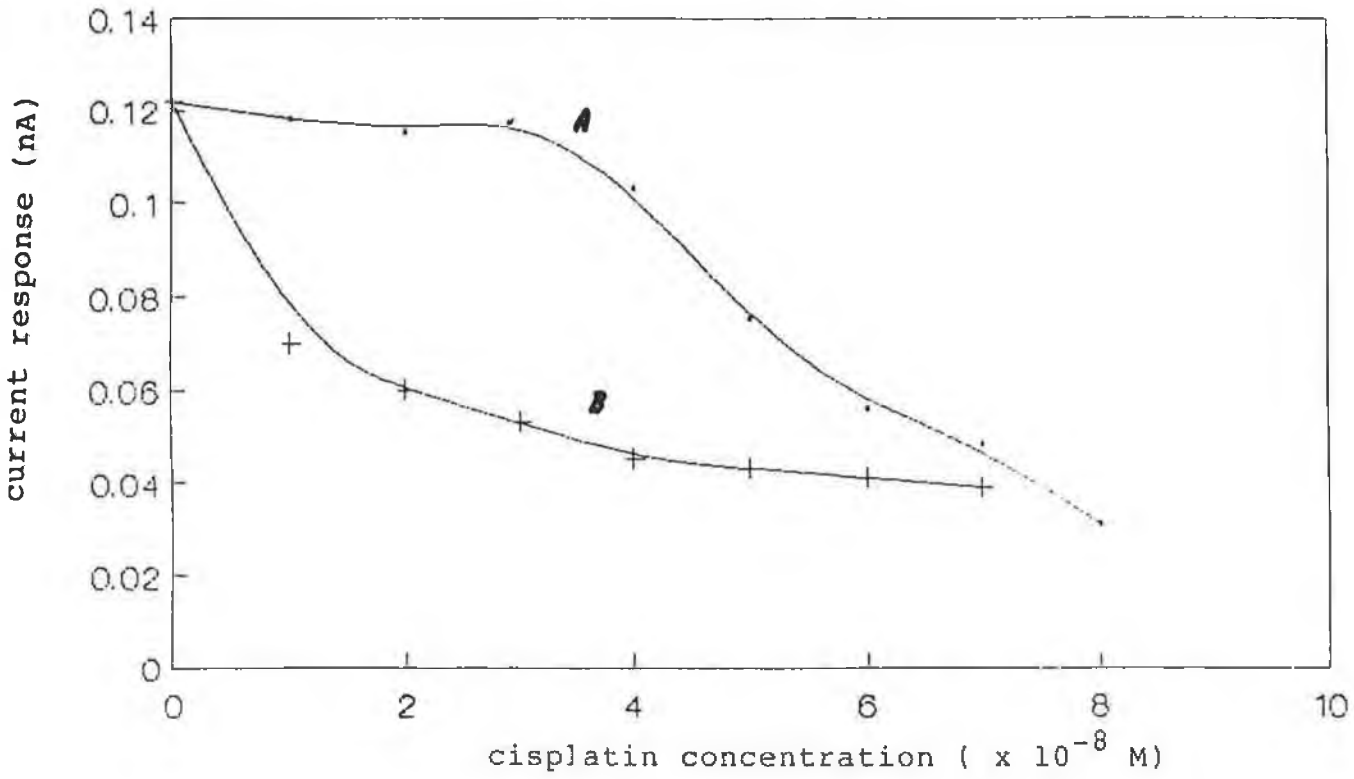

Figure 4.14. Effect of ageing of cisplatin on the current of peak B of cystine.
(A) Fresh solution
(B) Aged solution (4 days old)

4.5. REFERENCES

1. Riley C.M., Sternson L.A., Repta A.J., and Slyter S.A., Anal. Biochem., 1983,130,203.
2. Riley C.M., Sternson L.A., and Repta A.J., Anal. Biochem., 1982,124,167.
3. Andrews P.A., Wung W.E., and Howell S.B., Anal. Biochem., 1984,143,46.
4. Stankovich M.T., and Bard A.J., J. Electroanal. Chem., 1978,86,189.
5. Stankovich M.T., and Bard A.J., J. Electroanal. Chem., 1978,85,173.
6. Markus G., and Klarush F., J. Amer. Chem. Soc., 1957,79,139.
7. Kolthoff I., Anastasi A., and Tan B., J. Amer. Chem. Soc., 1958,80,3235.
8. Leach S., Mechers A., and Swanepoei D., Biochemistry, 1965,4,23.
9. Behr B., Bialowolska M., and Chodowski J.,J. Electroanal. Chem., 1973,46,223.
10. Cecil R., and Weitzman P.D.J.,Biochem. J., 1964,13,1.
11. Trijueque J.,Sanz C., Monleon C., and Vicente F., J. Electranal. Chem., 1988;251,173.
12. Hertl W., Anal. Biochem., 1987,164,1.
13. Forsman U., Anal. Chim. Acta., 1984,166,141.
14. Rodriquez-Flores J., Smyth M.R.,J. Electroanal. Chem., 1987,235,317.

15. Rodriquez-Flores J.,O'Kennedy R., and Smyth M.R.,Anal. Chim. Acta.,1988,212,355.

16. Wang J., Villa V., and Tapia T., Bioelectrochem. Bioenerg., 1988,19,39.

17. Palecek E., and Postbieglova I., J. Electroanal. Chem., 1986,214,359.

18. Stankovich M.T., and Bard A.J., J. Electroanal. Chem., 1977, 75,487.

19. Bond A.M., Thomson S.B., and Tucker D.J., Anal. Chim. Acta., 1984,156,33.

20. Van den Berg C.M.G.,Househam B.C., and Riley J.P., J. Electroanal. Chem., 1988,239,137.

21. Kutzel K., Clin. Chim. Acta., 1973,48,377.

22. Hitchman M.L., and Nyasulu F.W.M., J. Chem. Soc; Faraday Trans. J., 1986,82,1223.

23. Breyer B., and Radcliff F.J., Nature, 1951,167,79.

24. Kano K., Ikeda T., and Senda M., Agric. Biol. Chem., 1983,47(5),1043.

25. Smyth M.R., Buckley E., Rodriquez-Flores J., and O'Kennedy R., Analyst, 1988,113,31.

26. Yamamoto N., Nagasawa Y., Shuto S., Tsubomura H., Sawai M., and Okumura H., Clin. Chem., 1980,26(11),1569.

27. Squella J.A., Papic E., and Nunez-Vergara L.J., Bioelectrochem. Bioenerg., 1986,16,471.

28. Livertoux M.H., and Bessiere J., Bioelectrochem. Bioenerg., 1987,17,535.

29. Tanford C., J. Amer. Chem. Soc., 1951,73,2066.

30. Strick W., and Kolthoff I.M., J. Amer. Chem. Soc., 1949,71,1519.

31. Saroff H.A., and Mark H.J., J. Amer. Chem. Soc., 1953,75,1420.

32. Malik W.V., and Arora J.P.S., J. Electroanal. Chem., 1969,22,359.

33. Malik W.V., Ahmed S., J. Electroanal. Chem., 1973,47,155.

34. Arora J.P.S., Singh R.P., Soam D., and Scharma R., Bioelectrochem. Bioenerg., 1983,10,57.

35. Arora J.P.S.,Singh R.P., Soam D.,Singh S.P., and Kumar R., Bioelectrochem. Bioenerg., 1983,10,441.

36. Rodriquez J., Vinagre F., Barrachero A., and Sanchez A., Analyst, 1989,114,393.

37. Kolthoff I., and Barnum C., J. Amer. Chem. Soc., 1941,63,520.

38. Smyth M.R., and Smyth W.F., Analyst, 1978,103,530.

CHAPTER FIVE

VOLTAMMETRIC AND GRAPHITE FURNACE ATOMIC ABSORPTION SPECTROPHOTOMETRIC METHODS FOR THE DIRECT DETERMINATION OF INORGANIC PLATINUM IN URINE

5.1. INTRODUCTION

The determination of platinum (Pt) in plasma and urine of patients treated with the antineoplastic agent cisplatin requires a sensitive assay technique, and has proven an interesting challenge to the analytical chemist. The most widely used technique for the determination of platinum in body fluids following cisplatin therapy is graphite furnace atomic absorption spectrometry (GFAAS). Early pharmacokinetic experiments were undertaken to determine the total platinum levels in plasma or urine using this technique [1-4]. As already outlined in Chapter One, acute nephrotoxicity is the limiting factor in dosage escalation of cisplatin. The introduction of prehydration and a mannitol-induced diuresis substantially decreased the incidence of renal toxicity. Kelsen et al.[5] used GFAAS to perform a cisplatin nephrotoxicity study, to correlate acute nephrotoxicity with plasma platinum concentrations.

The advantage of this technique is that relatively little sample pretreatment is required, and urine, plasma and plasma ultrafiltrate can be introduced directly into the graphite furnace. However, in order to improve detection limits, many tissue samples are subjected to time-consuming and potentially hazardous, wet- or dry-ashing procedures prior to platinum analysis [6-9]. Typical wet ashing methods include the use of acids such as nitric or perchloric acids, and limits of detection using these methods are in the region of 0.1 ug/g of

wet tissue [7]. As these ashing techniques are potentially hazardous, Siddik et al. [9] reported on the application of tissue solubilisation in hyamine hydroxide (methylbenzenethonium hydroxide) in the GFAAS determination of total tissue platinum. Limits of detection were comparable between the hyamine hydroxide (0.25 μg/g) and nitric acid (0.15 ug/g procedures. However, the solubilisation of tissues offers several advantages over conventional digestion procedures. Larger numbers of samples can be processed with relatively greater safety using hyamine hydroxide, and solubilisation also eliminates the need for sample observation, which is necessary with the HNO_3 digests, to prevent charring.

Matrix removal may also be influenced by the temperature programmes used throughout sample analysis. Platinum is relatively non-volatile, and temperatures of between 2300^{o}C [8,10,11] and 2700^{o}C [7,9] are required for atomisation. However, when the samples are complex like plasma and tissue samples, the most important stage in the entire furnace programme is the ashing stage. The ultimate aim is to remove the matrix completely, leaving behind the analyte in a form which results in maximum atomisation. Therefore this step is very much matrix dependent, with plasma and urine requiring temperatures of 700 - 1200^{o}C [8,11,12], whilst tissue samples require higher temperatures for complete matrix removal [7,9].

Graphite furnace atomic absorption spectroscopy does provide the necessary sensitivity for monitoring Pt levels in

clinical samples. Due to the high temperarures required for atomisation, however, rapid decomposition of the pyrolytic graphite surface occurs leading to analytical inaccuracy. Also, this technique responds only to total levels of Pt and cannot differentiate between Pt complexes and their respective degradation and biotransformation products. Bannister et al. [8] developed a method of analysis for free circulating Pt species in blood plasma. The separation of protein bound and free Pt species was effected by centrafugal ultrafiltration, followed by the conversion of Pt in the ultrafiltrate to a cationic complex by reaction with ethylenediammine. This product was then collected on paper impregnated with a cation-exchange resin and Pt was eluted from the disk with 5 mM HCl. The limit of detection using GFAAS was 35 μg/l of plasma.

Platinum speciation, however, can be achieved by interfacing (either on-line or off-line) a separation/ chromatographic step with the GFAAS detection method. Fractionation of the HPLC eluent and subsequent determination by GFAAS is time consuming, but has been used by Riley et al. [13], who combined the separation of Pt in urine using column switching on solvent generated anion-exchangers, giving limits of detection of 2 μg/ml urine.

Platinum compounds can be determined based on electrochemical reduction or oxidation processes. Although the polarographic reduction of platinum (II) complexes has been the subject of investigations for years, its electrode reaction mechanism is still not completely understood [14]. The

complications associated with the reduction of these complexes has been reviewed by Harrison et al. [15]. Laitinen and Onstott [16] reported the appearance of unusual reduction waves (with maxima and minima) for the tetrachlorplatinate (II) ion at the DME. The catalytic currents observed at strongly negative potentials [17-20] have also been a subject of interest. The analytical utility of the catalytic current has been recognised previously; for instance Pt was determined in hydrochloric acid solutions [17] and after derivatisation with EDTA [18] or ethylenediammine [12,19,21-24]. In the latter case, a DPP assay for cisplatin was performed after acid oxidative hydrolysis of biological samples and reaction with ethylenediammine, giving limits of detection of 0.5 ng/ml platinum.

The interfacial behaviour of Pt complexes has also been utilised to reduce limits of detection. Wang et al.[25] exploited the interfacial accumulation of cisplatin at mercury electrodes as an effective preconcentration process prior to the voltammetric measurement. The voltammetric response was evaluated with respect to preconcentration time and potential, concentration dependence, nature of electrolyte, the presence of surfactants and other variables. Using a preconcentration potential of -0.20 V, a linear calibration plot was obtained up to 2.4×10^{-6} M, and the adsorptive stripping voltammetric technique was adapted for the indirect assay of cisplatin in untreated urine samples.

Previous stripping voltammetric methods for determining Pt include the masking of the sulphide or thiourea

peak by Pt, and the deposition of Pt on a graphite or glassy carbon electrode from solutions containing $PtCl_4^{2-}$ and $PtCl_6^{2-}$ ions following by anodic stripping voltammetry [26,27]. The sensitivity of these methods, however, is not high and only levels above 10^{-8} M platinum can be determined, compared to measurement of catalytic hydrogen waves produced by Pt complexed with ethylenediammine [19] or formazone [24], which give limits of detection of 10^{-10} M. Van den Berg et al. [28] improved the existing limits of detection (0.04 pM) by measurement of the catalytic hydrogen wave at a mercury electrode, following complexation of Pt with formazone (complex is adsorbed for 1-20 min at -0.925 V). This adsorptive cathodic stripping voltammetric method was used to determine Pt levels in sea water. However, the technique did suffer from the formazone peak that interferes with the measurement of the Pt peak, as the latter appears on a shoulder on the former.

The following section illustrates the usefulness of differential pulse polarography and adsorptive stripping voltammetry when applied to the determination of Pt after complexation with ethylenediammine. The technique was applied to the direct determination of Pt in urine samples, and the DPP technique was compared to a GFAAS method.

5.2. EXPERIMENTAL

5.2.1. Materials

All chemicals were of analytical reagent grade. The platinum atomic adsorption standard (P-6401) containing 1 mg/ml of platinum (Pt) in dilute HCl was obtained from Sigma Ltd. All solutions were prepared in water which had been obtained by passing distilled water through a Milli-Q water purification system. A buffer solution was prepared that was 0.5 M in boric acid and 0.59 M in ethylenediammine. This buffer was used in most of the voltammetric investigations. Human urine samples were donated by healthy volunteers.

5.2.2. Apparatus

Voltammetric investigations were carried out using a Princeton Applied Research (PAR) Model 264 polarographic analyser in conjunction with a PAR Model 303 SMDE electrode assembly and a Houston Omnigraphic Model 2000 x-y recorder.

An Instrumentation Laboratory (IL) Model 357 atomic absorption spectrometer was operated in conjunction with an IL Model 655 graphite furnace atomiser and pyrolytic graphite furnace cells for the GFAAS measurements.

5.2.3. Methods

For voltammetric investigations, a 10 mg/l stock solution of Pt was prepared by taking 0.1 ml of the atomic absorption standard solution and diluting to 10.0 ml with 0.15 M NaCl solution. From this solution, standards in the range 0.2 - 1.0 mg/l were prepared bt the appropriate dilution with boric acid-ethylenediammine solution. Prior to voltammetric investigations, the solutions to be analysed were placed in a boiling water bath for 20 min and allowed to cool to room temperature. The solutions were then de-gassed with oxygen-free nitrogen for 8 min prior to recording the appropriate voltammograms.

For graphite furnace atomic absorption spectrometric (GFAAS) investigations, a 10 mg/l stock solution was prepared by taking 0.1 ml of the atomic absorption standard solution and diluting to 10.0 ml with dilute HNO_3 (1+499).

For polarographic determinations of Pt in urine samples, 1.0 ml samples were diluted to 6.0 ml boric acid/ ethylenediammine buffer and placed on a boiling water bath for 20 min. After cooling to room temperature, the pH of the solutions were adjusted to 10.0 with 0.1 M NaOH, and the solutions were made up to 10 ml with water prior to voltammetric investigations. For GFAAS determinations, 1.0 ml urine samples were diluted to 6.0 ml with the dilute HNO_3 solution prior to direct injection of the sample solution into the furnace cell and running of the temperature programme.

The test solutions were always deoxygenated by purging with nitrogen for 8 min.

In the GFAAS investigations, the following instrumental parameters were used in the determination of Pt in both aqueous and urine samples:

light source	hollow cathode lamp
lamp current	10 mA
wavelength	265.9 nm
bandpass	0.5 nm
integration time	8 s (Pt in aqueous samples)
	12 s (Pt in urine samples)
purge gas	argon
flow rate	30/5 standard cubic
	feet/hour air
sample size	25 μl

Deuterium background correction was used throughout. The temperature programme employed with the furnace involved the following steps: drying for 5 s at 70^{0}C, then for 45 s at 110^{0}C; ashing for 20 s at 750^{0}C then for 20 s at 1000^{0}C; atomisation for 10 s at 2500^{0}C.

5.3. Differential Pulse Polarography (DPP) of Pt(II)

5.3.1. Basis of Method

Differential pulse polarography using the catalytic wave of $[Pt(en)_2]^{2+}$ was proposed by Alexander et al. [19] for the assay of traces of platinum in metal ore samples. The catalytic process is believed to follow the mechanism shown below:

$$[Pt(en)_2]^{2+}_{ads} + 2e^- \longrightarrow [Pt(en)_2]_{ads}$$

$$[Pt(en)_2]_{ads} + 2H^+ \longrightarrow [Pt(en)_2]^{2+}_{ads} + H_2$$

The mechanism indicates that the complex $[Pt(en)_2]^{2+}_{ads}$ (which acts as the catalyst) is reduced to a lower oxidation state, which is highly reactive and reduces protons to hydrogen.

5.3.1.1. Effect of pH

In optimising the conditions for the DPP determination of Pt(II), based on the catalytic wave generated by Pt(II) complexed with ethylenediammine, the complexation reaction was investigated at pH values between 7.0 and 11.0. At

pH 7.0, the DPP peak for the $[Pt(en)_2]^{2+}$ complex was relatively broad, and the peak current was lower than that observed at higher pH's. At pH 11.0, the DPP peak was masked to a large extent by the electrolyte decay. Between pH values of 8.0 and 10.0, the DPP waves were well defined, but a pH of 10.0 gave rise to the largest peak current and the best resolution from the electrolyte decay (Figure 5.1.).

5.3.1.2. Effect of the presence of chloride ions

In the initial studies, when the Pt(II) standards were prepared in the boric acid/ethylenediammine buffer (i.e. in a solution not containing chloride ions), the resulting DPP peaks gave rise to irreproducible responses, due to the instability of the Pt(II) in this buffer. In order to improve this situation, and to better mimic the matrix of urine, the Pt(II) standards were made up in 0.15 M NaCl prior to carrying out the complexation reaction. This resulted in better reproducibility of response and improved somewhat the shape of the DPP peak of the $[Pt(en)_2]^{2+}$ complex. The presence of chloride ions also resulted in a slight shift in the peak potential to more positive values, -0.50 V for $[Pt(en)_2]^{2+}$ complex when Pt standard was made up in 0.15M NaCl compared to a value of -0.57 V in distilled water (Figure 5.2.).

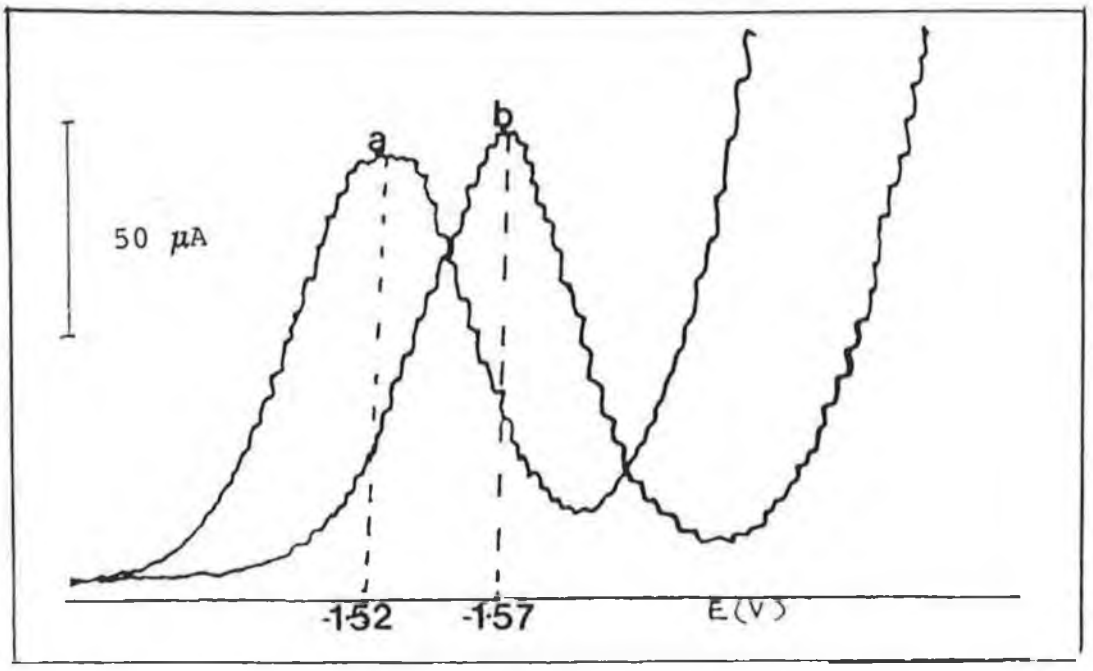

Figure 5.1. Effect of pH on DPP behaviour of $[Pt(en)_2]^{2+}$ complex

a) pH 8.0

b) pH 10.0

(concentration of Pt 1.0 μg/ml)

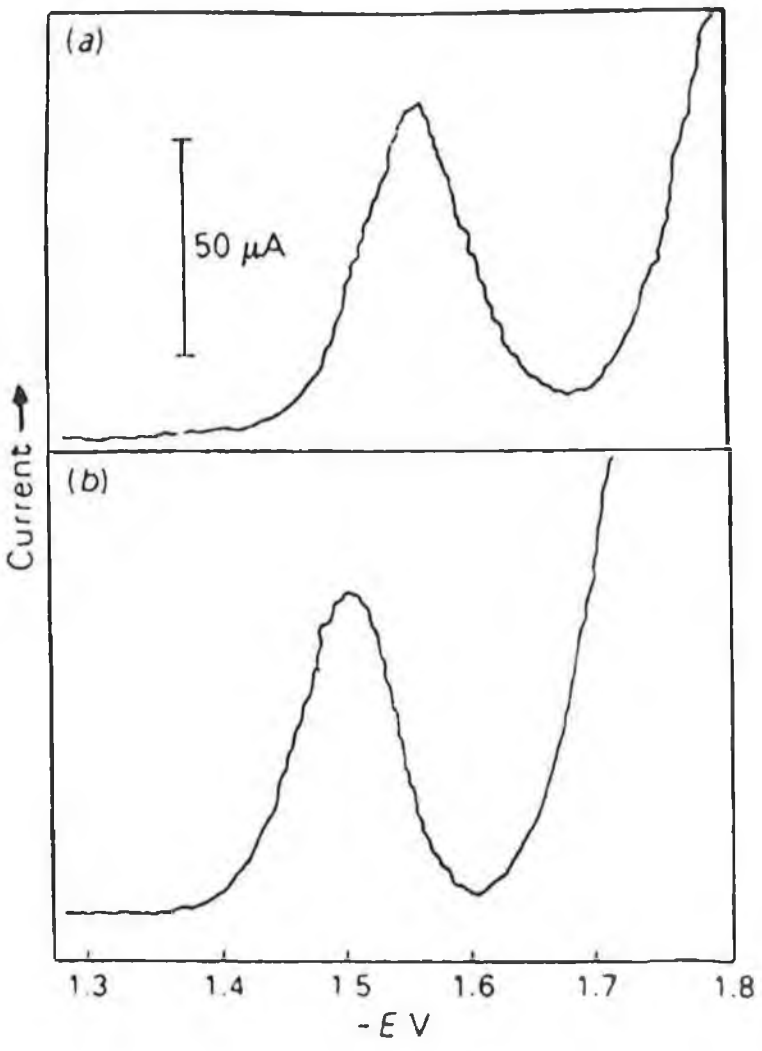

Figure 5.2. Differential Pulse polarographic behaviour of the $[Pt(en)_2]^{2+}$ complex (1.0 μg/ml in boric acid-ethylene diammine buffer, pH 10.0

a) when Pt standard was made up in distilled water; and

b) when Pt standard was made up in 0.15 M NaCl.

5.3.1.3. Effect of temperature on formation of the $Pt(en)_2^{2+}$ complex

Previous work [23] has shown that formation of the $[Pt(en)_2]^{2+}$ complex reaches a maximum between 15 and 20 min. A reaction time of 20 min was therefore employed for all investigations.

The temperature of the water bath where the complexation occurred was also carefully monitored throughout the initial studies. It was found that a temperature of at least 95^0C was needed for sucessful complexation of Pt(II) and ethylenediammine. Hence for all subsequent studies, a reaction temperature of 100^0C was used.

5.3.1.4. Calibration

Using the experimental conditions outlined above,a linear calibration curve was obtained for current (I) versus concentration (C) of Pt(II) (in aqueous solutions) between 0.2 and 1.0 μg/ml. Linear regression analysis of the data yielded a straight line plot which followed the equation $I = 2.29\ C - 8.51 \times 10^{-3}$ (correlation coefficient 0.99) (Figure 5.3a.). The standard solutions were re-analysed 24 hours later, resulting in increased current signals for the various Pt concentrations. Leaching of Pt or other metallic species from the glassware may provide interferents to the accurate analysis of Pt, hence it is

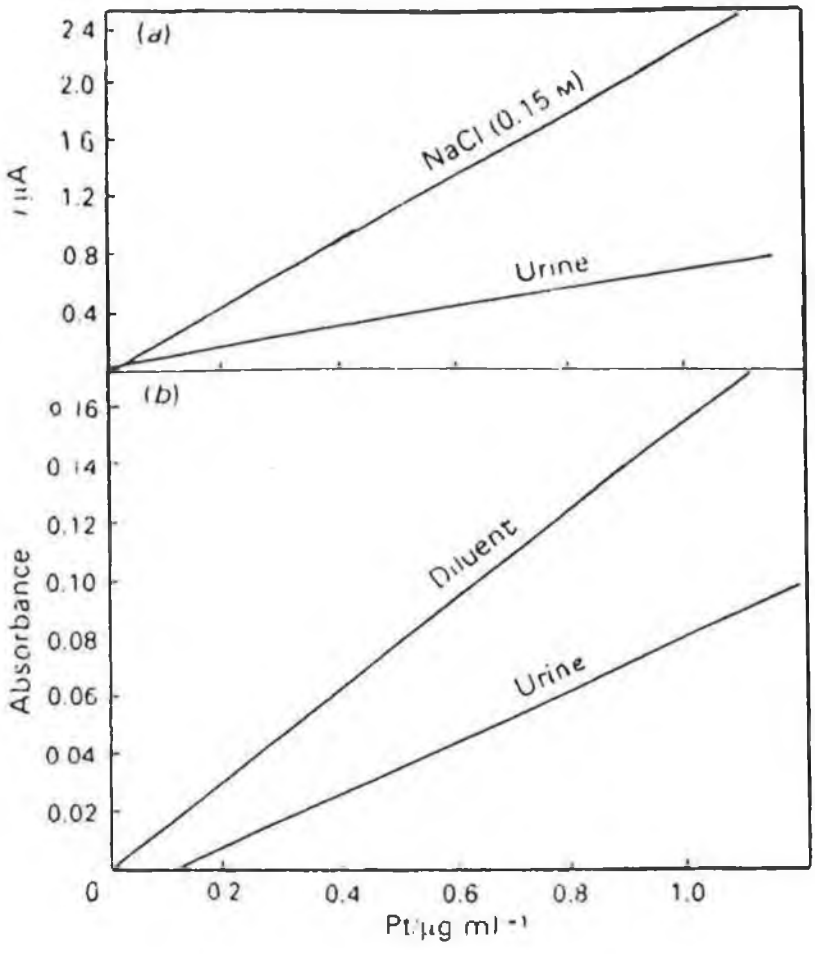

Figure 5.3. Calibration graphs obtained for a) DPP and b) GFAAS methods in aqueous solution and in urine.

necessary that the Pt standards be prepared freshly everyday.

5.3.1.5. Direct determination of Pt(II) in urine

Having established the optimum conditions for the polarographic determination of Pt(II) following complexation with ethylenediammine (in aqueous samples), it was decided to look at the possibility of using the complexation reaction to determine Pt(II) in urine samples. The procedure for the preparation and subsequent analysis of the urine samples has already been outlined in Section 5.2.3. On increasing Pt(II) concentration, an increase in current was seen at -1.66 V (Figure 5.4.). A calibration curve indicated that linearity was obtained over Pt(II) ranges of 0.2 - 1.0 μg/ml, with linear regression analysis of the data yielding a plot following the equation $I = 0.727\ C - 0.019$ (correlation coefficient 0.996) (Figure 5.3.a). The negative intercept and decrease in slope in comparison to the data obtained for the calibration plots of Pt(II) satandards in aqueous solutions, indicates that there is interference in the urine matrix that masks or binds to the platinum, hence reducing the levels that can accurately be determined. Limits of detection for the direct determination of inorganic Pt(II) in urine following complexation with ethlyenediammine is 0.4 μg/ml with a 31% recovery of the Pt complex.

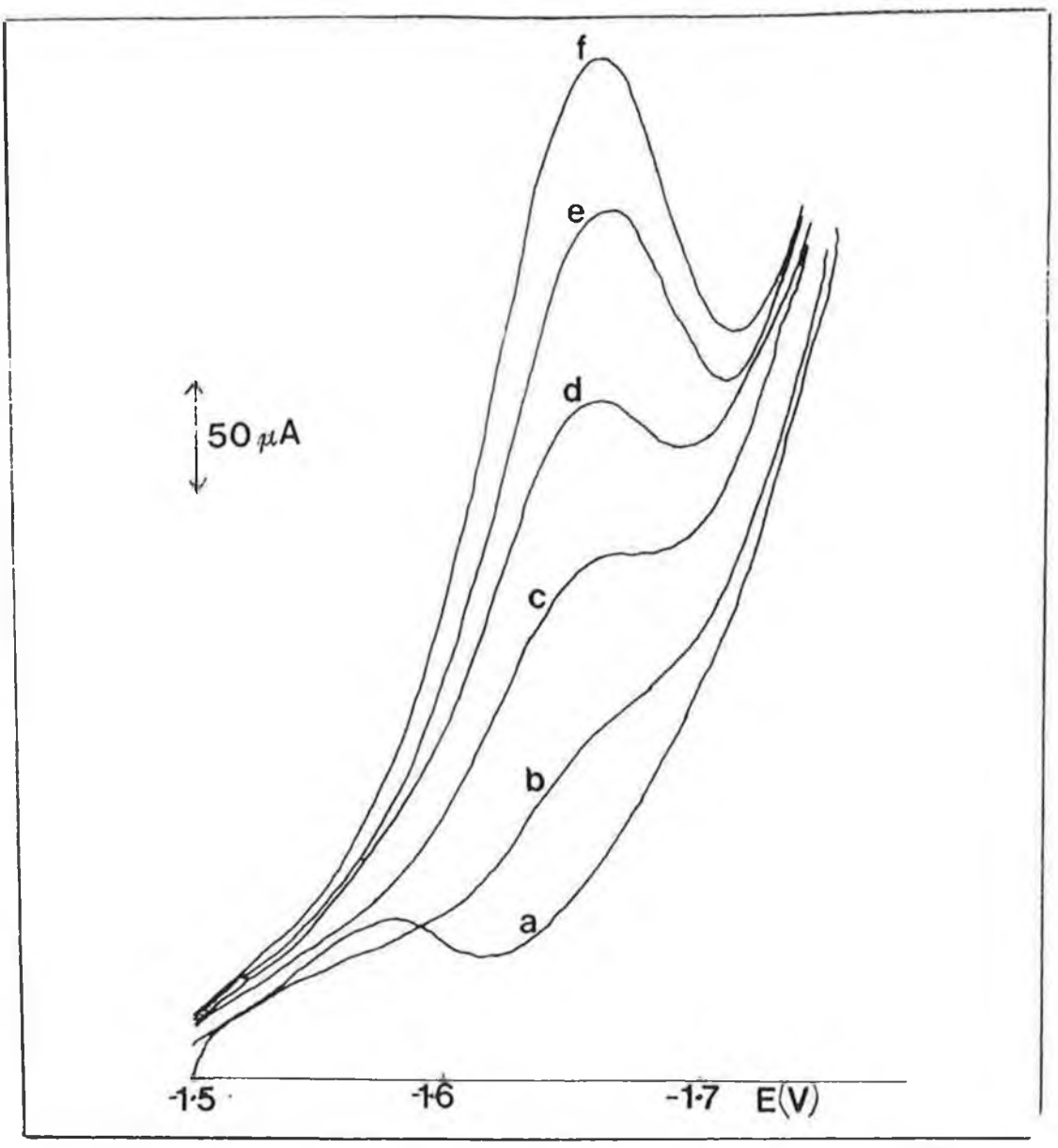

Figure 5.4. DPP of Pt standards in urine

a) black urine b) 0.2 μg/ml Pt

c) 0.4 μg/ml Pt d) 0.6 μg/ml Pt

e) 0.8 μg/ml Pt f) 1.0 μg/ml Pt

5.3.2. Graphite furnace atomic absorption spectroscopy (GFAAS)

5.3.2.1. Optimisation of operational parameters

In GFAAS, care must be taken to select the proper conditions for the drying, ashing and atomisation stages. When dealing with trace metals in purely aqueous solutions, the ashing phase has no real significance. However, as in this case, when trace metals are to be determined in varying amounts of complex matrices (plasma, urine ,tissues, etc,), the ashing stage is perhaps the most important phase in the entire furnace programme. Thermal destruction of the matrix of a sample is very much sample dependent, but the ultimate aim is to remove the matrix completely, leaving behind the analyte in a form which results in maximum atomisation efficiency. However, it should also be noted, that the use of too high an ashing temperature or time can result in the loss of significant quantities of the analyte before the atomisation stage is reached.

A programme of sequential operations was optimised bearing the above points in mind. The programme outlined in Section 3.2.3. is similar to that reported by Pera and Harder [7], but the ashing temperature in this programme was maintained at $1000^{0}C$, instead of $1500^{0}C$, in order to guard against loss of platinum before atomisation. 10 ul aliquots of Pt(II) standards prepared in diluent (see Section 5.2.3.) were analysed for Pt concentrations over the range 0.2 - 1.0 μg/ml. Linear

regression analysis of the data yielded a straight line plot which followed the equation $A = 0.144C + 5.66 \times 10^{-3}$ (correlation coefficient 0.990) (Figure 5.3.b). Having found that this programme was successful in the analysis of Pt in aqueous solutions it was decided to try to reproduce this success for the direct determination of Pt in urine samples.

5.3.2.2. Direct GFAAS determination of Pt in urine

A calibration curve relating to the direct determination of platinum (II) in urine was found to be linear over comparable ranges studied in aqueous solutions. Linear regression analysis of the data yielded the following plot following the equation $A = 0.081C - 3.866 \times 10^{-3}$ (correlation coefficient 0.999) (Figure 5.3.b.).

A negative intercept and decrease in slope compared to that noted for aqueous solutions highlights the problems involved in the direct determination of Pt in urine (i.e. without any extraction or preconcentration steps). The high ashing temperature of $1000^{0}C$, and indeed the high atomisation temperature ($2500^{0}C$), theoretically should have removed any endogenoeus urine interferents. Higher ashing temperatures were investigated (with the atomisation temperature kept constant), but these only resulted in a decrease of absorbance of the Pt standards. Hence, the optimum ashing temperature useful for the direct detection of Pt in urine was in fact the original temperature used.

Using this technique concentrations of platinum(II) were determined directly in urine down to 0.4 μg/ml with a 44% recovery of the analyte.

5.4. Adsorptive Stripping Voltammetry

Adsorptive stripping voltammetry has become increasingly popular in recent years for the determination of species which cannot be determined by anodic and cathodic stripping voltammetric techniques, but which can undergo accumulation at an electrode surface by adsorption [29,30]. Stripping techniques are not particularly suited to the determination of the platinum group metals [26], but, Wang et al. [25] have reported a method for the determination of cisplatin using AdSV. We therefore investigated the application of AdSV to the determination of inorganic platinum following its complexation with ethylenediammine, as reported in Section 5.3.1.

5.4.1. Initial investigations

A short study was initially undertaken to look at the feasibility of using AdSV to determine the $[Pt(en)_2]^{2+}$ complex. When a supporting electrolyte of 0.1 M KCl -0.01 M ethylenediammine (50:50) was investigated using an accumulation potential (E_{acc}) of -1.00 V, and accumulation times (t_{acc}) between 0 - 300 s, a very slight increase was noted in the current around -1.45 V. A large increase in current was found, however, for a peak at -1.72 V, which has characteristics of a catalytic wave due to hydrogen evolution (Figure 5.5.a). The

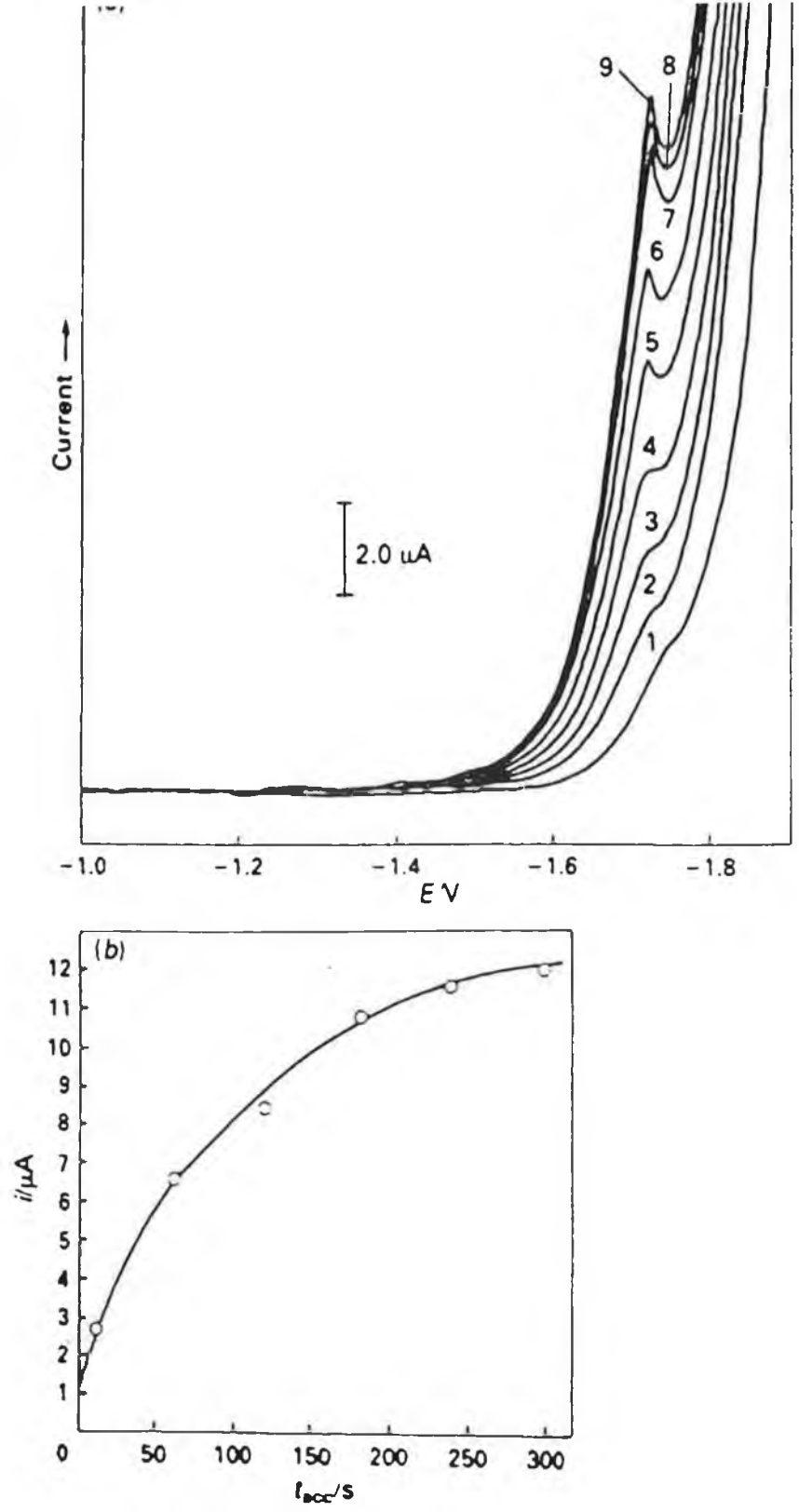

Figure 5.5a. Effect of t_{acc} on the adsorptive stripping voltammetric behaviour of the $[Pt(en)_2]^{2+}$ complex (4 ng/ml) in 0.1 M KCl- 0.01 M ethylenediammine (50/50) solution. b) Plot of current vs t_{acc} relating to a) . t_{acc}: (1) background); (2) 0; (3) 10; (4) 30;(5) 60; (6) 120; (7) 180; (8) 240; and (9) 300 s.

current due to this peak increased in a non-linear manner as shown in Figure 5.5.b, reaching a limiting value for t_{acc} around 300 s. Using a supporting electrolyte of 0.1 M KCl, increases were found in the current both at -1.56 V (peak A) and at -1.72 V (peak B) (Figure 5.6.a). The current for peak A, increased linearly for t_{acc} up to 120 s, whereas peak B (due to catalytic hydrogen evolution) shifted to more negative potentials, and its current increased non-linearly over the range of accumulation times studied, until it eventually merged with the supporting electrolyte decay (Figure 5.6.b). The supporting electrolyte most suitable for analytical purposes was therefore found to be the 0.1 M KCl - 0.01 M ethylenediammine (50:50) solution, as the potential of the catalytic wave due to the adsorbed Pt(II) complex was not affected by increasing t_{acc} in this system.

A further investigation was subsequently carried out a few months later, the objective being to look at the effect of E_{acc}, pulse amplitude, drop size and concentration of ethylenediammine on the determination of Pt(II). Two major peaks were noted during this study; peak A at - 1.38 V and peak B at - 1.57 V (Figure 5.7.). The shift (of approximately 200 mV) in peak potentials of peaks A and B compared to those previously reported are likely to be due to replacement of reference frits and fillings from one study to the next.

The behaviour of ethylenediammine was then monitored as a function of time (t_{acc}) with a constant E_{acc} of - 0.95 V. One sharp peak at - 1.38 V was observed. This peak increased

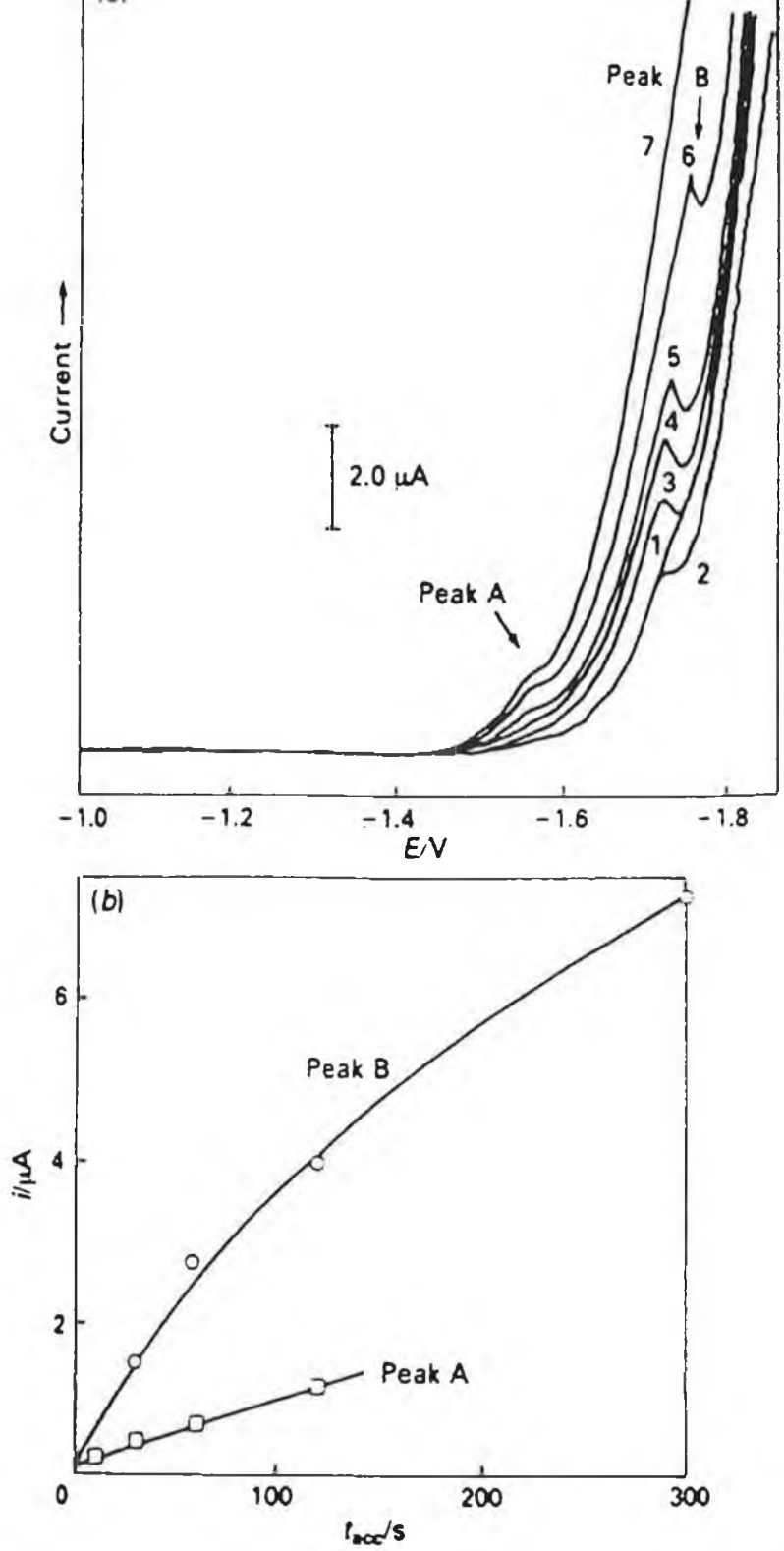

Figure 5.6. a) Effect of t_{acc} on the adsorptive stripping voltammetric behaviour of the $[Pt(en)_2]^{2+}$ complex (4 ng/ml) in 0.1 M KCl. b) Plot of current vs t_{acc} relating to a) t_{acc}: (1) background; (2) 0; (3) 10; (4) 30; (5) 60; (6) 120 and (7) 300 s.

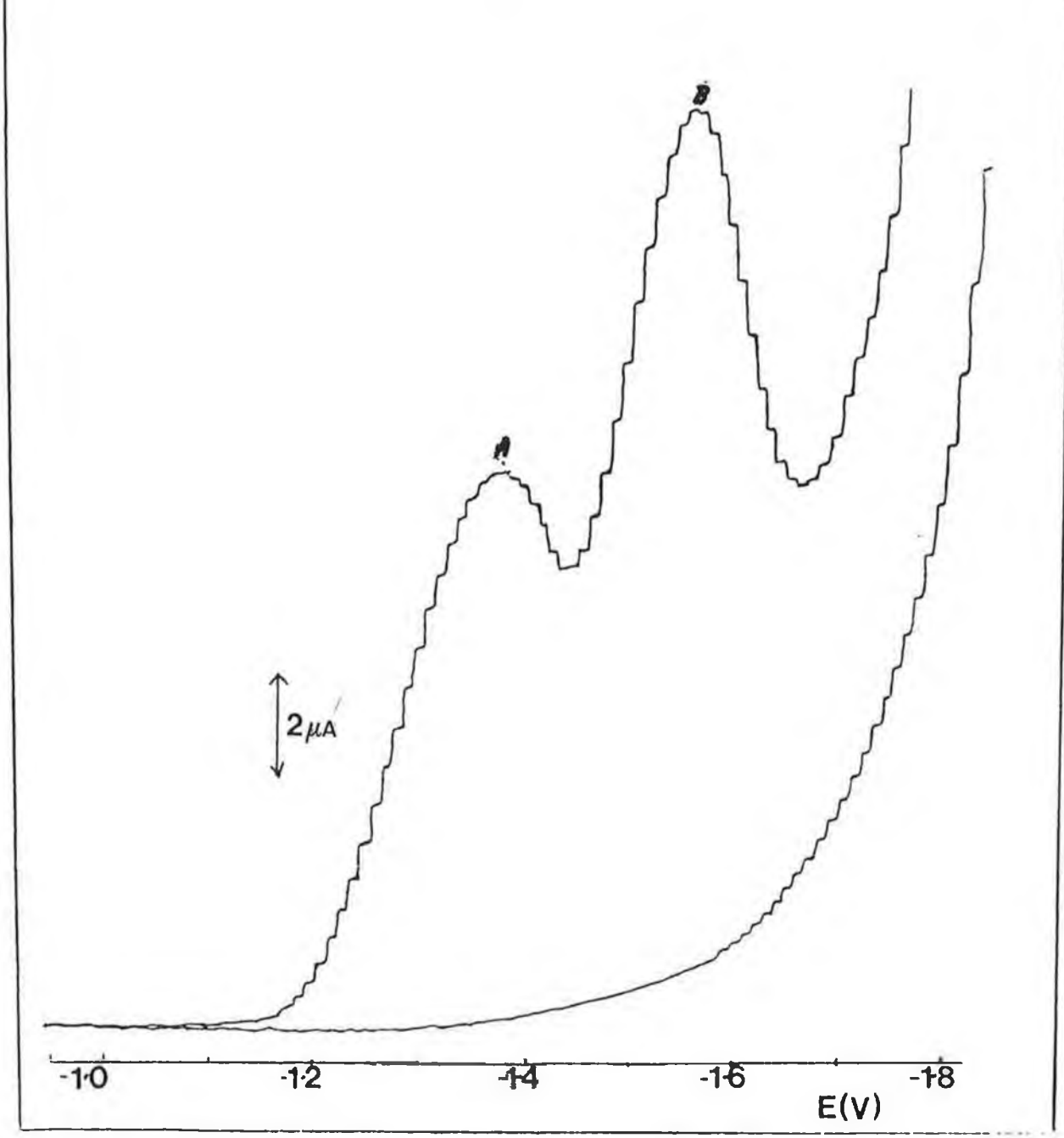

Figure 5.7. Typical voltammetric behaviour of $[Pt(en)_2]^{2+}$ complex. t_{acc} = 30 s; E_{acc} = -0.95 V. Concentration of Pt = 0.2 μg/ml in 0.1 M KCl-0.01 M ethylenediammine (50:50).

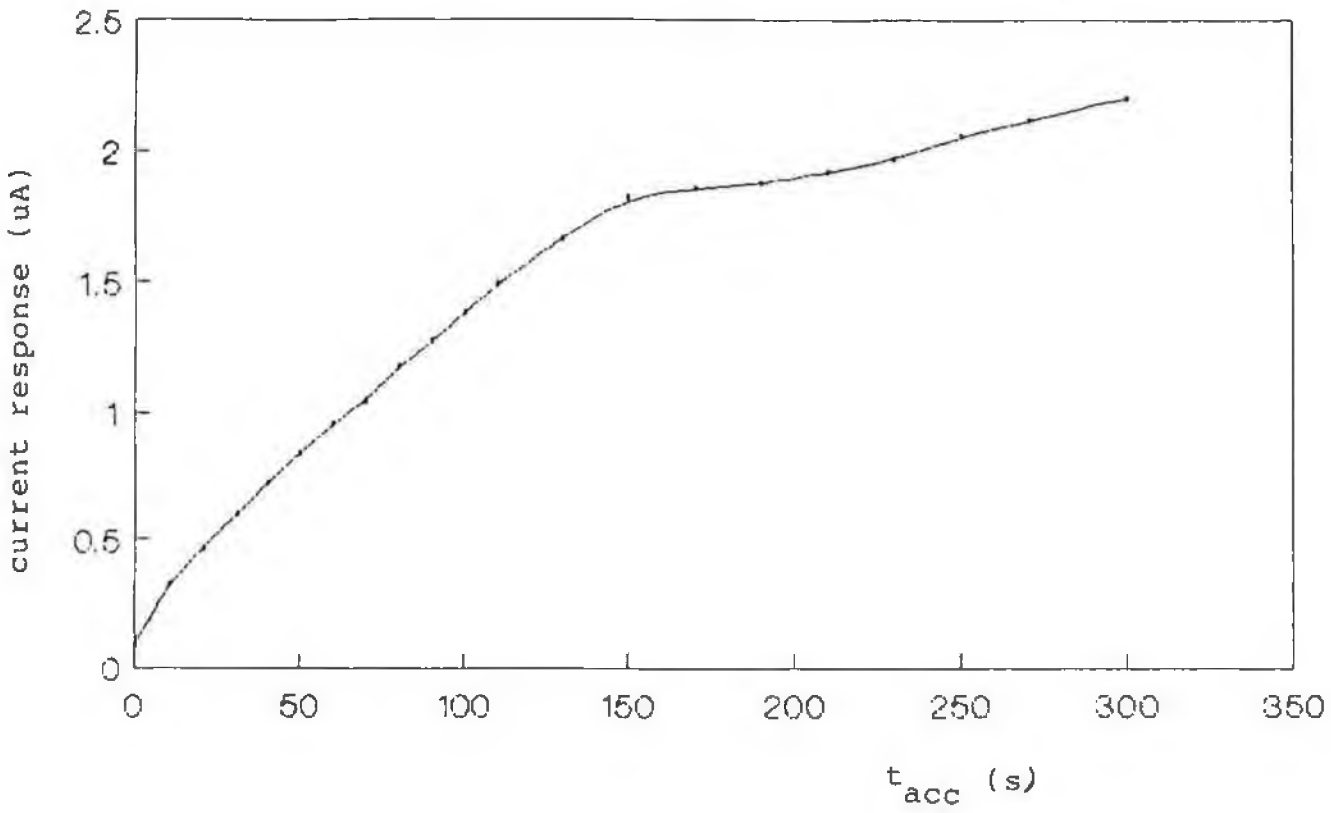

Figure 5.8. Dependence of peak current of 0.59 M ethylenediammine on t_{acc}. E_{acc} -0.95 V; scan rate 10 mV/s; pulse amplitude 10 mV; drop area 0.025 mm^2.

in current linearly up to a time of 150 s, where, above this accumulation time, saturation of the electrode surface occurred, giving rise to the plateau region seen in Figure 5.8. No wave was observed in the potential region for the catalytic wave due to $[Pt(en)_2]^{2+}$. The peak at - 1.38 V is therefore due to the reduction of the complexing agent on its own. Hence, the adsorptive stripping voltammetric behaviour of $[Pt(en)_2]^{2+}$ gives rise to two peaks which do not greatly interfere in the measurement of one another. This would appear to be a slight improvement in selectivity over the method reported by van den Berg and Jacinto [28], who found that the formazone (which was used to complex Pt(II)) peak, interferes with the measurement of the platinum peak, which appears as a shoulder on the formazone peak.

5.4.2. Effect of accumulation potential and time

The effect of the accumulation potential on both peak currents was evaluated over the range - 0.70 -> 1.30 V (Figure 5.9.). The adsorption potential affects the amount of complex which adsorbs, and at potentials between - 0.80 and - 0.95 V, the largest peaks were observed for $[Pt(en)_2]^{2+}$. A gradual decrease of the current for this peak was noted at potentials more positive than - 0.80 V and more negative than - 0.95 V. The peak current for the complexing agent, i.e. peak A, gradually increased from - 0.70 V to the optimum current response at - 1.10 V, where at potentials more negative than this, a rapid

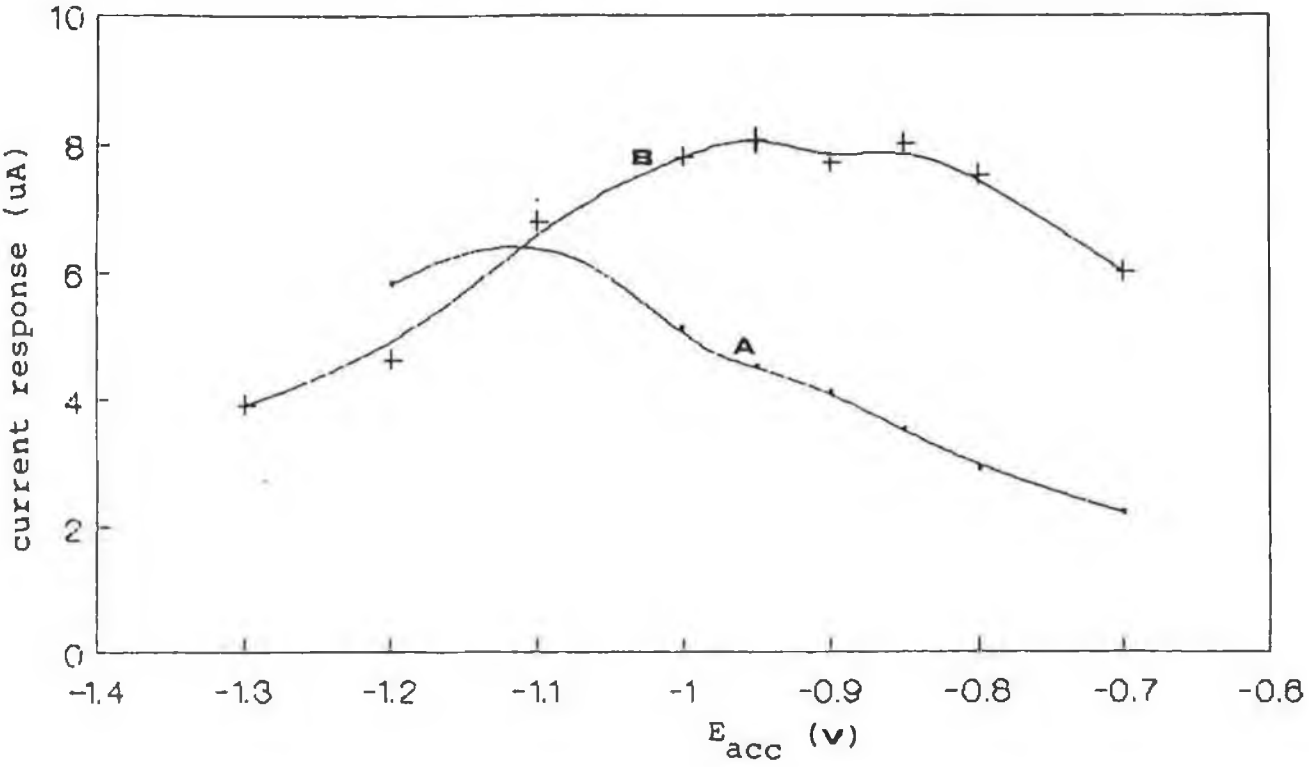

Figure 5.9. Dependence of peak currents for peaks A and B on E_{acc}. [Pt(II)] 0.25 μg/ml; t_{acc} 60 s; scan rate 10 mV/s; pulse amplitude 50 mV; and drop area 0.025 mm^2.

decrease in current response was noted. The optimal adsorption potential for analytical purposes for the detection of Pt(II) in its complexed form was chosen as - 0.95 V. This potential is required for trace platinum concentrations, whereas an adsorption potential of - 0.70 V suffices for higher platinum concentrations (the peak height of ethylenediammine at this potential is reduced by almost 50%). The dependence of the adsorptive stripping peak currents of $[Pt(en)_2]^{2+}$ on the accumulation time at three concentration levels is shown in Figure 5.10. The longer the accumulation time, the more $[Pt(en)_2^{2+}]$ adsorbed, and the larger the peak current. Solutions containing stock concentrations of 10,50,and, 100 µg/ml Pt were prepared, and 50 ul of each was added to the cell to give a final concentration of Pt(II) in the cell of 0.05, 0.25, and 0.5 µg/ml. For concentrations of 0.5 and 0.25 µg/ml Pt, the peaks increased linearly at first, and then the current response leveled off as the accumulation time was steadily increased. As expected from the adsorption processes, deviation from linearity was observed at shorter accumulation periods for solutions of higher Pt(II) concentrations. However, with a concentration of 0.05 µg/ml Pt, adsorption peaks only developed after an accumulation time of 60 s. These peaks were not fully resolved from the complex peak compared to those obtained for Pt(II) at higher concentrations. Non-linear behaviour was also observed on increasing acumulation times above 60 s. This behaviour would suggest that a concentration of > 10 µg/ml Pt(II) is required before full complexation between metal and complexing agent is observed using the adsorptive stripping technique.

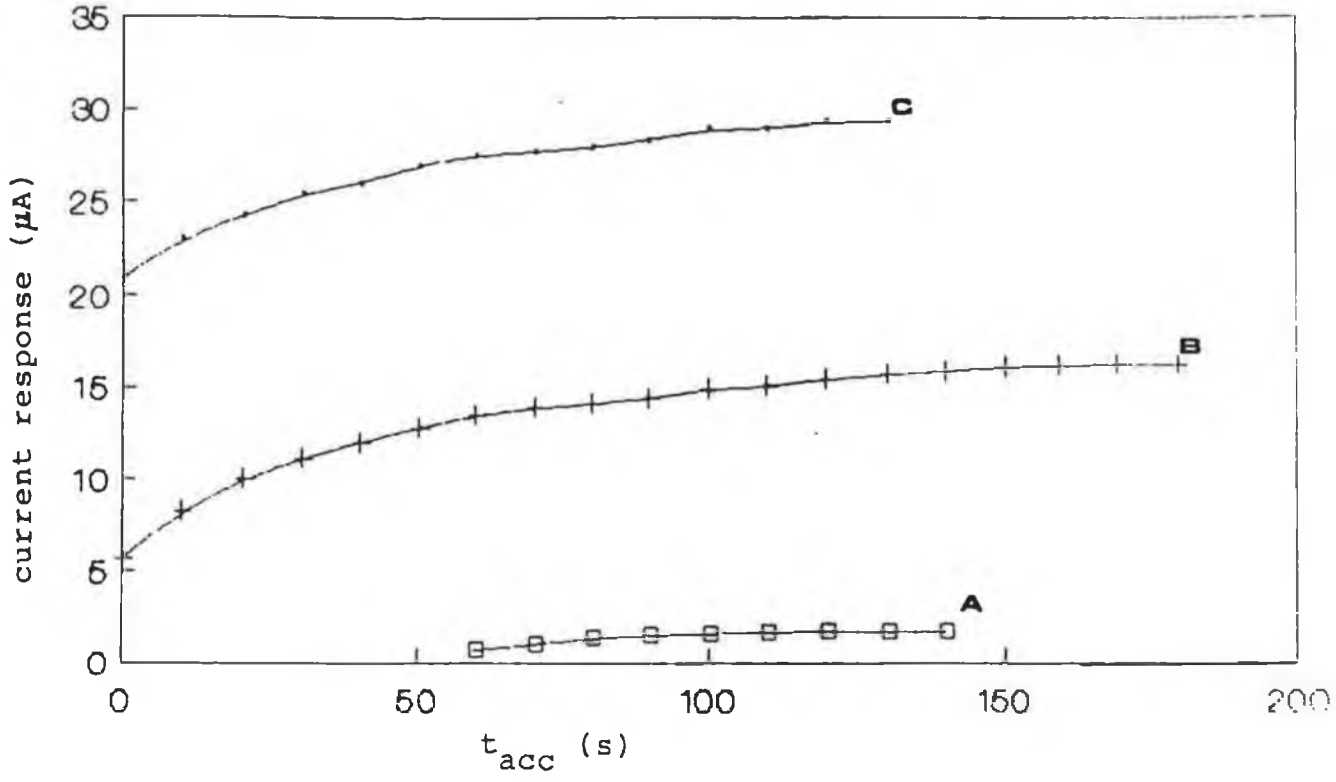

Figure 5.10. Dependence of $[Pt(en)_2]^{2+}$ peak current on t_{acc} for (A) 0.05 μg/ml (B) 0.025 μg/ml and (C) 0.5 μg/ml Pt. Conditions as in Fig. 5.8.

5.4.3. Effect of drop size, scan rate and pulse amplitude

The effect of drop size, scan rate and pulse amplitude were also studied in order to find the optimum conditions for the determination of Pt(II) following complexation. A mercury drop of 0.025 m^2 resulted in the largest peak currents for both processes. This was expected as the greater the surface area of the electrode, the greater the amount of analyte adsorbed. A scan rate of 10 mV/sec and a pulse amplitude of 100 mV also resulted in better shaped and reproducible voltammograms of $[Pt(en)_2]^{2+}$ and ethylenediammine.

The adsorbed $[Pt(en)_2]^{2+}$ can be measured using different voltammetric waveforms. Linear scan and differential pulse modes were compared, with the differential pulse mode yielding better defined peaks following accumulation, compared to the linear scan mode. Therefore, the differential pulse mode was used in all subsequent work.

5.4.4. Effect of ethylenediammine concentration

The effect of concentration of the complex on the adsorptive stripping behaviour of $[Pt(en)_2]^{2+}$ was studied over a concentration range of 1 - .001 M ethylenediamine (Figure 5.11.). At concentrations > 0.59 M, the peak at - 1.55 V decreased in height and was also not fully resolved from the

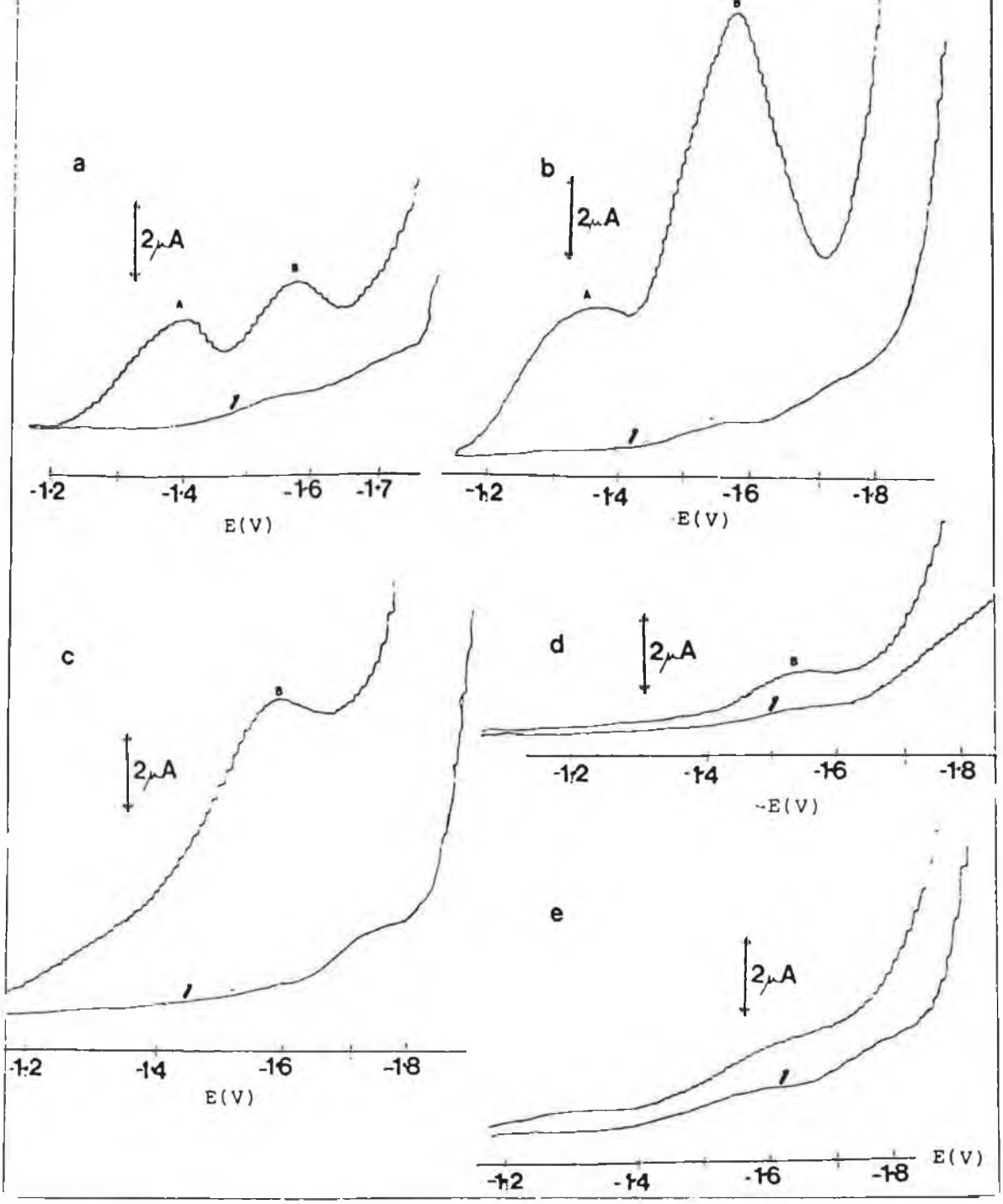

Figure 5.11. Effect of ethylenediammine concentration on the AdSV behaviour of $[Pt(en)_2]^{2+}$ complex (peak B) and ethylenediammine (en) (peak A). Pt(II) concentration in all cases was 0.25 μg/ml; t_{acc} 60 s.

(a) 1M en (b) 0.59 M en

(c) 0.1 M en (d) 0.01 M en

(e) 0.001 M en (1 = background)

decay of the background electrolyte. As expected, peak A was not observed at these lower concentrations. A 1 M ethylenediammine concentration reduced the peak currents for both peaks A and B, where a concentration of 0.59 M ethylenediammine resulted in better resolution from the decay of the background electrolyte, and also optimum peak currents for $[Pt(en)_2]^{2+}$, in particular. For further work, a concentration of 0.59 M ethylenediammine was therefore selected.

The effective preconcentration associated with the adsorption process results in low detection limits. Using an accumulation time of 60 s and adding increasing 5 μl aliquots of a stock solution of 25 μg/ml Pt in a cell volume of 10 ml, a calibration curve yielded the following equation I = 17.94C - 0.69 (correlation coefficient 0.987). The limit of detection corresponds to 12.5 ng/ml Pt in the cell (i.e 5 μl of 25 μg/ml Pt in 10 ml of electrolyte solution.

For higher detection limits, shorter preconcentration times suffice. The dependence of the peak current on the Pt concentration, using a preconcentration period of 30 s is shown in Figure 5.12. The response was linear up to 1.25 μg/ml Pt (slope of the linear portion 21.796 μA/ug/ml; correlation coefficient 0.99). The limit of detection using an accumulation time of 30 s and increasing the additions of 5 μl aliquots of 50 μg/ml Pt solution to 10 ml of electrolyte in the cell was 25 ng/ml.

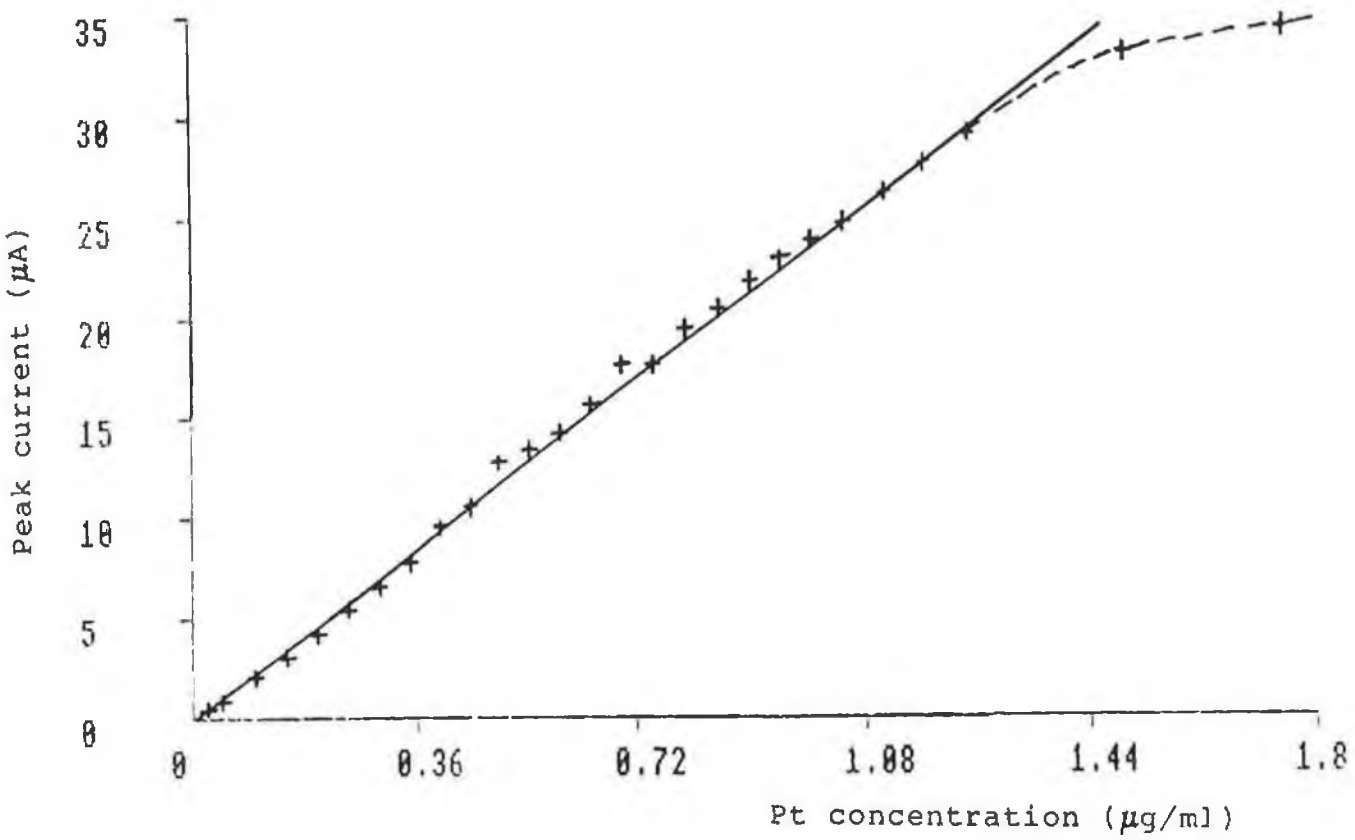

Figure 5.12. Dependence of $[Pt(en)_2]^{2+}$ complex peak current on Pt(II) concentration using t_{acc} of 30 s, scan rate 10 mV/s, drop size 0.025 mm^2.

5.5. The application of AdSV for the determination of Pt in its complexed form directly in urine

The adsorptive stripping voltammetric conditions that had previously been optimised for the determination of Pt (after complexation) in aqueous solutions, were then examined for the effective determination of Pt in urine samples. Urine samples were collected and centrifuged for 15 min, after which 1 ml aliquots were spiked with appropriate volumes of the Pt standard, and then diluted to 10 ml with 0.59 M ethylenediammine, 0.5 M boric acid buffer solution. These solutions were then boiled for 20 min in a water bath, allowed to cool to room temperature and the pH adjusted to 10.0. A calibration curve for the determination of inorganic Pt in urine, folowing an accumulation period of 60 s is shown in Figure 5.13. The current response was found to be linearly related to concentration according to the equation $I = 1.47C - 0.53$ (correlation coefficient 0.98). Using this technique, the limit of detection was 0.75 μg/ml. Deviations from linearity occurred at concentrations of > 2.4 μg/ml, where a third peak at -1.70 V was noted. On running similar urine samples that were Pt-free under the same experimental conditions, this third peak was provisionally identified as an endogenous component of urine, where, at high urine concentrations, this peak interferes with Pt measurements. This deviation from linearity at high concentrations of Pt and urine, plus the negative intercept on the x-axis (concentration axis) suggests that

there are components in the urine matrix that compete with the $[Pt(en)_2]^{2+}$ complex for adsorption on the surface sites of the electrode. These components appear to displace Pt from the surface. Hence to improve the existing limits of detection, a longer and time consuming sample clean-up step is probably required to remove these inherent interfering components.

However, the results presented here, where no pretreatment of the urine is undertaken, allows the quick detection of Pt in urine to levels that would be expected during cisplatin therapy (see Chapter 1). Also the technique does not suffer from interferences from the complexing agent during the measurement of Pt and this is an improvement on the work presented by van den Berg and Jacinto [28]. It should be noted however that the limits of detection are not as good as van den Berg and Jacinto [28], due to the higher background currents observed at very negative potentials.

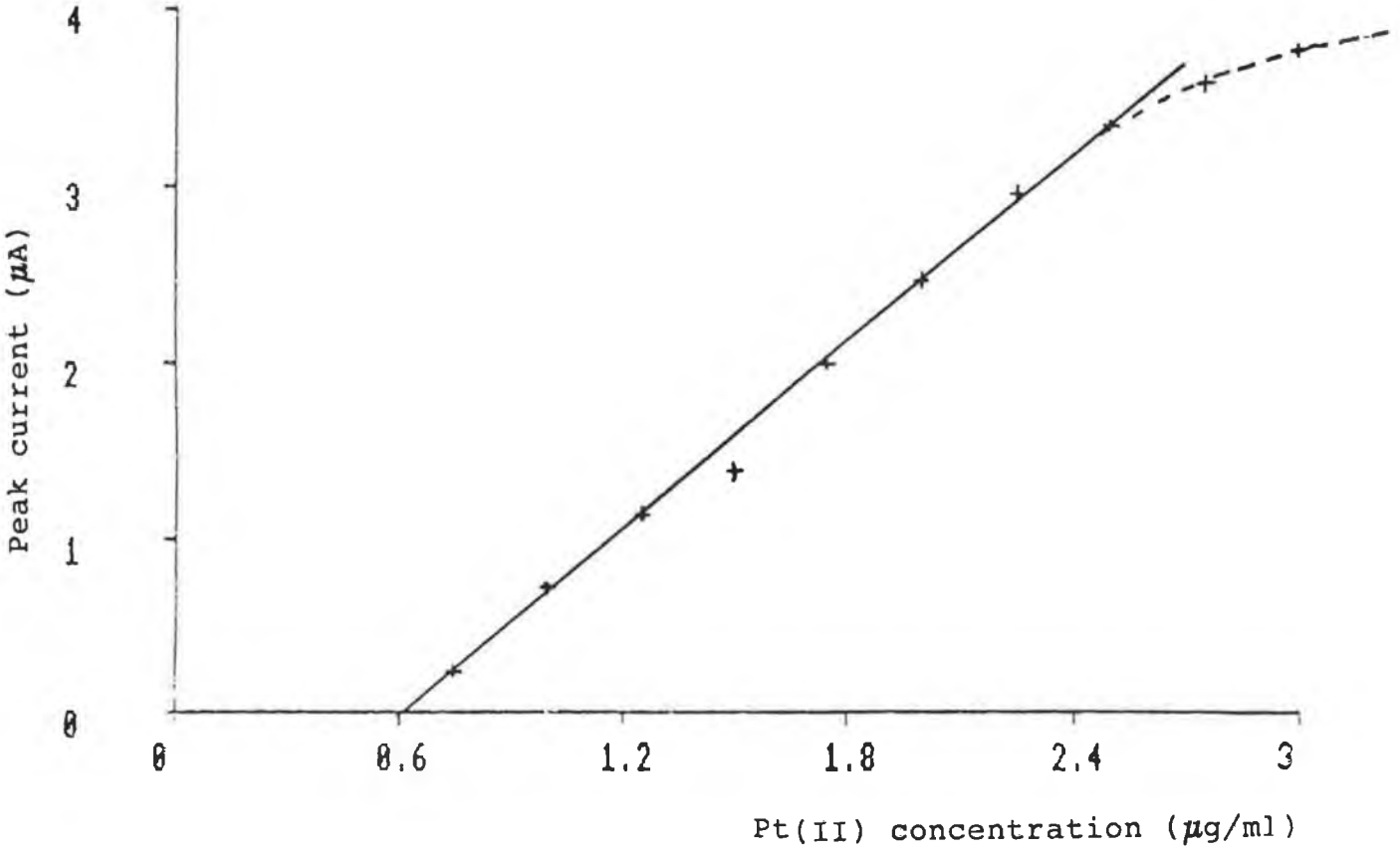

Figure 5.13. Dependence of $[Pt(en)_2]^{2+}$ complex peak current on Pt(II) concentration in urine, using t_{acc} of 60 s, scan rate 10 mV/s, drop area 0.025 mm^2.

5.6. REFERENCES

1. Litterst C.L., Gram T.E., Dedrick R.L., Leroy A.F., and Guarino A.M., Cancer Res., 1976,36,2340.
2. Leroy A.F., Lutz R.J., Dedrick R.L., Litterst C.L., and Guarino A.M., Cancer Treat. Rep., 1979,63,59.
3. Gormley P.E., Bull J.M., Leroy A.F., and Cysyk R., Clin. Pharmacol. Ther., 1979,25,351.
4. Leroy A.F., Wehling M.L., Sponseller H.L., Friauf W. S., Soloman R.E., Dedrick R.L., Litterst C.L., Gram T.E., GuarinoA.M., and Becker D.A., Biochem. Med., 1977,18,184.
5. Kelsen D.P., Alcock N., and Young C.W., Am. J. Clin. Oncol., (CCT) 1985,8,77.
6. Jones A.H., Anal. Chem., 1976,48,1472.
7. Pera M.F., and Harder H.C., Clin. Chem., 1977,23,1245.
8. Bannister S.J., Chang Y., Sternson L.A., and Repta A.J., Clin. Chem., 1978,24,877.
9. Siddik Z.H., Boxall F.E., and Howell S.B., Anal. Biochem., 1987,163,21.
10. Riley C.M., Sternson L.A., and Repta A.J., Anal. Biochem., 1982,124,167.
11. Andrews P.A., Wung W.E., Howell S.B., Anal. Biochem., 1984,143,46.
12. Shearan P., and Smyth M.R., Analyst, 1988,113,609.
13. Riley C.M., Sternson L.A., Repta A.J., and Siegler R.W., J. Chromatogr., 1982,229,373.

14. Eiferink F., Van der Vijgh W.J.F., and Pinedo H.M., Anal. Chem., 1986,58,2293.

15. Harrison J.A., and Thompson J., Electrochim. Acta., 1973,18,829.

16. Laitinen H.A., and Onstott E.I., J. Am. Chem. Soc., 1950,72,4569.

17. Slendyk I., and Herasymenko P., Z. Phys. Chem. A., 1932,162,223.

18. Ezerskaya N.A., and Kiseleva I.N., Zh. Anal. Khim., 1969,24,1684.

19. Alexander P.W., Hoh R., and Smythe L.E., Talanta, 1977,24, 543.

20. Ezerskaya N.A.,and Kiseleva I.N., Zh. Anal. Khim., 1984,39,1541.

21. Vrano O., Kleinwachter V., and Brabec V., Experimentia, 1984,40,446.

22. Vrano O., Kleinwachter V., and Brabec V., Talanta, 1983,36288.

23. Bartosec I.,Cattinio M.T., Grasselli G., Guaitani A., Urso R., Zucco E., Libretti A., and Garattini S., Tumori, 1985,69,595.

24. Zhao Z., and Freiser H., Anal. Chem., 1986,58,1498.

25. Wang J., Peng T.,and Lin M-S., Bioelectrochem. and Bioenerg., 1986,16,395.

26. Vydra F., Stulik K., and Julakova E., "Electrochemical Stripping Analysis" Horwood, Chichester, 1976, p283.

27. Kriksotakis K., and Tobschall H.J., Fresenius Z. Anal. Chem., 1985,320.156.

28. Van den Berg C.M.G., and Jacinto G.S., Anal. Chim. Acta., 1988,211,129.

29. Wang J., "Stripping Analysis: Priniciples, Instrumentation, and Analysis," Verlag Chemie, Dearfield Beach, FL, 1985.

30. Franklin Smyth W., in Smyth M.R., and Vos J.G., Editors, "Electrochemistry, Sensors and Analysis", Elsevier, Amsterdam, 1986, pp29-36.